The Role of Uncertainty for Lumped Parameter Modeling and Optimization of Low Temperature Geothermal Resources

Sven Scholtysik

Thesis of 60 ECTS credits
Master of Science in Sustainable Energy Science - Iceland School of Energy

January 2015

The Role of Uncertainty for Lumped Parameter Modeling and Optimization of Low Temperature Geothermal Resources

Sven Scholtysik

Thesis of 60 ECTS credits submitted to the School of Science and Engineering
at Reykjavík University in partial fulfillment of
the requirements for the degree of
Master of Science in **Sustainable Energy Science - Iceland School of Energy**

January 2015

Supervisors:

Dr. Ágúst Valfells, Supervisor
Associate Professor, Reykjavik University

Dr. Hlynur Stefánsson, Co-Supervisor
Associate Professor, Reykjavik University

Dr. Halldór Pálsson, Co-Supervisor
Associate Professor, University of Iceland

Examiner:

Dr. Guðrún Arnbjörg Sævarsdóttir, Examiner
Dean of The School of Science and Engineering, Reykjavik University

The Role of Uncertainty for Lumped Parameter Modeling and Optimization of Low Temperature Geothermal Resources

Sven Scholtysik

60 ECTS thesis submitted to the School of Science and Engineering
at Reykjavík University in partial fulfillment
of the requirements for the degree of
Master of Science in Sustainable Energy Science - Iceland School of Energy.

Student: January 2015

Sven Scholtysik

Supervisors:

Dr. Ágúst Valfells

Dr. Hlynur Stefánsson

Dr. Halldór Pálsson

Examiner:

Dr. Guðrún Arnbjörg Sævarsdóttir

_____

Date

_____

Sven Scholtysik
Master of Science

The Role of Uncertainty for Lumped Parameter Modeling and Optimization of Low Temperature Geothermal Resources

Sven Scholtysik

January 2015

Abstract

With a growing population and ongoing industrialization, energy demand is rising on a global scale. Satisfying this demand in a sustainable way, while minimizing mankind's impact on climate change, is a significant challenge for our and future generations. One of the options that is apt to make a difference, is the use of low emission energy sources for heating purposes. One of these sources is Earth's ubiquitous geothermal potential. Understanding this potential and its limitations is of utmost importance. Despite having a large impact on optimization and management of geothermal resources, the influence of uncertainty has not been studied extensively. Consequently, this thesis discusses the role of uncertainty in detail. Using net present value maximization as the objective function, the sources of uncertainty are identified by creating a customized net present value model, which splits costs and benefits into different variables. These variables are analyzed for their tendency towards uncertainty. One of the influencing variables is the reservoir's physical reaction to production, as it allows forecasting of realistic exploitation values. In order to test how much information is needed to produce good forecasting results, an initial lumped parameter model fit is obtained to identify the complexity of the best fit for four low temperature reservoirs in Iceland. In order to simulate decreasing uncertainty, the operational data is cut into smaller portions. By gradually extending the data range and iterative fitting, a development of the coefficient of determination is analyzed, finding that after ten seasonal cycles of data input, the model fit reaches a significant level of certainty. This time horizon can act as a stabilizing factor in the economic optimization and improve the accuracy of economic forecasting. Furthermore, the best fits do not show differences in model complexity for different levels of uncertainty.

Keywords: geothermal energy, lumped parameter modeling, optimization, net present value, uncertainty

Hlutverk óvissu í Lumped parameter líkönum og bestun á lághita jarðvarmasvæðum

Sven Scholtysik

Janúar 2015

Útdráttur

Á sama tíma og fólksfjöldi jarðar vex, eykst orkuþörf jarðarbúa gífurlega. Ein stærsta ógn mannkynsins er að svara þessari orkuþörf á sjálfbæran máta og með endurnýjanlegum orkugjöfum sem lágmarka vistspor til framtíðar. Einn af stærstu möguleikunum þegar kemur að því að minnka útblástur gróðurhúsa lofttegunda snertir upphitun híbýla. Í stað þess að nota jarðefnaeldsneyti til húshitunar er nauðsynlegt að nýta þá orku sem til er í iðrum jarðar. Til að unnt sé að nýta þá orku á bestan hátt er nauðsynlegt að skilja eðli ysta hluta jarðar,gera sér grein fyrir þeim ferlum sem þar eiga sér stað og skilja möguleika, takmörk og óvissuþætti sem snúa að nýtingu auðlindarinnar. Þrátt fyrir að vera mjög mikilvæg breyta í nýtingu jarðvarmans er óvissa í nýtingu frekar lítið rannsakaður hluti fræðisviðsins. Þessi ritgerð snertir á óvissu í vinnslu jarðvarma, áhrif hennar á fjármögnun og framtíðaráhorf. Notast var við líkön sem hámarka núvirði jarðvarmavinnslu og kennsl borin á helstu óvissuþætti vinnslunnar. Nýtt líkan var smíðað sem gerir greinarmun á vinnslukostnaði og tekjum og þeir þættir síðan greindir með tilliti til óvissuþátta í jarðvarmavinnslu. Ein stærsta breytan þegar kemur að rekstri jarðhitasvæða er svörun jarðhitageymisins við aukinni framleiðslu. Góður skilningur á jarðhitageyminum eykur langtímanotkun og minnkar óvissu þegar kemur að langlífi framleiðslu. Til að greina hversu miklar upplýsingar eru nauðsynlegar til að geta spáð fyrir um óvissuþætti var notast við „lumped parameter“ líkan var notað til að greina fjögur lág-hitasvæði á Íslandi. Notast var við framleiðslugögn til að meta breytingu á jarðhitageyminum og áhrif þeirra á óvissu metin. Framleiðslugögnum var bætt við líkanið þangað til fastinn, „coefficient of determination“, fór að verða greinilegur. Gögnum var bætt við líkanið unns 10 hringrásum var lokið, en þá var óvissan orðin mjög lág. Tímaskalinn virkar því sem stöðugleikaþáttur í jarðhitavinnslu og eykur fjárhagslegt jafnvægi og getur haft umtalsverð áhrif á fjárhagsspár.

Lykilorð: jarðvarmaorka, lumped parameter líkön, bestun, núvirði, óvissa

Acknowledgements

I would like to acknowledge Ágúst Valfells for his supervision, support, encouragement and guidance throughout the whole thesis, and for financial support through the Landsvirkjun Energy Research Fund; Hlynur Stefánsson, Halldór Pálsson, Egill Júlíusson and Silja Rán Sigurðardóttir for providing feedback, practical support and valuable insights; Tiffany Roche for her work on the operational data, Guðni Axelsson and Sigríður Sif Gylfadóttir for providing me with programmes and advice, Gretar Ívarsson for providing maps, Skúli Guðmundsson for advice on statistical matters and Almar Barja for interesting discussions and transportation.

Furthermore, I would like to thank the staff of Reykjavik University and Iceland School of Energy, Halla Hrund Logadóttir and Verity Louise Sharp, for always supporting the work that I did and providing me with helpful ideas.

Finally, I want to thank my family, my friends here in Iceland and abroad and my girlfriend Rebecca for always supporting me, proof reading the thesis and enduring my rants about geothermal energy and everything else.

Contents

List of Figures

List of Tables

Nomenclature

Abbreviations

AEO	Annual Energy Outlook
BBL	Barrel
BN	Billion
$CAPM$	Capital Asset Pricing Model
CF	Cash Flow
CSV	Comma Separated Values
DCF	Discounted Cash Flow
$E.G.$	Exempli Gratia
EGS	Enhanced Geothermal Systems
EIA	Energy Information Administration
$ETAL$	Et Alii
ETC	Etcetera
FIG	Figure
GHG	Greenhouse Gases
HDR	Hot Dry Rock
$IBID$	Ibidem
$IDDP$	Icelandic Deep Drilling Project
IEA	International Energy Agency
$ISOR$	Íslenskar Orkurannsóknir

LPM	Lumped Parameter Model
M	Million
NPV	Net Present Value
$OECD$	Office for Economic Cooperation and Development
OMR	Oil Market Report
OR	Orkuveita Reykjavíkur
PHD	Doctor of Philosophy
PV	Present Value
SI	Le Système International d'Unités
TDS	Total Dissolved Solids
US	United States
$WACC$	Weighted Average Cost of Capital

Variables

$\bar{R}^2$	Adjusted coefficient of determination	
$\bar{R}^2_N$	Adjusted coefficient of determination, normalized	
$\bar{y}$	Average of the observed values	
β	Correlation degree	
$\dot{m}_i$	Production in period i	[kg/s]
$\dot{m}_{e,i}$	Demand in period i	[kg/s]
η_i	Efficiency factor	
ι	Time period range	
ρ	Density of water	[kg/m^3]
σ_N	Conductivity between tanks N and the external environment of the system	[m $\cdot s$]
$\sigma_{j,k}$	Conductivity between tanks j and k	[m $\cdot s$]
ε	Tank number range	
B_i	Benefit in period i	[$]

C_A	Annuity cost	[$]
C_C	Construction cost	[$]
C_E	Electricity cost	[$]
C_el	Electricity price	[$/kWh]
C_I	Investment cost	[$]
C_M	Maintenance cost	[$]
C_O	Other cost	[$]
C_R	Running cost	[$]
C_W	Achievable price	[$/m^3]
C_{Eq}	Equipment cost	[$]
C_{La}	Land purchase cost	[$]
C_{Li}	Labor cost, investment phase	[$]
C_{Lr}	Labour cost, operational phase	[$]
C_{St}	Storage and transportation cost	[$]
CF_i	Cash flow in period i	[$]
D_C	Debt capital	[$]
D_i	Depreciation in period i	[$]
E_C	Equity capital	[$]
E_i	Earnings in period i	[$]
E_V	Book value	[$]
g	Gravitational acceleration	[m/s^2]
H_0	External drawdown	[m]
h_1^{max}	Maximum drawdown	[m]
$h_{i,j}$	Drawdown for tank j in time period i	[m]
i	Time period	
j	Tank number - flow from	
K	Storage coefficient matrix	[N x N]

k	Tank number - flow to	
K_j	Storage coefficient of tank j	[m $\cdot s^2$]
$LCOE$	Levelized cost of electricity	[$/kwh]
n	Sample size	
p	Number of model parameters	
P_W	Energy needed to pump up water	[W]
P_{pump}	Power rating of a pump	[W]
$p_{s,a}$	Polynomial of degree s-a	
pb	Payback period	[a]
r	Discount rate	
R^2	Coefficient of determination	
r_D	Cost of debt	
r_E	Cost of equity	
r_F	Rate of return, risk free	
r_M	Rate of return, market	
R^2_N	Coefficient of determination, normalized	
S	Conductivity matrix	[N x N]
SS_{res}	Residual sum of squares	
SS_{tot}	Total sum of squares	
t	Tax rate	
X_W	Exergy	[J]
y_i	Observed value in period i	
y_m	Number of pumps	

Chapter 1

Introduction

Energy is needed worldwide, around the clock and every day of the year. The demand for it is increasing rapidly along with a growing world population and industrialization of development countries [13] [14]. During the last years, minimizing mankind's impact on climate change through reducing carbon dioxide emissions by promoting the use of alternative energy sources could be found on political agendas all around the world [15] [16] [17]. Despite these international efforts to promote the use of sustainable energy as a supply source to satisfy the energy demand, burning fossil fuels still acts as the primary energy source of the world in the 21st century [14]. Fossil fuels have to be categorized as non-renewable on a human scale, since its redevelopment takes a lot of time. Additionally combustion of fossil fuels produces a rather high level of greenhouse gas (GHG) emissions. Forecasts for fossil fuel usage are showing steady growth within the next decades because of their comparatively low costs [18].

Geothermal energy, which is exploited by mining thermal energy from the earth's crust, is one of the most promising alternatives to fossil fuels. Pursuing the use of geothermal energy could help satisfy some of the energy demand and reduce greenhouse gas emissions on a global level. Having a long history of human usage, geothermal energy profits from existing, dependable technology and a naturally inherited ubiquity. These factors lead to moderate costs and enormous development potential. Furthermore geothermal energy can be regarded as sustainable on a human time scale as long as the extraction amount of geothermal fluid does not exceed the level of possible recharge in the reservoir. This leads to a reservoir specific sustainable production limit, which is restricted by the geological set up (e.g. rock porosity, aquifer characteristics, etc.)[19] [20] [21].

1.1 Context

Local characteristics and economic circumstances determine the exploitation strategy and influence the optimization of a geothermal project substantially. In the beginning of every project, which deals with the development of geothermal resources, the specific local characteristics of the reservoir are usually not known. Therefore, geological, geophysical and geochemical measurements are used to gain information through surface and subsurface exploration. Additional information is generated as exploratory drilling is pursued [22]. In the operational stage of a project, information about how the reservoir reacts to production is generated continuously. The obtained data can be used as an input for reservoir modeling. The data sets are fitted to a reservoir model, which distillates the taken measurements into valuable information, which then can be used for optimizing exploitation strategies and maintaining production in an economical and sustainable equilibrium [23].

1.2 Research focus

The research for this thesis focuses on the role of uncertainty for the optimization and lumped parameter modeling of low temperature geothermal resources. It is analyzed, what the main sources of uncertainty for economic optimization are. Furthermore, the research focuses on how the decrease of uncertainty, respectively the increase of available operational data changes the outcome of lumped parameter modeling. Throughout the research, a theoretical detailed cash flow model for the Net Present Value (NPV) calculation is introduced. Its maximization is used as the standard objective function for the optimization. The research is tackled with an interdisciplinary approach in order to paint a holistic picture.

1.3 Objective of the thesis

The research pursued for this thesis tries to find answers to the following questions:

- What is the role of uncertainty in lumped parameter modeling for low temperature geothermal resources?
- What are the main sources of uncertainty for the economic optimization of low temperature geothermal resources?

- Can the outcome of lumped parameter modeling act as a stabilizing factor in the economic optimization of low temperature geothermal resources?
- Are there practical time horizons for decreasing uncertainty?

1.4 Structure of the thesis

This thesis starts off with background information on geothermal energy. Geothermal systems are classified and the main characteristics and challenges of natural hydrothermal, geopressured, enhanced and magmatic geothermal systems are analyzed. This is followed by a discussion about the different ways of using geothermal energy. The work presented in this thesis focuses on low temperature geothermal resources with only the liquid phase being present in the system. The chapter continues with background information on reservoir modeling. The basic idea of modeling is described and the four main reservoir model types: conceptual, simple analytic, detailed numerical and lumped parameter models are introduced. The focus is laid upon lumped parameter modeling and its distinct differences to numerical modeling. It is stated that, for the research within this thesis, a lumped parameter modeling approach is used. Furthermore a short introduction to optimization is given.

Chapter three shifts the focus to the methods, which were used to pursue the research of the thesis. The sources of data and theoretical information are discussed and the software used is described. Information about the geothermal fields, from which measured data is taken, is presented and the lumped parameter modeling approach is explained. Its mathematical foundation is presented by using a three tank model example. The theoretical background of testing the fit of the model is discussed. The maximization of the Net Present Value is introduced as the standard objective function. Special focus is given to the construction of a suitable Cash Flow (CF) for low temperature geothermal exploitation. Additionally the influence of the discount rate is analyzed and the concept of the Weighted Average Cost of Capital (WACC) with the usage of the Capital Asset Pricing Model (CAPM) is suggested. Furthermore, the constraints of the optimization problem are introduced and explained. The chapter also gives an overview of how the operational data was gained and processed in order to use it as an input for the lumped parameter modeling.

Chapter four focuses on the results of the lumped parameter modeling and the optimization. The NPV model from chapter three is used and the main sources of uncertainty in the model are identified. For the lumped parameter part, the operational data is checked

for consistency, and an initial model fit for all available data sets was performed in order to identify the model complexity of the best fit. The results of this initial fit are discussed and displayed numerically as well as graphically. The data is split into several parts and fits with decreasing uncertainty are simulated and compared to control model results. Additionally drawdown forecasting is undertaken for two examples.

Chapter five leads to the discussion of the results. It is explained how the optimization is prone to uncertainty and which difficulties may arise when quantification is expected. It is displayed how uncertainty sources, which were identified in chapter four, comprise themselves of a subset of variables, which are prone to indistinct behavior over time. Furthermore, the main outcomes of the analysis of the behavior of the lumped parameter model fit with decreasing uncertainty are discussed. The implications these findings have on economic optimization are pointed out and the question if NPV maximization is most suitable objective function, when minimizing uncertainty is the goal, is discussed. Additionally, chapter five provides a conclusion of the research, identifies areas to improve the work and suggests future research opportunities.

1.5 Graphical overview of the work

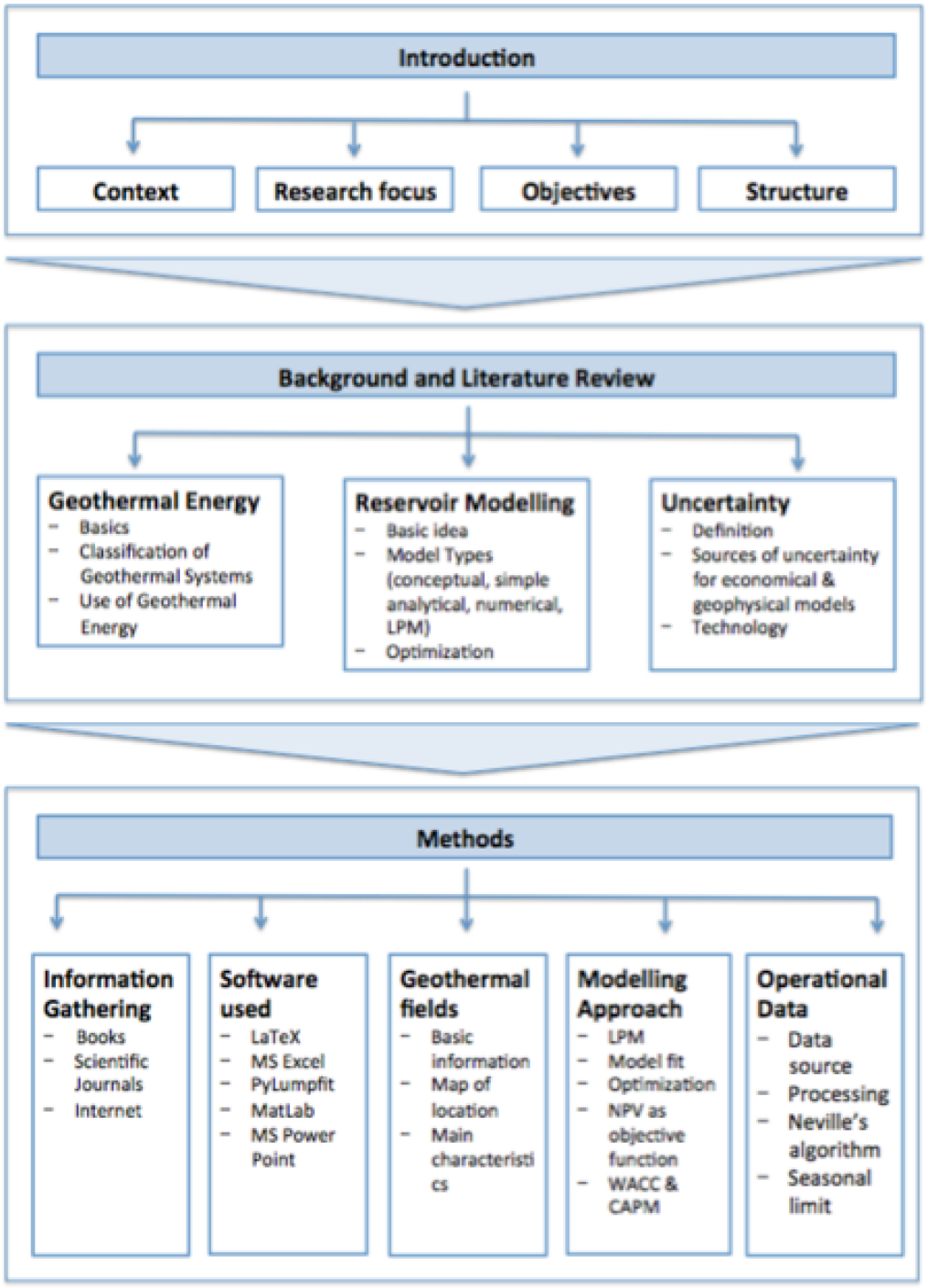

Figure 1: Graphic overview of the thesis' structure - part 1

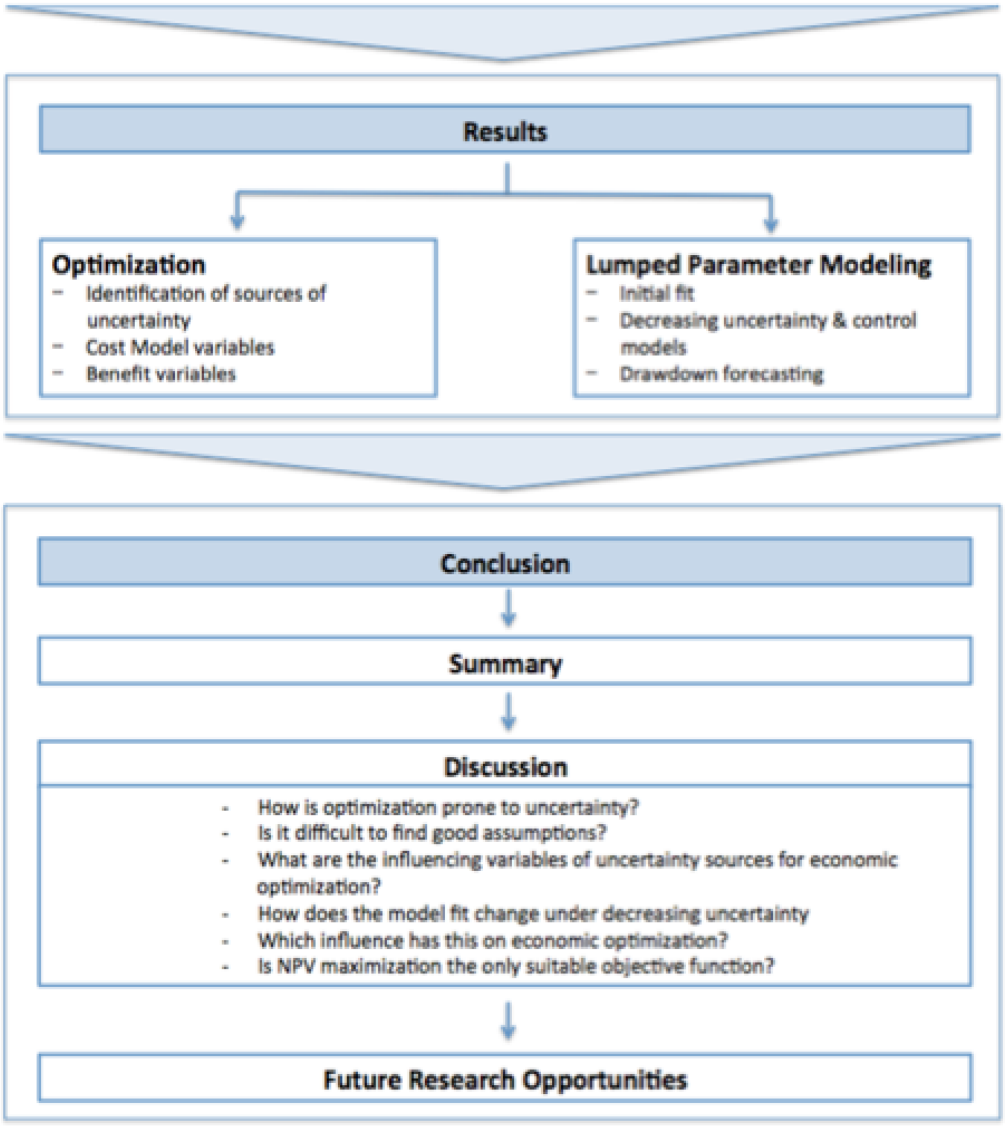

Figure 2: Graphic overview of the thesis' structure - part 2

Chapter 2

Background and literature review

This chapter introduces the main principles and ideas of geothermal energy, reservoir modeling, optimization and uncertainty.

2.1 Geothermal Energy

This section introduces a classification scheme for geothermal systems and gives an overview of different characteristics of high and low temperature geothermal fields. The chapter concludes with different applications of geothermal energy.

2.1.1 Geothermal Energy Basics

Geothermal energy derives from the exploitation of thermal energy which is stored in the earth's crust [24]. Since conductive and convective heat transfer is ubiquitous in the earth's mantle, thermal energy is distributed all around the globe [25]. Nevertheless, the distribution pattern is not uniform and geothermal gradients differ according to geological settings [26]. The geothermal gradient is measured as an increase of temperature per unit of depth. An overview of areas with a steep geothermal gradient, displayed on a world map, can be found in Figure 3 [1]. It is remarkable how closely these areas approximate the plate boundaries.

The heat flow rate through the crust differs between terrestrial and oceanic crust. The terrestrial flow rate averages 0.65 W/m^2 and the flow rate under oceanic crust averages 0.10 W/m^2 [27]. The average temperature gradient ranges from 25 °C to 30 °C per kilometer, which mainly results from the decay of potassium, uranium and thorium isotopes.

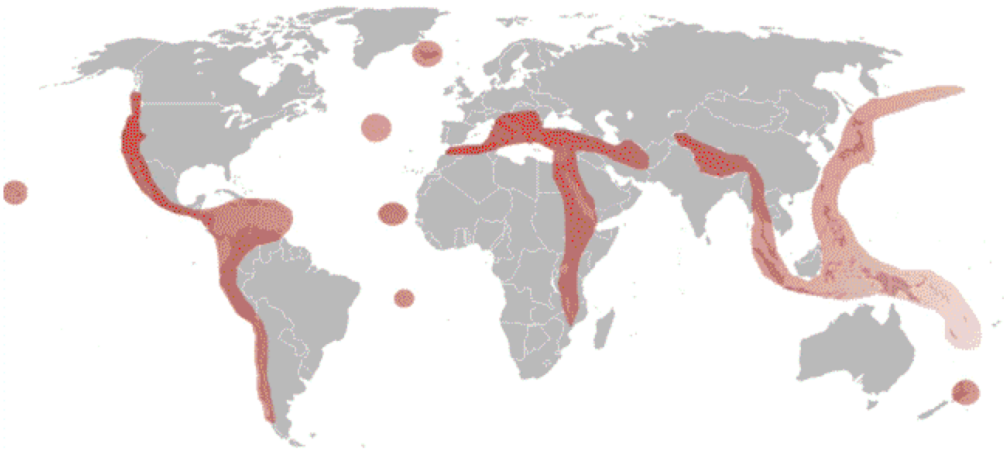

Figure 3: Worldwide distribution of geothermal hot spots. Areas with exceptionally steep temperature gradients are marked in red and follow tectonic plate boundaries closely.[1]

However, the gradient can be influenced locally by intrusions of molten rock (lava)[27]. The gradient is the steepest at tectonic plate boundaries, where temperature usually rises quickly while gaining depth [28]. People who inhabited these areas were historically among the first to explore the use of geothermal energy. Proof of early use of geothermal energy is present in areas where geothermal fluid reaches the surface of the earth and creates hot springs [29] [30] [31]. This manifestation of geothermal energy was used for bathing and washing clothes for more than 7000 years [32], where industrial use of geothermal energy, either directly or for power production, didn't begin until the early twentieth century. One of the first industrially used geothermal fields was Lardarello in Italy, where electricity was produced from geothermal steam in 1902 [33].

Industrial use requires accessibility of the resource. Accessibility is achieved anywhere through drilling production wells to a certain depth until the desired temperature is reached. As drilling for geothermal fluid is one of the major cost factors in geothermal development and is generally more expensive than drilling for oil and gas, economic accessibility is a requirement as well [34] [35] [36]. Development is therefore limited to areas where where drilling costs are manageable due to steep geothermal gradients and a favorable geological setting.

2.1.2 Classification of Geothermal Systems

This chapter focuses on the classification of geothermal systems and gives an overview of the characteristics of four different system types.

2.1.2.1 Natural Hydrothermal Systems

Natural hydrothermal systems produce geothermal fluid without any added technological help. This type of system requires a natural heat source, and rocks with enough permeability to allow a convection dominated system. Usually they are found at tectonic plate boundaries, which not only are generally areas with steep geothermal gradients, but also feature local high permeability formations [27] [37]. Water in hydrothermal systems is often of meteoric origin. Water falls as precipitation and percolates through permeable layers until it reaches the heat source (e.g. magmatic intrusion), heats up and travels upward towards the surface [22]. There are exceptions to this, like the Reykjanes field in Southwestern Iceland, where the geothermal fluid contains seawater as well [38] [39]. In general, natural hydrothermal systems are further divided into two categories: vapor dominated systems and liquid dominated systems [27] [22] .

A vapor dominated system is formed if the pressure of the reservoir allows the geothermal fluid to boil and eventually vaporize. These systems are relatively easy to exploit and occur seldom. If they occur, they might be suitable for base load electricity production. Examples include Geysers in the USA and Larderello in Italy [40] [41] [42] [43].

A liquid dominated system is formed if the pressure of the reservoir does not allow the geothermal fluid to boil. These systems are more common than vapor dominated systems, but they are generally more difficult to exploit, as the concentration of total dissolved solids (TDS) in the fluid might pose as a booster for scaling. Scaling can be a big problem at the transition passage between a two phase flow and a one phase flow. This transition is made when the fluid is flashed [27] [40] [43] [44].

2.1.2.2 Geopressured Systems

Geopressured geothermal systems consist of reservoirs filled with sedimentary rock and water which is excluded from exchange with surrounding rocks [45] [46]. Due to a rapid filling with sediments, the pressure in the reservoir is commonly higher than the hydrostatic pressure [40]. The geothermal fluid might be exposed to a pressure up to 600 bar while reaching a temperature of about 180°C [27]. Generally, geopressured systems are assumed to be saturated with methane and have around 100,000 ppm TDS. Geopressured systems were first found in the Gulf of Mexico region, where research was carried out during the 1970s and 80s. US research found additional reservoirs in Alaska, California and the Rocky Mountain region [47] [48]. These types of systems have been found to be

profitable only under very special circumstances. However, technological development might change this in the future [40] [49] .

2.1.2.3 Hot Dry Rock

Many locations on Earth have a relatively steep geothermal gradient but have insufficient fluid content or permeability. These systems are called hot dry rock (HDR) formations or enhanced geothermal systems (EGS)[27] [22] [40]. Given a sufficient borehole depth, such systems are available everywhere - creating a very large resource base. However, access is restricted heavily by economic factors such as drilling and infrastructure cost [35] [50] [51]. Nevertheless, the ubiquitious nature of EGS is a promising feature. Currently this technology is still in its development phase and attracts investors like the Google Foundation [52]. The technology behind it is hydraulic fracturing, a technology well known from the oil and gas industry, where it is used to access shale oil and gas reservoirs. A partially horizontal injection well is drilled and a mixture of water and chemicals is pumped into the ground with great pressure. Given the high pressure, the rock formations fracture and consequently create a fairly large surface area for heat exchange. As an application for the geothermal industry, the water is heated up in the hot rock formation and is pumped up through a production well where it can be flashed and its vapor phase can be used for electricity production [53]. A good overview of this still new technology can be found in Armstead and Tester's "Heat Mining" [54] and in Brown's "Mining the Earth's Heat" [55].

2.1.2.4 Magma

In contrast to using a cooling magmatic intrusion as the heat source, as natural hydrothermal systems do, magma systems use a heat source which comes from molten rock. Due to the high temperatures of magma, this type of heat source is theoretically desirable for electricity production, however, the high temperature poses as a considerable danger to equipment durability. As research and first experiments in Iceland show, drilling to a depth of 2100m and a temperature of about 900°C is possible but is accompanied by operational difficulties [56]. The Iceland Deep Drilling Project (IDDP) had the goal to drill 4.5km into the supercritical zone that was suspected in the Krafla geothermal area, located under the Krafla volcano in northern Iceland. The drilling process had to be stopped at 2100m when magma with a temperature of 900°C flowed into the borehole [57]. In contrast to the first occurrence of a magmatic disturbance in Hawaii [40], the project team continued to examine the borehole. They were able to achieve production at a well head

temperature of 450°C and a superheated dry steam with a pressure of between 40 and 140 bar. This production test had to be stopped after two years due to mechanical failure. [58]

The project aims to continue testing the possibilities of using magma as a heat source. Currently a discussion is ongoing whether the Reykjanes geothermal zone in southwestern Iceland might pose as a possible location for IDDP 2 [59].

2.1.3 Use of Geothermal Energy

The varying characteristics of different geothermal systems account for different uses. This subchapter focuses on the different applications of geothermal energy. For a general overview of different uses, the work of Lindal in 1973 is suggested [60].

2.1.3.1 Power Production

One of the most common uses of high temperature geothermal resources is electricity production. Commonly one of the following three power plant types is used [27] [22]:

- Dry steam power plants
- Flashing power plants
- Binary power plants

Dry steam power plants are the simplest form of geothermal power plants and can only be operated in vapor dominated high temperature geothermal fields, within which the vapor contains almost no liquid. In ideal conditions the dry steam can be extracted easily and used directly in electricity generation [22] [27].

Flashing power plants are generally quoted as the most common form of geothermal power plants. The geothermal fluid is brought to the surface under pressurized conditions. The pressure is released gradually in a so-called flash tank, which leads to partial vaporization of the fluid. The vapor phase is then used to run a turbine and generate electricity, while the liquid phase might be used for reinjection or further industrial uses. Even after multiple flashing stages, a liquid phase usually still exists [22] [27].

Binary power plants are commonly used when the reservoir temperature is not high enough to produce a vapor phase in the geothermal fluid. The fluid is pumped to the surface and flows through a heat exchanger that transfers the heat to a closed working fluid cycle. The working fluid used has usually a lower boiling point than the geothermal

fluid and is consequently vaporized. The vapor is used to run a turbine. The working fluid then condenses and is used again for the next vaporization cycle [22] [27].

There is an ongoing discussion whether producing electricity from geothermal resources should be considered sustainable or not. The majority of scientists believes, that if the local resource is exploited below or at the recharge rate, sustainability can be achieved [19] [61] [21] [62] [20].

Worldwide, geothermal energy is still a rather small sector of the energy industry, although electricity generation from geothermal power plants is constantly rising. This development is displayed in Figure 4 [2]. Furthermore, new technologies ensure a positive outlook for the geothermal industry internationally.

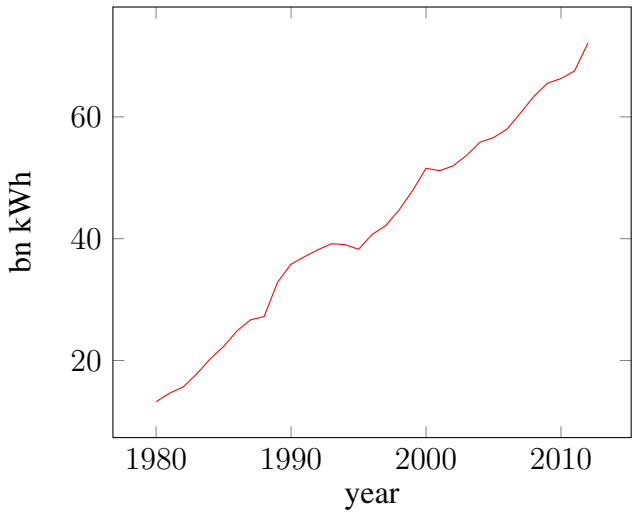

Figure 4: Worldwide annual electricity generation from geothermal resources in billions of kWh from 1980 to 2010 [2].

2.1.3.2 Space Heating

Space heating is one the most popular industrial uses for geothermal fluid that comes from low temperature geothermal resources [60] [27]. As the supply temperature for space heating should roughly be between 60 and 90°C, brine from geothermal power plants might be used as well. This business model is apt to be feasible and is already applied for example in Reykjavik [63], where the space heating system uses brine from the high temperature power plant at Nesjavellir and other different low temperature reservoirs which are situated in the city's vicinity [64] [10]. After the space heating process, the geothermal fluid usually has a temperature of about 25 to 40 °C. If this temperature range is met, the fluid can for example be used further for snow melting in public areas. This again is demonstrated in Reykjavik, Iceland [65].

2.1.3.3 Further Industrial Uses

Geothermal energy has many more applications. Historically it has been used for bathing and washing purposes, but technology development continues to open doors for more diversified applications like [60] [27]:

- Food drying
- Heating for distillation
- Chemical extraction
- Greenhouses
- Aquaculture
- Sterilization
- Refrigeration

Generally, uses beside space heating and electricity generation are of smaller scale, but can be of importance for the local communities surrounding the geothermal resource. In colder climates like Iceland, the application as a heating source for greenhouses is of importance, as it enhances the possibilities of growing fruits and vegetables locally [66]. Additionally, food drying is a co-existing industry which can offer substantial benefits to the business owners. For further information, reading Árni Ragnarsson's article upon this topic is recommended [67]. Overall, geothermal resources offer a variety of industrial uses, which can be exploited in a sustainable and socially acceptable way, while offering profitable business opportunities.

2.2 Reservoir Modeling and Optimization

This chapter gives an overview of reservoir modeling and optimization. Starting with the objectives and basic ideas of modeling, the chapter explores different model types and their fit for geothermal reservoirs. The optimization part of this chapter will give a general overview of the topic.

2.2.1 Modeling

This subchapter focuses on the objectives and basic ideas of modeling, as well as it gives an overview of the main model types.

2.2.1.1 Basic Idea of Modeling

The basic idea of modeling is to create a theoretical framework that simplifies real processes to a point where they can be described mathematically or graphically. Furthermore, a model should hold the all the information necessary to make it possible for the user to understand the modeled process [68]. Stachowiak discusses that a model is characterized by three attributes:

1. Visualization - a model is always a visualization of a real or artificial original.
2. Shortening - generally a model does not capture all attributes of the original. It rather displays information that seems useful to the creator.
3. Pragmatism - the model is not assigned to its original. It functions as a substitute for specific subjects, during a specific time interval, at specific theoretical and practical operations [68].

This characterization is rather philosophical but gives a good overview of the basic idea of modeling. In the following chapter different model types are introduced.

2.2.1.2 Model Types

In the academic field of reservoir engineering, geothermal models are usually divided into four categories. These categories are according to the work of Grant and Bixley [23]:

- Conceptual models

- Simple analytic models
- Lumped parameter models
- Detailed numerical models

In the following, each category is characterized in more detail.

2.2.1.2.1 Conceptual Models Conceptual models are usually the first step in modeling geothermal systems. This is the case, as they are the quickest and easiest to produce since they only give a general graphic overview of the system. A common way to visualize a conceptual model is a cross section of the according field, showing the main geological structures and processes of the reservoir and its surrounding areas. A conceptual model integrates data from different scientific disciplines (e.g. geology, geochemistry, etc.) into one big picture and aims to help interpret the data[69] [70]. Grant and Bixley mention certain qualities a sound conceptual model for geothermal systems should have [23]:

- Simplicity - it should be as simple as possible.
- Completeness - it should provide all the information needed to get a holistic picture.
- Neutrality - all data should be of the same quality.
- Originality - it should use observed rather than interpreted data, since interpreted data might already be minorly altered due to the interpretation process.

A model featuring the above mentioned characteristics can be visualized in many different ways. Figure 5 and Figure 6 show two very different conceptual models of a high and a low temperature geothermal system.

Acting as a descriptive, qualitative model, a conceptual model can ideally give information on the reservoir size, the location of the heat source, the location of upflow and recharge zones, the flow patterns of the fluid and potentially existent subsystems. This list should not be understood as complete and not all information is always available at every stage of the development of a conceptual model. Nevertheless, the model should be designed in a way that helps to concentrate and visualize the available information and act as a supporting tool for all scientists involved in the management of the geothermal system.

2.2.1.2.2 Simple Analytic Models Another approach to modeling is taken by the simple analytic model. It usually simplifies the characteristics of the system to a great extent

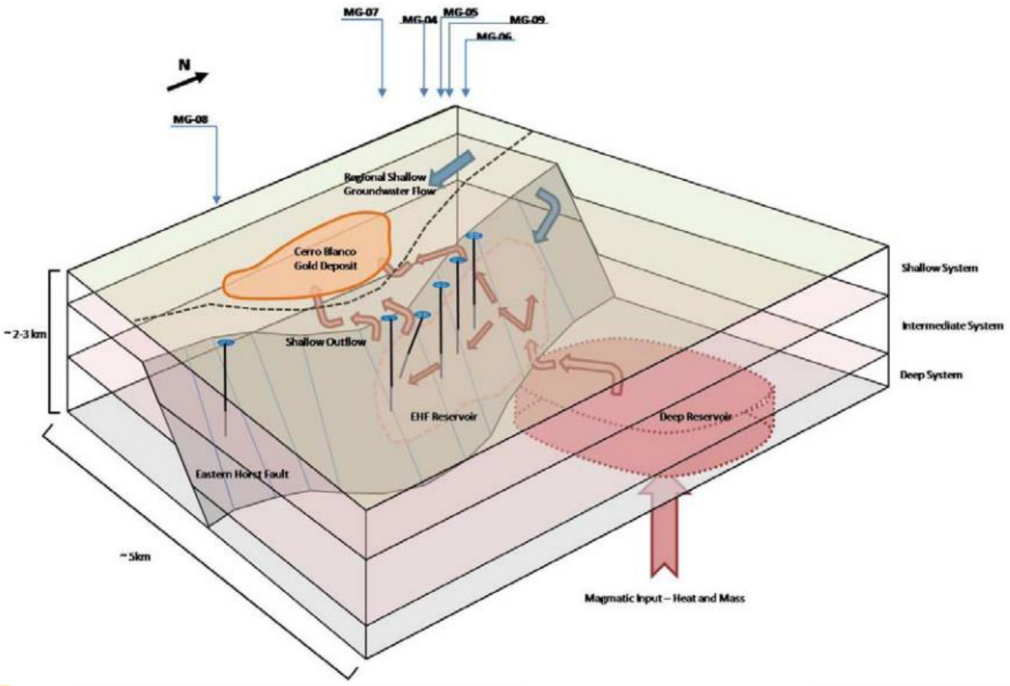

Figure 5: Conceptual model of the Mita geothermal system, Guatemala (McDowell and White, 2011 [3]).

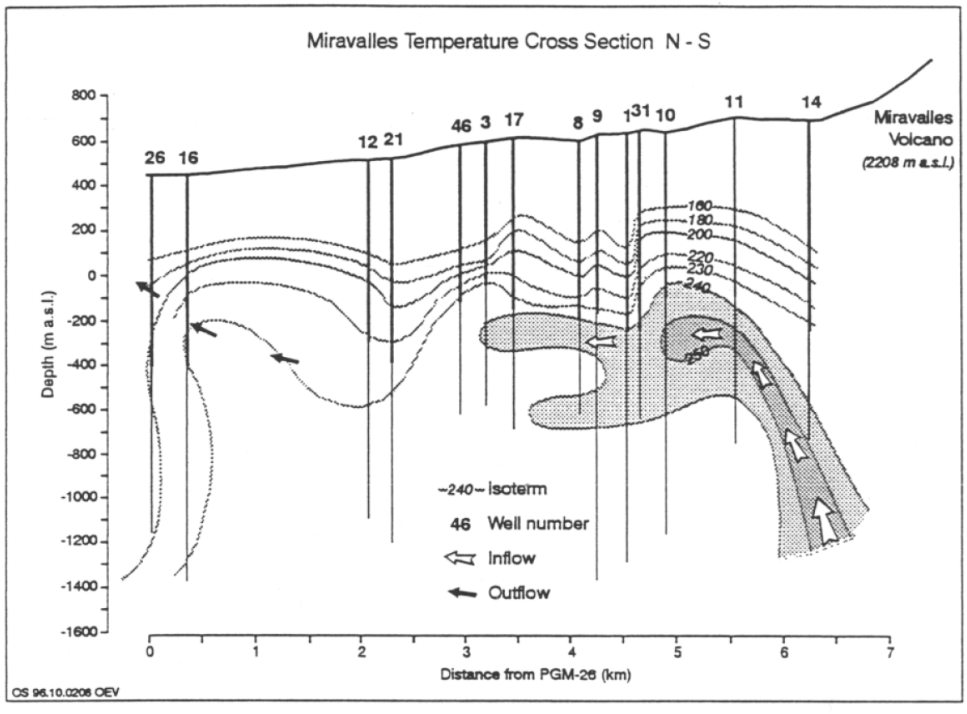

Figure 6: Conceptual model of the Miravalles high-temperature geothermal system in Costa Rica, shown in a N-S cross-section (Vallejos, 1996 [4]).

and assumes constant properties. Simulations of either temperature, pressure or chemistry are the norm. As this approach is manageable in a reasonable amount of time, this modeling approach can be considered to be time and cost saving in comparison to the more complex models.

2.2.1.2.3 Detailed Numerical Models A detailed numerical model divides a geothermal system into multiple interconnected blocks, which then get assigned individual physical properties. Creating and managing these blocks requires a lot of time since the number of blocks easily reaches thousands. The blocks on the surface are connected to a two dimensional grid, which determines the block distribution throughout the system. [71]. Figure 7 shows an example of a surface structure grid and Figure 8 shows the grid in the ground, with varying height of the blocks according to depth.

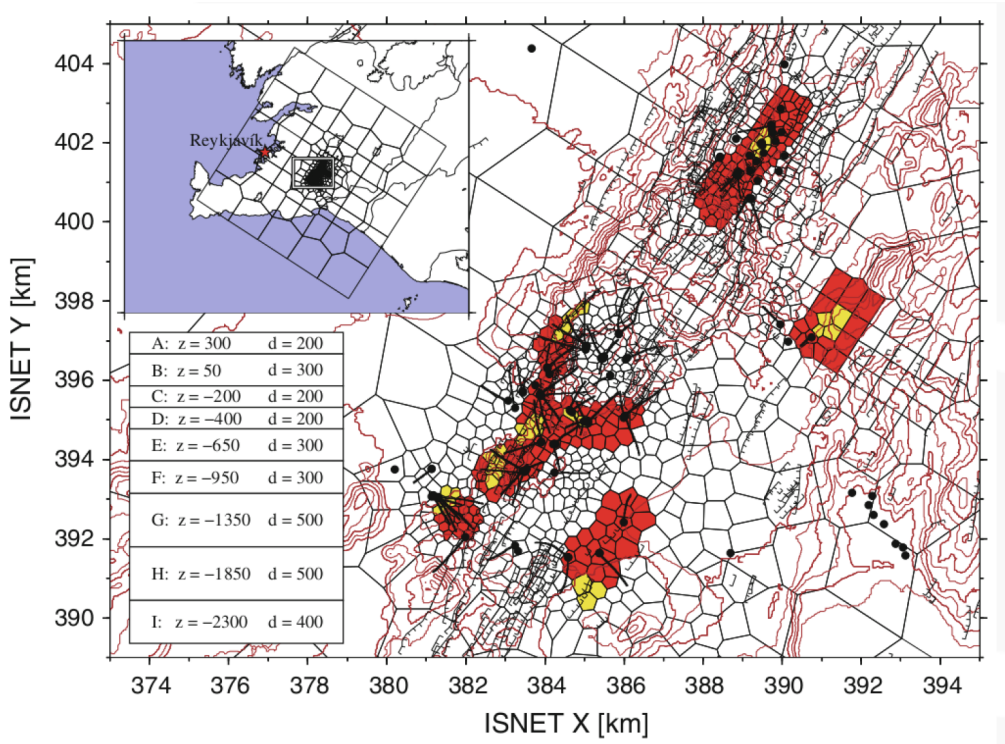

Figure 7: Surface grid of a detailed numerical model, covering the Hengill area in Iceland [5].

Computing requires dedicated programs and a considerable amount of processing power. The outcome is a very detailed model, which allows the user to find answers to complex questions, such as the the ideal location for drilling injection wells. For further reading "Mathematical modeling of fluid flow and heat transfer in geothermal systems" by Karsten Pruess is recommended [72].

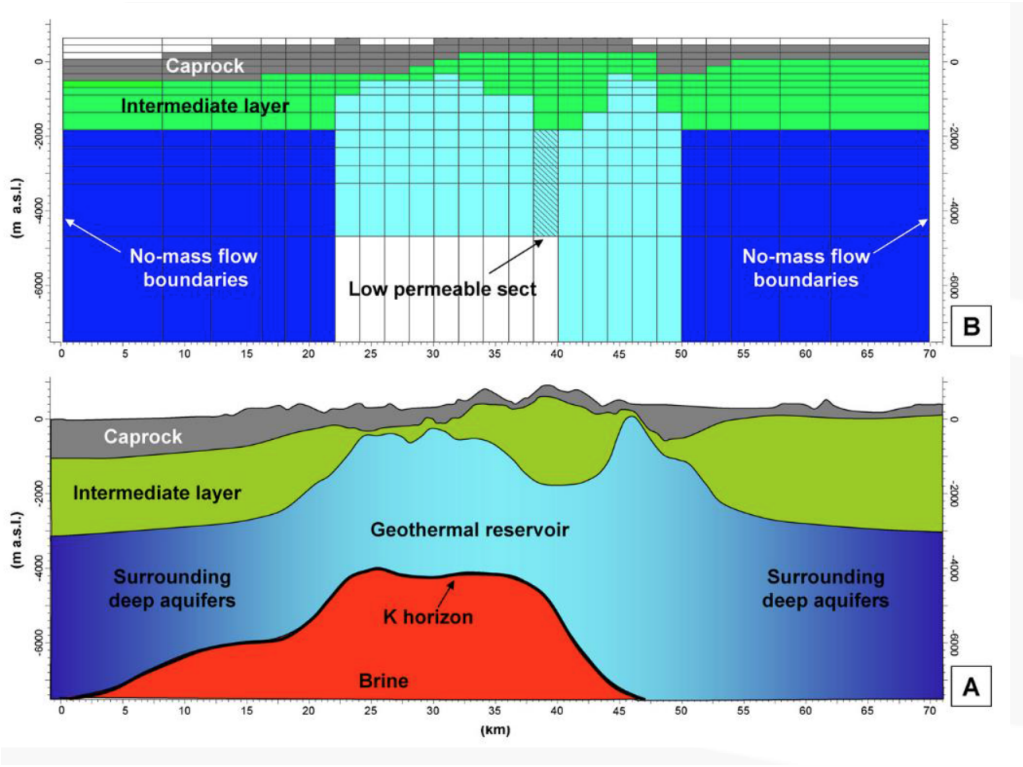

Figure 8: Block distribution within a detailed numerical model with varying depth [6].

2.2.1.2.4 Lumped Parameter Models As described before, detailed numerical modeling of geothermal systems is a time and capital consuming process that sometimes is not necessary for the management of the the according system. Another approach which has proven itself as a time and money saving alternative is the lumped parameter modeling approach. It has been proven to successfully simulate various low temperature systems in Iceland [73] [74] [75]. In general LPMs might be used if

- data availability for the reservoir in question is limited and therefore detailed numerical modeling is futile,
- modeling funds are limited,
- modeling time is limited,
- a pre-stage for numerical modeling is desired,
- validity of other model results need to be checked [76].

Usually lumped parameter models can be considered a simpler version of the more advanced numerical models and are created to match historical production and physical properties. Once the model matches reality sufficiently, the model could be used to forecast future changes of the system.

The theoretical foundation of lumped parameter modeling is the concept of dividing the geothermal system into two or more individual data tanks. This contrasts the hundreds or even thousands of modeling blocks of detailed numerical models. Typically one block represents the production zone of the system, while the other blocks represent recharge zones. The according equations can often be reduced to differential equations. The model can either be regarded as open or closed. It is open when geothermal fluid can be exchanged with the surroundings. This is usually represented by a resistor/connector which is connected to an outside reservoir of infinite dimensions and constant pressure. Within each block the properties are uniform, hence no internal differences exist. Withdrawal from the production tank will influence all connected tanks, according to the set properties for individual tanks and connectors [75]. Although having uniform tanks might seem to be disadvantageous, LPMs actually provide a good result for modeling low temperature geothermal reservoirs. No major drawbacks are seen from the uniformity because low temperature geothermal reservoirs are considered nearly isothermal and have almost uniform fluid chemistry. [77].

Figure 18 displays a visualization of a three tank model, where the first tank represents the central part of the reservoir and the other tanks represent the outer parts of the reservoir. The tanks are connected and geothermal fluid can flow between the tanks.

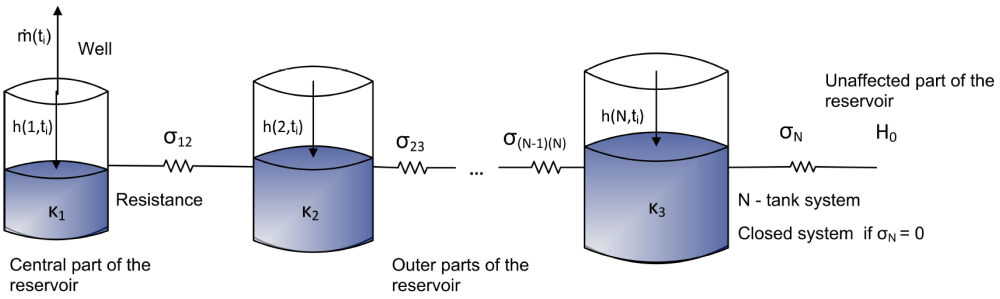

Figure 9: Conceptual graphic of the functionality of a three tank Lumped Parameter Model [7]

More details about the model displayed in Figure 9 are given in chapter 3.4, as it is the model that is used for the practical part of the thesis.

2.2.2 Optimization

Maximizing or minimizing an objective function is the basic goal of an optimization model. For the main part of this thesis, the objective function is the maximization of the net present value (NPV). In this section the NPV concept and the associated calculations are explained.

The NPV method uses a conceptual and complex approach to calculate the value of a certain project. The two basic principles of this discounted cash flow method can be described as follows:

- The time value of money – according to the theory of time preference, it is more desirable to obtain a certain amount of money today than tomorrow.
- The risk premium - the risk of not getting a certain amount of money depreciates its worth [78].

The mathematical foundation of the NPV method is the summed up estimations of future Cash Flows, which are discounted with a distinct discount rate [79]. This is displayed in the following equation.

$$NPV = \sum_{i=1}^{I} \frac{CF_i}{(1+r)^i} \tag{1}$$

where

- CF_i = cash flow in period i
- r = discount rate

The sum of all discounted positive future Cash Flows is the Present Value (PV). By subtracting the investment costs at the point of time $i = 1$, the so called Net Present Value is created [80].

The discount rate should be chosen in a way that reflects the risk of the Cash Flow. Determining the appropriate discount rate r is therefore one of the most important challenges with this method, as it has a high potential to influence the calculated value [81].

The Weighted Average Cost of Capital (WACC) is widely used as a discount factor within the industry. It is a calculative parameter that reflects the average rate that a company has to pay to all its security holders and weighs each category of capital appropriately [82] [83]. The WACC is calculated in the following way :

$$\text{WACC} = \left[\frac{E_C}{E_V} \cdot r_E\right] + \left[\frac{D_C}{E_V} \cdot r_D \cdot (1-T)\right] \tag{2}$$

where

- E_C = equity capital
- r_E= cost of equity
- E_V = book value

- T = tax rate
- D_C = debt capital
- r_D = cost of debt

The costs of debt are determined by averaging the existing debt positions of a company. In contrast to this, the costs of equity are commonly calculated by the Capital Asset Pricing Model (CAPM) [84] [85]. This is a theoretical framework that calculates the costs of equity in accordance to the individual risk of the company. The CAPM calculates the costs of equity in the following way:

$$r_E = r_F + \beta \cdot (r_M - r_F) \tag{3}$$

where

- r_F = risk free interest rate (= return on a 10 year government bond at evaluation date)
- β = correlation degree of the value development of the evaluated share with the value development of the market portfolio (beta = 1). Is available through market information services for listed companies. Otherwise, a peer group analysis is used.
- r_M = stock index yield

Combining all the equations, the NPV of a project can be expressed as:

$$\text{NPV} = \sum_{i=1}^{I} \frac{CF_i}{(1 + [\frac{E_C}{E_V} \cdot (r_F + \beta \cdot (r_M - r_F))] + [\frac{D_C}{E_V} \cdot r_D \cdot (1 - T)])^i} \tag{4}$$

where the variables are the same as those used in prior equations.

2.3 The Role of Uncertainty in Geothermal Optimization

This chapter focuses on uncertainty. It gives a definition of the term and states sources of uncertainty in economical and geophysical models, while giving relevant examples.

2.3.1 Definition and Influence of Uncertainty

Uncertainty is a term widely used in academic life. At the same time, a precise definition is not easy to come by, as every scientific discipline uses the term to mean slightly different things. Its very basic meaning, which is applicable throughout all academic disciplines, is given by the Merriam-Webster dictionary as "lack of sureness about someone or something. Uncertainty may range from a falling short of certainty to an almost complete lack of conviction or knowledge, especially an outcome or result." Uncertainty may influence all stages of a project and is therefore to be categorized as relatively ubiquitous. Two aspects influenced by uncertainty are the outcomes of economical and geophysical models. These models are integral parts of any geothermal project and therefore of utmost importance for its successful execution.

2.3.2 Sources of Uncertainty in Economical Models

One of the main sources of uncertainty in economical models are the variables of net present value (NPV) calculations. The calculation is mainly comprised of two parameters: the cash flow and a discount rate. These two parameters are the two main drivers of uncertainty for the calculation outcome. In reality, the cash flow is an aggregation of different financially positive and negative effects. Each of the components has an influence on the outcome and is therefore a contributor to uncertainty. This is explained and analyzed in more detail in chapters three, four and five. The discount rate on the other hand is often only a single parameter and has the power to influence the results of the calculation dramatically. Figure 10 shows the difference in outcome for a constant cash flow of $100,000 over 20 time periods while being discounted at 5% and 15%.

Additional examples for uncertainty in economic models are easily found through the study of published forecasts. A prime example for the extent of unforeseen development are oil price forecasts. Oil being one of the most discussed commodities on this planet, many people have an interest in forecasting the price of a barrel (bbl) of oil correctly.

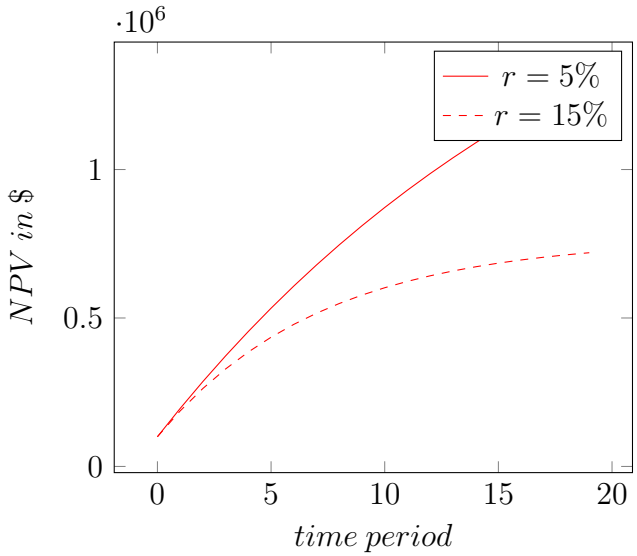

Figure 10: Net Present Value development over 20 time periods with varying discount rates. A discount rate of 5% is shown by the red line. A discount rate of 15% is shown by the dashed red line.

The U.S. Energy Information Administration (EIA) publishes an Annual Energy Outlook (AEO) which includes an oil price forecast per barrel [86]. Figure 11 contrasts the forecasted prices (red) from selected AEO issues with the actual price (blue) in 2006 U.S. Dollars [8].

It is clearly visible that the forecasted price hardly matches the actual development. This example displays the high level of uncertainty and the difficulties for experts to incorporate it into their forecast accordingly. For details about the difficulties and uncertainties in oil price forecasting, the work of James D. Hamilton is recommended [87] [88] [89].

Another important forecast for economists is the forecast of currency exchange rates. Being discussed in literature for decades[90] [91] [92] [93], these forecasts have great influence on international projects and companies that conduct business in different regions of the world. As currency rates are very sensitive to economic and political influences, forecasting becomes delicate [94] [95].

2.3.3 Sources of Uncertainty in Geophysical Models

In addition to its influence on economical models, uncertainty can also influence the outcome of geophysical models. Being an integral part of any geothermal operation, geo-

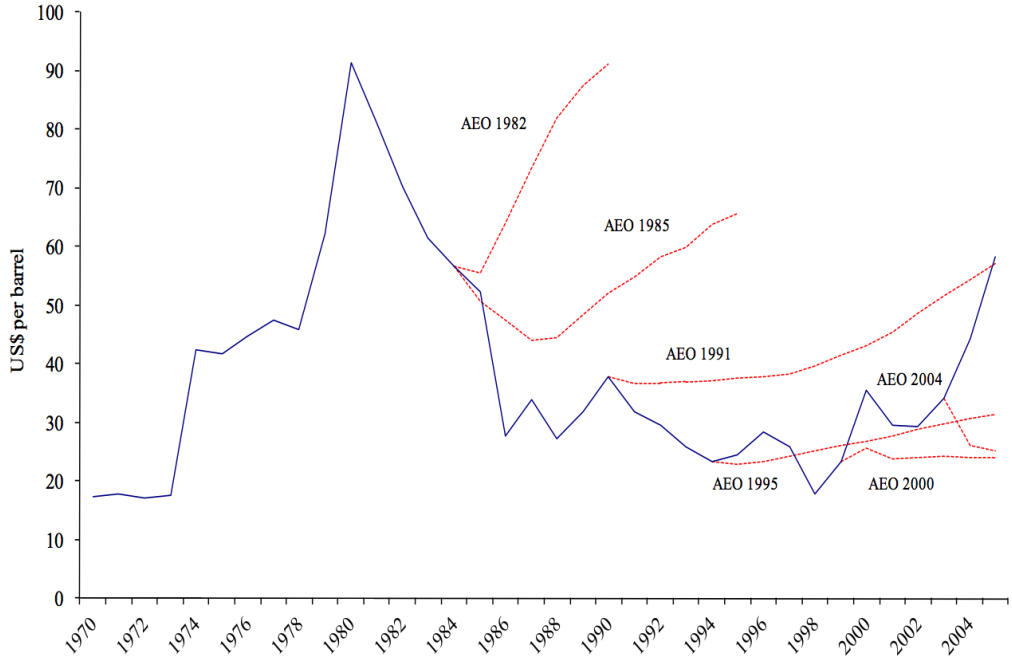

Figure 11: Comparison of the Annual Energy Outlook oil price forecast of 1982, 1985, 1991, 1995, 2000 and 2004 with the observed oil price development[8]. The AEO forecasts are marked by the dashed red lines, whereas the observed price is shown by the blue line.

physical models build the foundation for exploratory and economic success. This chapter explores various examples of sources of uncertainty in geophysical models.

2.3.3.1 Lack of Data

One of the main contributors to uncertainty in geophysical models for the development of geothermal resources is often the lack of data. When the first estimates of specific resource properties are made, information about the system is usually scarce. This scarcity stems from insufficient exploration. Exploratory budgets make up a large percentage of the cost of geothermal exploitation [96] [97]. Financing this initial project phase can be problematic as investors hesitate regularly when confronted with the overall high exploratory success risks [98] [99]. The information that is available ususally stems from geological surveying and geophysical and -chemical surface measurements. Detailed information from subsurface exploration analyses is often not available until later project phases as funding cannot be guaranteed [100]. The lack of data encourages uncertainty in the outcome of reservoir models.

2.3.3.2 Evolving Systems

Geothermal resources are living and evolving systems in many ways. The aforementioned geological, -physical, and -chemical analyses give a good picture during the initial developing and exploitation stages of the project. However, many of the characteristic features of the resource may react to the actual production from the reservoir. For example, resistivity measurements of given rock formations within the reservoir often react to physical changes (e.g. exploitation, earthquakes, etc) of the reservoir [101] [102] [103]. This means that the resistivity measurements used for the inital modeling can become inaccurate and therefore need to be updated to ensure data integrity. There is evidence that not only resistivity, but also permeability of rocks and the chemical composition of the geothermal fluid may change with time and consequently might vary during the production period.[104] [105]. The alterations of physical and chemical properties lead inevitably to uncertainty. Additionally, the water level is highly responsive to production. In order to optimize the management of the geothermal resource, detailed information on the dependency of the water table to the production rate need to be provided.

2.3.3.3 Model Simplicity

Another source of uncertainty is determined by the nature of the model itself. As discussed in chapter 2.2.1.1, one of the main ideas of modeling is simplification or as Stachowiak calls it - shortening of reality [68]. A model does not contain all information available. Only information which is considered as important by the model creator is included in the final product. Consequently, certain parts of reality are not incorporated. This is a cause of uncertainty, as this unincorporated information could lead to slightly different outcomes of the model.

2.3.4 Technological Development

Technological development might be a potential source of uncertainty, since it is hard to include technology's rate of development into a forecast model. Once again, an applicable example can be found in the oil and gas industry, where technological development made the exploitation of shale oil and gas possible. This changed the level of proved resources dramatically, as can be seen in the published EIA data [9], which is compiled graphically in Figures 12 and 13. The overall level and its ongoing development differed tremendously from the development in the past and defied predictability as technological

development and economic factors made shale oil and gas an economically exploitable option.

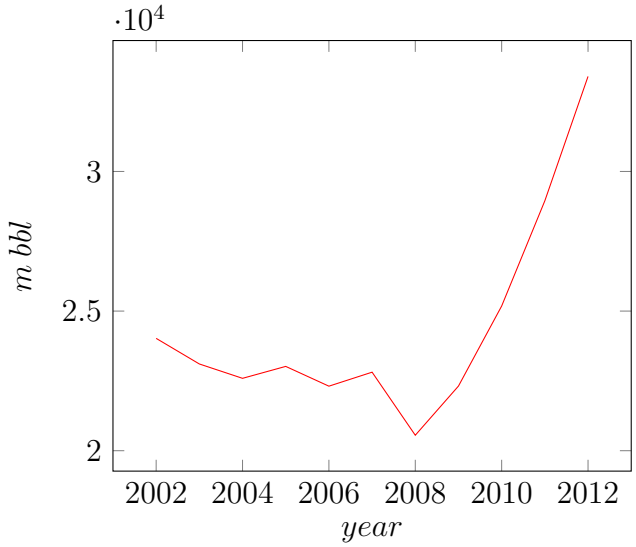

Figure 12: Proved crude oil reserves in the United States in million bbl from 2001 to 2012 [9]

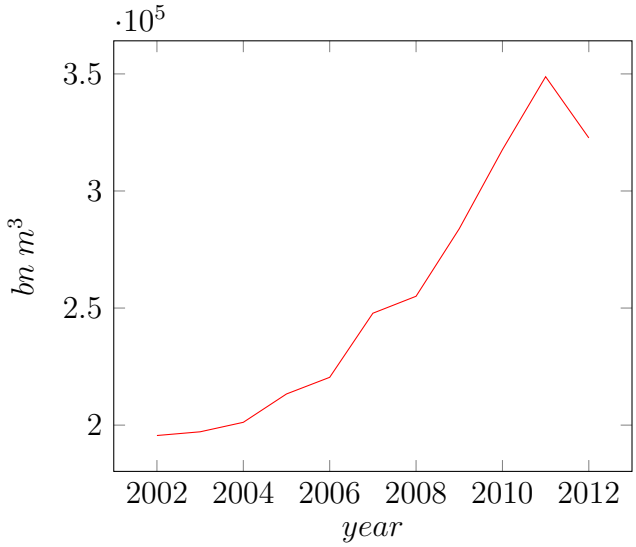

Figure 13: Proved wet natural gas reserves in the United States in million bbl from 2001 to 2012 [9]

Chapter 3

Methods

This chapter provides the reader with all information that is needed to understand the practical work that was pursued to answer the question of how uncertainty influences the fit of lumped parameter models and which parameters influence the economic optimization when NPV maximization is the set goal. Information about the techniques and methods which were used, is displayed. The chapter starts with general information of how the literature review was performed. This is followed by a description of the software that was used and information on the geothermal fields from which the operational data was taken. Additionally, the lumped parameter model is discussed and the optimization problem is laid out. The chapter concludes with information about the operational data and how it was processed.

3.1 Gathering of Information

The research for this paper was mainly pursued by collecting data from textbooks, scientific peer reviewed journals and official organizations like the International Energy Agency, the U.S. Energy Information Administration, OECD, et cetera. The author collected the information and reviewed them critically. By comparing quantitative information from different issuers about the same subject, quantitative differences prevail. Reasons for these differences are subject to further investigation. Nevertheless, the qualitative statements do not differ within the consulted resources.

3.2 Software

For the lumped parameter modeling PyLumpfit was used. It was programmed by and obtained from Iceland Geosurvey (ISOR). PyLumpfit represents the latest version of the widely used software Lumpfit which was written in Fortran77. The software was used with full permission. PyLumpfit fits the observed and measured operational data to a model by using a non-linear iterative least-squares method. Processing of the operational raw data was done by using the algorithms provided by Tiffany Roche. The algorithms were run in MatLab. General calculations for processing data were mainly performed by using Microsoft Excel. Graphs included in this thesis were created by using Microsoft Excel and LaTeX. Overview flow charts were created in Microsoft PowerPoint.

3.3 Geothermal Fields

The geothermal fields which are used as data providers for the research of this thesis are Laugarnes, Ellidaar, Reykir and Reykjahlid. All fields are used for district heating purposes in Reykjavik, although only Laugarnes and Ellidaar lie within the city limits. A map of the location of the fields was published by Gunnlaugsson [10] and is displayed as Figure 14. There is disagreement among the literature if Reykir and Reykjahlid should be considered one field since they are geographically close and geologically related [10] [106] [107]. In line with Sigurdardottir [7], Reykir and Reykjhlid are regarded as one field for this research but are also analyzed separately. Table 1 gives an overview of the main characteristics of the fields. The data was provided from Orkuveita Reykjavikur.

Table 1: Selected data for Ellidaar, Laugarnes, Reykir and Reykjahlid

Field	Avg. Temperature (°C)	Number of production well in 2010	Average production in 2010 (kg/s)	Production for Reykjavik (%)
Ellidaar	87	8	61	3
Laugarnes	128	10	129	7
Reykir	82	22	344	18
Reykjahlid	93	12	410	21

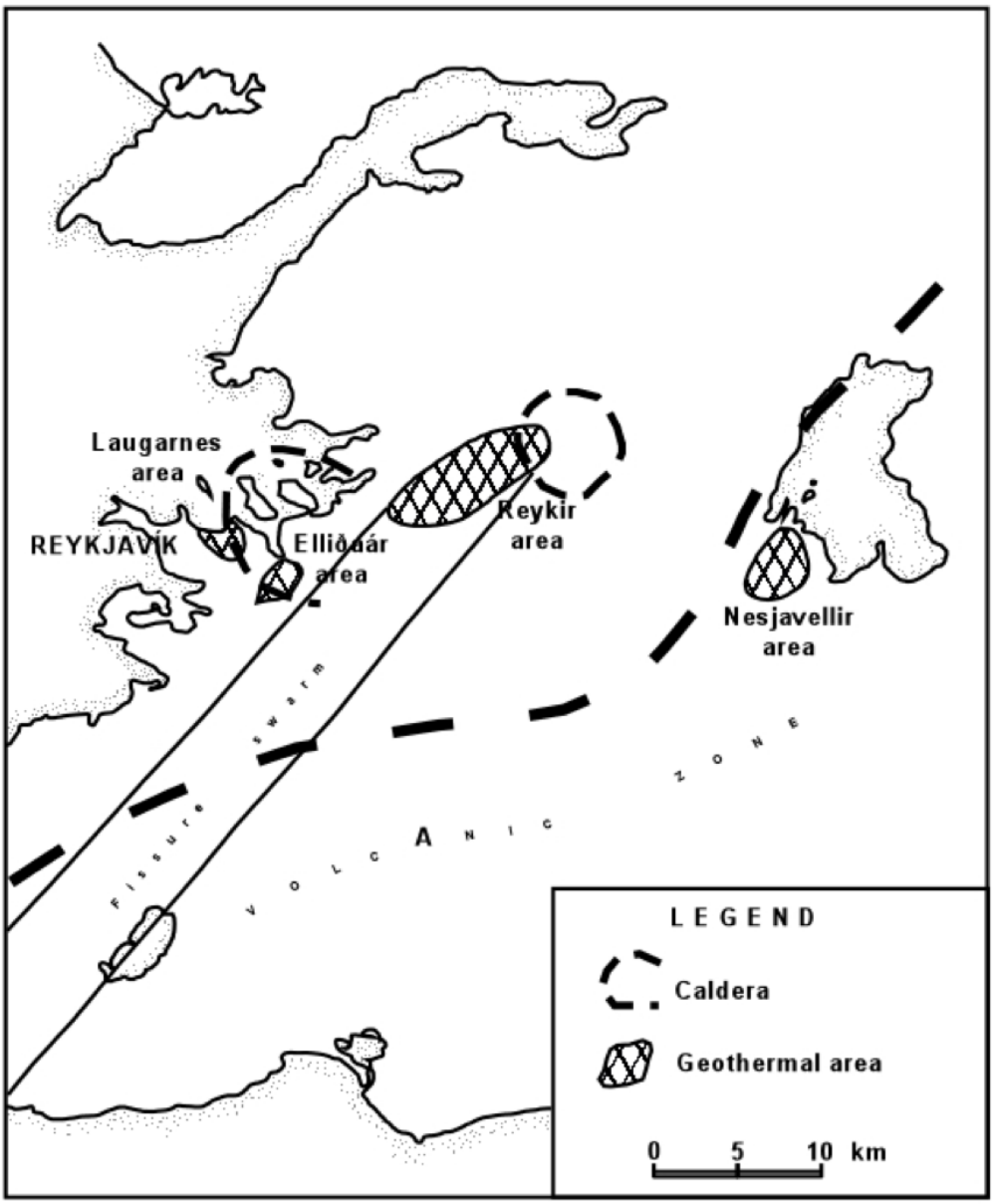

Figure 14: Location of low and high temperature geothermal fields used for district heating in Reykajvik [10]

3.3.1 Laugarnes

The field Laugarnes, which is located in downtown Reykjavik, represents the field with the highest average temperature, whereat the average production rate is to be found in the range of roughly 120kg/s. The water table data which is used within this thesis comes from reference wells RV-34 and RV-7. It covers the time span from January 1967 to November 2010 in the case of RV-7 and from February 1985 to November 2010 in the case of RV-34. Both data sets have a monthly resolution. For Laugarnes, the production

data was taken from wells RV-5, RV-9, RV-10, RV-11, RV-15, RV-17, RV-19, RV-20, RV-35 and RV-38.

The location of the boreholes, as well as the reference well, can be found in figure 15.

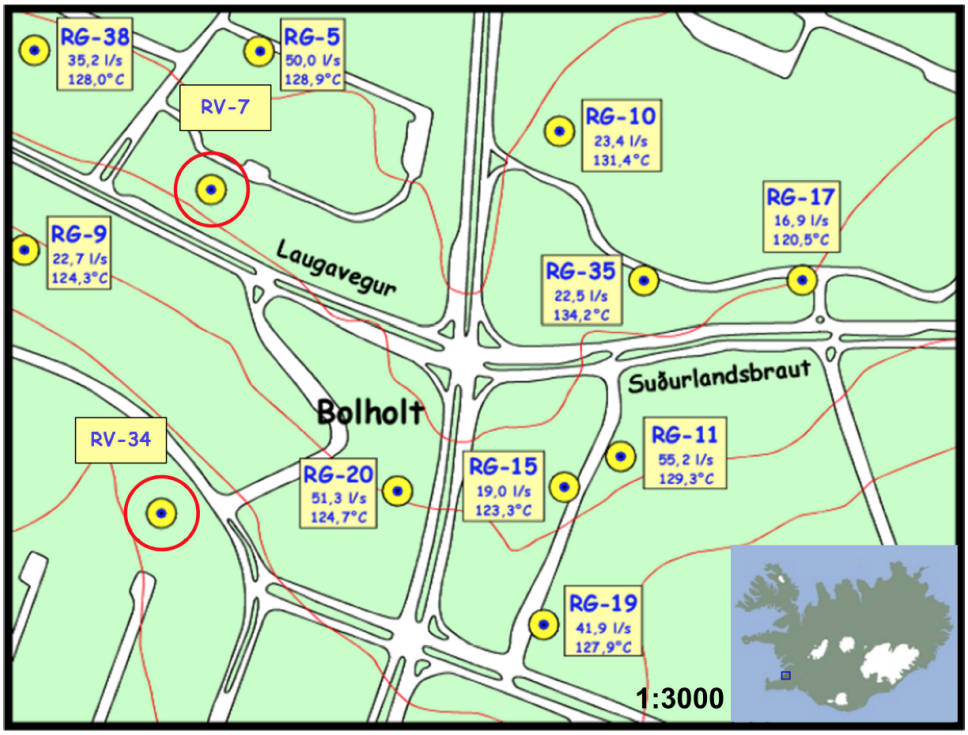

Figure 15: Map of the well location at the geothermal field Laugarnes. Reference wells are marked with a red circle [11].

3.3.2 Ellidaar

Out of the three fields, Ellidaar has the lowest production rate and the lowest average temperature. The water table is taken from reference well RV-27 and covers the time span from October 1969 to November 2010 with monthly resolution. For Ellidaar, the production data was taken from wells RV-23, RV-26, RV-29, RV-30, RV-31, RV-36, RV-37 and RV-39. The location of the boreholes, as well as the reference well, can be found in figure 16.

3.3.3 Reykir and Reykjahlid

Reykir lies not within Reykjavik's city limits but 20 km northeast in the municipality of Mosfellsbaer. The water table data used for this thesis was measured at reference wells

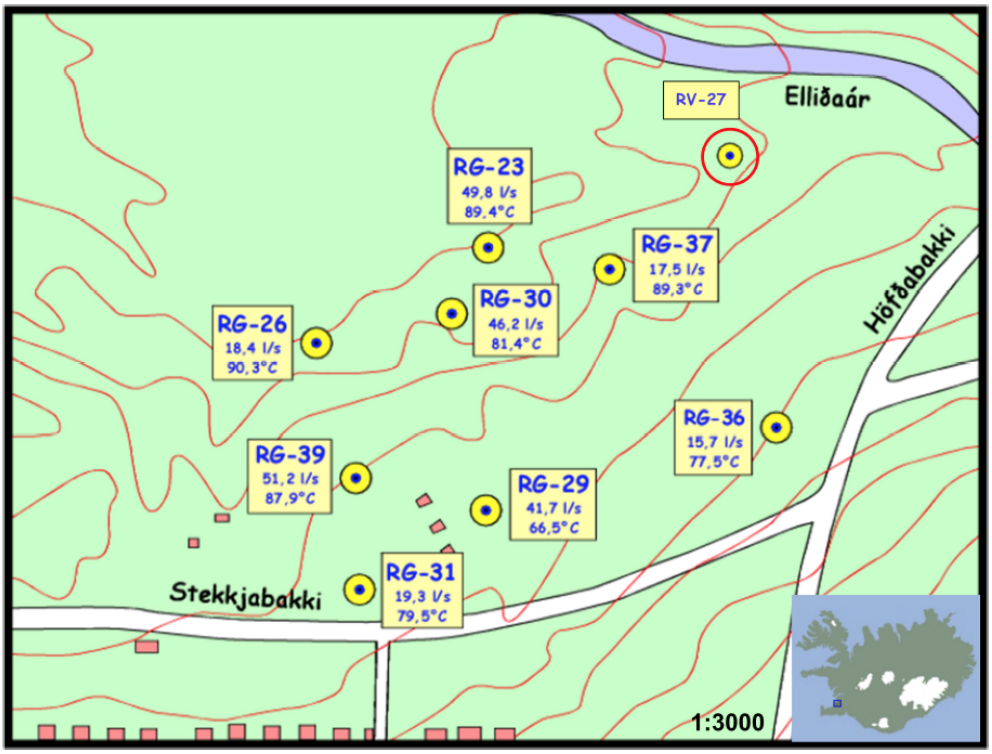

Figure 16: Map of the well locations at the geothermal field Ellidaar. Reference wells are marked with a red circle. [11]

MG-1 and SR-32. For borehole MG-1, data collection started in May 1976, whereat collection of data at SR-32 started in March of 1980. Both data sets are available with monthly resolution.

Being Reykir's neighboring field, Reykjahlid's data resembles the geographical and geological characteristics. The water table data that is used within this thesis was collected at reference well MG-28 and covers the time span from March 1985 to November 2010 with monthly resolution.

For Reykir the production data was taken from wells MG-3, MG-4, MG-6, MG-8, MG-9, MG-11, MG-12, MG-13, MG-14, MG-15, MG-16, MG-17, MG-18, MG-20, MG-22, MG-23, MG-24, MG-25, MG-26, MG-27, MG-30 and MG-31.

For Reykjahlid the production data was taken from wells MG-5, MG-19, MG-21, MG-29, MG-32, MG-33, MG-34, MG-35, MG-36, MG-37, MG-38 and MG-39..

The location of the boreholes, as well as the reference well, can be found in figure 17.

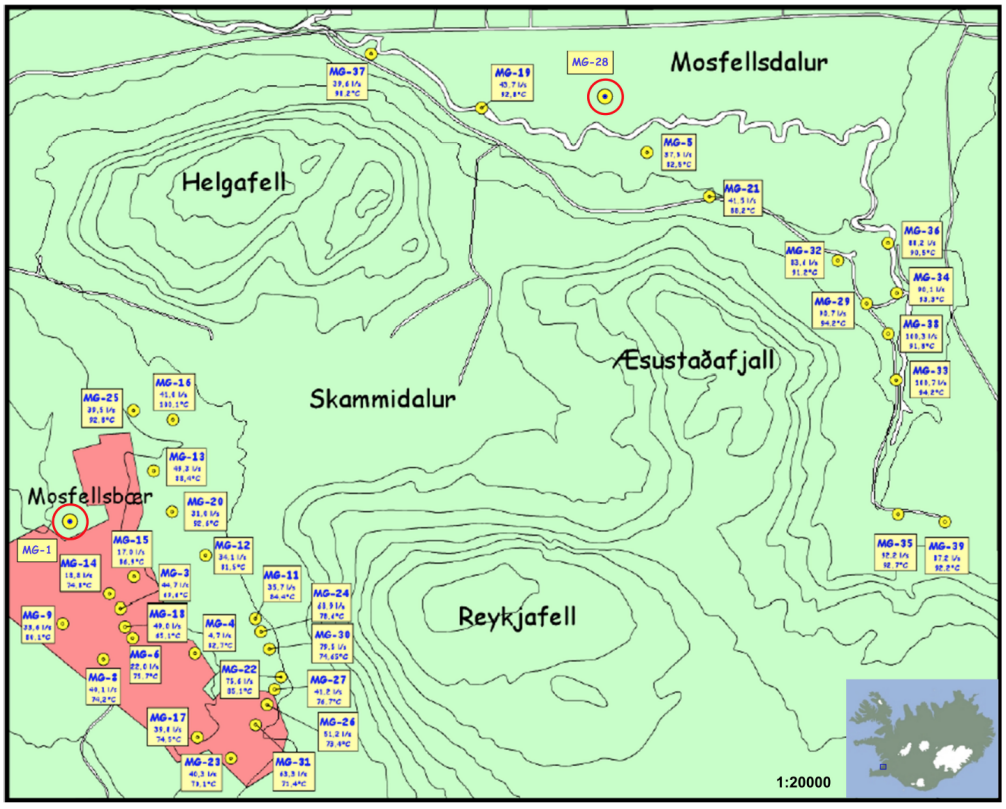

Figure 17: Map of the well locations at the geothermal fields Reykir and Reykjahlid. Reference wells are marked with a red circle. [11]

3.4 Modeling Approach

The modeling approach for this research is based on the dissertation of Silja Rán Sigurdardóttir [7]. The following chapter gives an overview of how the models are constructed.

3.4.1 Lumped Parameter Model

The model represents a liquid phase hydrothermal reservoir. The modeling is carried out with a lumped parameter approach. As described in chapter 2.2.1.2.4, a three tank model is used for explanation. This is in accordance to Sarak [77] and Axelsson [75] who also preferred a three tank approach.

The tanks are interconnected via flow resistors that simulate the local permeability and therefore geothermal fluid is able to flow through them. The first tank represents the reservoir center, which can be regarded as the production part of the reservoir. Tank two and three pose as the outer parts of the reservoir.

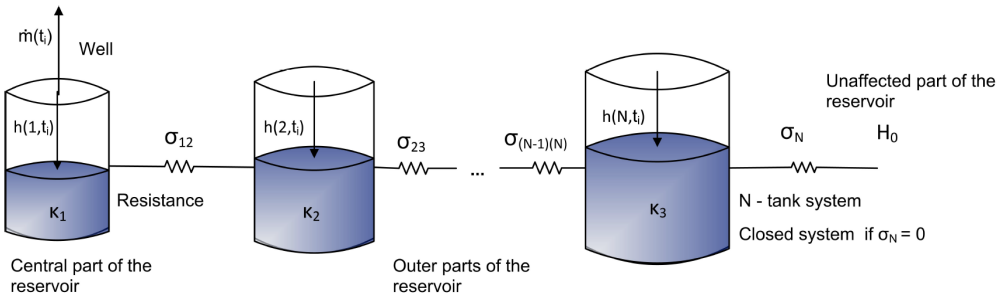

Figure 18: Conceptual graphic of the functionality of a three tank Lumped Parameter Model [7].

The state of the tanks is characterized by a drawdown h_j where j is the tank number $\forall j \in \varepsilon := \{1...N\}$. In the model used for explanatory purposes N = 3.

The nomenclature for the flow resistors/connectors between the tanks is as follows. Connector $\sigma_{j,k}$ runs between tank j and k. Allowing fluid to travel into and out of the system, the last connector σ_N connects tank N to a constant pressure source, which can be regarded as the recharge supplier. If $\sigma_N = 0$ the system is to be characterized as closed,if $\sigma_N \neq 0$ the system is open.

The production of the system is displayed as $\dot{m}_i \quad \forall \dot{m} \in \mathbb{R}_+, \forall i \in \iota := \{1...I\}$.

Trans-tank flow is determined by differences in drawdown in the different tanks and is defined as:

$$K_1 \frac{dh_1}{dt} = \sigma_{12}(h_2 - h_1) + \frac{\dot{m}}{\rho g} \tag{5}$$

$$K_2 \frac{dh_2}{dt} = \sigma_{12}(h_1 - h_2) + \sigma_{23}(h_3 - h_2) \tag{6}$$

$$K_3 \frac{dh_3}{dt} = \sigma_{23}(h_2 - h_3) + \sigma_3(h_0 - h_3) \tag{7}$$

where K represents a storage coffecient. For a system with N tanks it can be defined as:

$$\mathbf{K}\frac{\partial}{\partial t}\mathbf{h} = \mathbf{S} \cdot \mathbf{h} + \mathbf{u} \tag{8}$$

whereas

$$\mathbf{K}=\begin{bmatrix} K_1 & 0 & \dots & 0 \\ 0 & \ddots & \ddots & \vdots \\ \vdots & \ddots & K_{N-1} & 0 \\ 0 & \dots & 0 & K_N \end{bmatrix}$$

$$\mathbf{h}=\begin{bmatrix} h_1 \\ \vdots \\ h_N \end{bmatrix}$$

$$\mathbf{u}=\begin{bmatrix} \frac{\dot{m}}{pg} \\ 0 \\ \vdots \\ 0 \\ \sigma_N H_0 \end{bmatrix}$$

$$\mathbf{S}=\begin{bmatrix} -\sigma_{12} & \sigma_{12} & 0 & \dots & 0 \\ \sigma_{12} & -(\sigma_{12}+\sigma_{23}) & \sigma_{23} & \ddots & \vdots \\ 0 & \ddots & \ddots & \ddots & 0 \\ \vdots & \ddots & \ddots & \ddots & \sigma_{(N-1)N} \\ 0 & \dots & 0 & \sigma_{(N-1)N} & -(\sigma_{(N-1)N}+\sigma_N) \end{bmatrix}$$

3.4.2 Testing The Model Fit

As described in chapter 3.2, the software that is used for fitting the data to a lumped parameter model is PyLumpfit. The main output which PyLumpfit gives to the user is the so-called coefficient of determination, or R^2. This coefficient, ranging from 0 to 1, gives an indication of how well the model fits the data. Even though the scientific community is in discussion about it, a value closer to 1 is generally preferred. R^2 is usually calculated as

$$R^2 = 1 - \frac{SS_{\text{res}}}{SS_{\text{tot}}} \tag{9}$$

where y_i is the observed value at time i, $\bar{y}$ is the average of the observed values and f_i is the modeled value at time i [108].

$$SS_{res} = \sum_i (y_i - f_i)^2 \tag{10}$$

is the residual sum of squares.

$$SS_{tot} = \sum_i (y_i - \bar{y})^2 \tag{11}$$

is the total sum of squares.

$$\bar{y} = \frac{1}{I} \sum_{i=1}^{I} y_i \tag{12}$$

is the mean of the observed data.

The coefficient of determination is partly used within this thesis as it is the Icelandic industry standard, to measure a model fit for geothermal lumped parameter modeling. Theoretically a more appropriate measurement would be the $\bar{R}^2$, which corrects the value for unwanted effects related to a changing amount of observed data points and is calculated as:

$$\bar{R}^2 = 1 - \frac{(n-1) \cdot (1 - R^2)}{n - p - 1} \tag{13}$$

where n is the sample size and p is the number of model parameters [109]. The results chapter includes results as R^2 and $\bar{R}^2$.

3.4.3 Optimization

For the optimization part, the NPV concept that was introduced in chapter two is used as the objective function. This chapter describes some changes and specifications to the concept.

3.4.3.1 Adjustments of the NPV Model

The NPV WACC model described before, poses as the theoretical framework for measuring the value of a project. In order to use the model properly for low temperature geothermal projects, some amendments and clarifications have to be made.

In order to calculate the cash flow which is generated from the project, the earnings before interest, depreciation and amortization (EBITDA or E_i) have to be calculated. Therefore costs and benefits need to be defined clearly.

The costs include the investment and the running cost. The investment cost can be calculated as

$$C_I = C_{Eq} + C_{Li} + C_C + C_O + C_{La}, \quad C_I \in \mathbb{R} \tag{14}$$

where

- C_I = investment cost
- C_{Eq} = equipment cost (for example pumps)
- C_{Li} = labor cost during the investment phase
- C_C = construction cost
- C_O = other costs
- C_{La} = cost for land purchase

The running costs can be defined as

$$C_{Ri} = C_{Mi} + C_{Ei} + C_{Lri} + C_{Sti} + C_{Ai}, \quad C_{Ri} \in \mathbb{R} \quad \forall i \in \iota \tag{15}$$

where

- C_R = running costs
- C_M = maintenance cost
- C_E = electricity cost
- C_{Lr} = labor cost during the operation period
- C_{St} = storage and transportation cost
- C_A = annuity cost

The electricity cost can be calculated as

$$C_E = \sum_{i=1}^{I} \frac{C_{el} \cdot g \cdot \dot{m}_i \cdot h_{1,i}}{\eta_i} \tag{16}$$

where

- C_{el} = electricity price
- g = gravitational acceleration
- η_i = efficiency factor

The annuity cost are to be considered if the investment is partly financed by loans. The annuities are considered fixed and can be calculated as

$$C_A = C_I \cdot (1 - \frac{E_C}{E_V}) \cdot \frac{(1+r)^p \cdot r}{(1+r)^{pb} - 1} \tag{17}$$

where

- C_i = investment cost
- E_C = equity capital share
- r = interest rate
- pb = payback period

All components of the running and the investment cost can occur in reality but don't need to occur.

The benefits are calculated as

$$B_i = \frac{\dot{m}_i \cdot C_W \cdot \Delta t}{\rho}, \quad C_B \in \mathbb{R} \quad \forall i \in \iota \tag{18}$$

where C_W is a fixed achievable price per cubic meter of hot water and ρ represents the density of water.

Therefore the earnings are calculated as

$$E_i = B_i - C_I - C_{Ri}, \quad E_i \in \mathbb{R} \quad \forall i \in \iota \tag{19}$$

The cash flow has to be corrected by the tax rate and depreciation. Hence the cash flow is calculated as

$$CF_i = (E_i - D_i) \cdot (1 - T_i), \quad CF_i \in \mathbb{R} \quad \forall i \in \iota \tag{20}$$

where

- D_i = depreciation in period i
- t_i = corporate tax rate in period i

3.4.3.2 Constraint 1

Drawdown is a function of demand. A discrete integration through the modified Euler method [110] [7] gives:

$$h_{i+1} = (K - \frac{\Delta t}{2}S)^{-1}((K + \frac{\Delta t}{2}S)h_i + \frac{\Delta t}{2}(u_{i+1} + u_i)), \quad \forall i \in \iota \tag{21}$$

where

$$\mathrm{u} = \begin{bmatrix} \frac{\dot{m}}{pg} \\ 0 \\ \vdots \\ 0 \\ \sigma_N H_0 \end{bmatrix}, \quad \forall i \in \iota$$

3.4.3.3 Constraint 2

In the model, production $\dot{m}$ cannot exceed demand $\dot{m}_{e,i}$.

$$\dot{m} \leq \dot{m}_{e,i}, \quad \forall i \in \iota \tag{22}$$

3.4.3.4 Constraint 3

Extracting water from a given well requires a certain amount of power, calculated as

$$P_{well} = \dot{m} \cdot g \cdot h \tag{23}$$

where h is the height which the water has to be pumped.

Additionally, water contains a specific exergy X_W. The total exergy of the water pumped can be calculated as

$$X_W = \dot{m} \cdot e_x \tag{24}$$

where e_x is the specific exergy of the fluid.

For the sustainability constraint, it is assumed that the amount of energy that is needed to pump up water has to be equal or less than a given fraction of the according exergy.

$$P_W \leq \delta \cdot X_W \tag{25}$$

The maximum drawdown is calculated as

$$h_1^{max} = \frac{e_x \cdot \delta}{g} \tag{26}$$

The drawdown of the reservoir is not allowed to exceed the maximum drawdown.

$$h_{l,i} \leq h_1^{max} \tag{27}$$

3.4.3.5 Constraint 4

Equation 27 calculates the power that is needed per well to pump water to the surface. The total power that is used for pumping at time i can be calculated as

$$P_{power,i} \leq P_{pump} \cdot \sum_{i=1}^{i} y_{mi} \tag{28}$$

where

- P_{pump} = power rating of one pump
- y_{mi} = number of pumps at time i

3.4.3.6 Optimization Problem

Considering the information given in previous chapters, the optimization model can be defined as [7]:

$$\text{maximize NPV} = \sum_{i=1}^{I} \frac{CF_i}{(1+WACC)^i} \tag{29}$$

subject to

$$h_{j,i+1} = (K - \frac{\Delta t}{2}S)^{-1}((K + \frac{\Delta t}{2}S)h_{j,i} + \frac{\Delta t}{2}(u_{u+1} + u_i))$$

$$P_{power,i} \leq P_{pump} \cdot \sum_{m=1}^{i} y_m$$

$$0 \leq \dot{m}_i \leq \dot{m}_{e.i}$$

$$0 \leq h_{1,i} \leq h_1^{max}$$

$$y_i \geq 0$$

$$\text{initial values: } h_{j,1} = h_0, \quad \dot{m}_1 = m_0, \quad y_1 \geq 1$$

$$y_i \in \mathbb{Z}_+ \text{ and } h_{j,i}, \dot{m}_i \in \mathbb{R} \forall i \in \iota \text{ and } \forall j \in \varepsilon$$

3.5 Operational Data

The operational data comprises data sets for all four low temperature geothermal fields. The raw drawdown/production data was supplied by Orkuveita Reykjavikur and covers different time sets for each field. The data was processed by the author, who used the Matlab code written by Tiffany Roche who is a graduate student from Polytech in France

and worked at Reykjavik University as a summer researcher with Ágúst Valfells. Tiffany was in charge of creating algorithms for cleaning the data, converting it into the right format and interpolating missing data via Neville's Algorithm. Neville's algorithm interpolates the data and estimates a data trend, taking the existing data and the slope of the production/drawdown curve into account. Mathematically this can be expressed as:

$$p_{i,i}(x) = y_i,\ 0 \leq i \leq n, \tag{30}$$

$$p_{s,a}(x) = \frac{(x_a - x)p_{s,a-1}(x) + (x - x_s)p_{s+1,a}(x)}{x_a - x_s},\ 0 \leq s < a \leq n. \tag{31}$$

where $p_{s,a}$ is a polynomial of the degree a-s which incorporeates the points x_k and y_k $\forall \quad k = [s, s+1, ..., a]$ and $s, a \in \mathbb{Z}_+^*$ [111].

Neville's algorithm can produce feasible results as long as the missing data is not missing on a part of the polynomial which is characterized by alternating monotonic increase and decrease and is additionally limited by an external limitation.

To visualize this issue, Figure 19 shows a seasonal production curve in red which is limited by a seasonal maximum or production capacity limit at y=4. Data is missing for a part of periods 11 and 12. Applying Neville's algorithm in this case leads to exaggerated estimation for the missing data as the slope leading to the maximum production is very steep. This is schematically shown by the black dashed production estimation for periods 11 and 12. The graph shows that the production is estimated too high, when considering the local maxima before and after the estimated data.

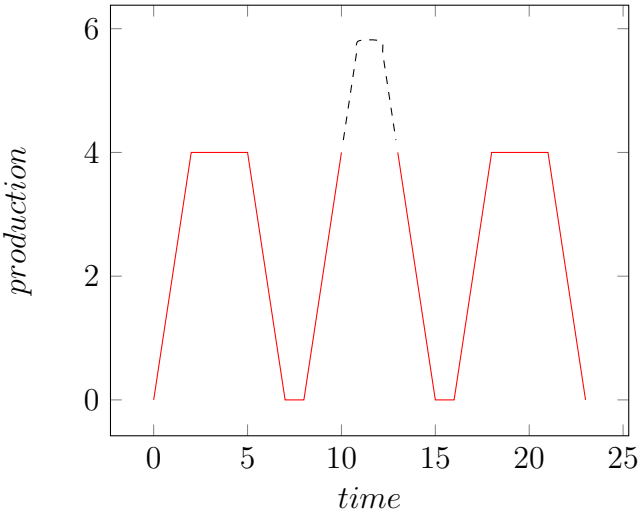

Figure 19: Schematic estimation of seasonal production by using Neville's algorithm. The estimation is marked by the dashed black line, where measured production data is marked red.

In order to avoid overestimating the missing data, a seasonal maximum $\dot{m}_{smax}$ is determined and all estimations $\dot{m}_{sest}$ above the maximum are lowered by $\dot{m}_{sest} - \dot{m}_{smax}$.

The outcome of Tiffany Roche's algorithms is provided in a csv file in the format of "DD-MMM-YYYY, Production, Drawdown 1, Drawdown 2". In order to use the data as an input for PyLumpfit, it needs to be processed further. After splitting the CSV values into separate columns, the months are consecutively numbered and the data is rearranged to "Month number, Drawdown, Production" and saved as an input CSV file for Py Lumpfit.

The operational data is fitted, using PyLumpfit, via the non-linear iterative least-squares method, which tries to create a model function $y(x) = f(x; \alpha_1, \ldots, \alpha_m)$ from a set of observed values $y_i (i = 1, \ldots, n)$. The best solution is considered to be the one which minimizes the sum of squared differences between the model function and the observed values:

$$\min_{\vec{\alpha}} \|\vec{f} - \vec{y}\|_2^2 \tag{32}$$

where

$$\sum_{i=1}^{n} (f(x_i, \vec{\alpha}) - y_i)^2 = \|\vec{f} - \vec{y}\|_2^2. \tag{33}$$

while $m \geq n$.

Chapter 4

Results

This chapter focuses on the results of the research. It displays the sources of uncertainty for NPV maximization, the workflow of the LPM part and portrays its outcomes.

4.1 Optimization and Uncertainty

With NPV maximization as the objective function of the theoretical optimization, uncertainty comes into action for different variables. As stated in chapter three, the cost model consists of different input variables. As equation 1 shows, the two influential variables for NPV calculations are the cash flow and the discount factor.

The influence of the discount factor was already discussed partly in chapter 2.3.2 and displayed in Figure 10. A rather practical and manageable way to try to limit the uncertainty connected to the discount factor was proposed in chapter 2 - the WACC was implemented and acts as a rather stable discount factor as long as the underlying capital structure of the project is not changed.

Equally interesting is the influence of uncertainty on the variables that make up the Cash Flow. Equations 13 - 19 offer an overview of the main actuating variables.

4.1.1 Investment Cost and Uncertainty

Depending on the point in time when the optimization is run, the investment cost can be subject to uncertainty. If the optimization is run after the investment phase is over, the investment costs are not subject to uncertainty as they are fixed. However, the assumption of fixed investment cost is usually not appropriate for geothermal projects since a

modular framework for development of the resource is often used and existing production equipment is extended or new equipment is purchased. In fact, optimization results are often used as input for informed decisions on adjusting the production volume and therefore variable investment cost should be considered. Equation 13 shows the variables that make up the investment cost in the model.

Equipment cost is subject to price fluctuations which are hard to forecast since many influential factors come into play. This is the case if the piece of equipment is the outcome of a project and/or company itself. Following are some of the input variables for the equipment cost:

- The rate of technological development can change the development cost of the equipment.
- Labor cost for producing the equipment may change, as regional, national or industry specific wage levels alternate.
- Transportation cost comes into play when the equipment is delivered to the construction/project site. These cost can vary widely according to fuel cost, which are linked to commodity prices and refining margins.
- Feedstock prices may change and can influence the equipment cost in both ways. Fluctuations in the feedstock price may stem from potentially changing production cost, labor cost and shipping of the feedstock to the equipment manufacturer.

Another variable that is apt to influence the level of the investment cost is labor cost during the investment period. As for the labor cost of producing new equipment, the labor cost during the construction period are subject to change in line with regional, national or industry specific wage levels.

Furthermore, construction cost may change over time due to feedstock price variations and labor cost changes.

Lastly, land purchase cost are subject to uncertainty as the land valuation might change due to infrastructural changes to the surrounding land, population migration to or from the area, and the occurrence of natural hazards.

4.1.2 Running Cost and Uncertainty

The second big part of the proposed cost model are the periodically occurring running costs. The running costs are subject to uncertainty as many influencing parameters might change over time. Equation 14 calculates the running costs as the sum of maintenance

cost, electricity cost, labor cost during the operation period, storage and transportation cost and annuity cost. As it is the case for the variables that constitute the investment cost, the variables of the running cost are prone to uncertainty too.

Maintenance cost is subject to change as the price for products that are needed to maintain the operating equipment might vary. Influencing variables are the same as for the equipment cost: feedstock prices, technological development and labor cost.

Labor cost during the operation period underlie the same influences as labor cost during the construction period.

Storage and transportation cost might arise and is subject to uncertainty as labor cost of maintaining pipelines may vary and the prize of the land used for storage and transportation is again prone to effects due to infrastructural changes to the surrounding land, population migration and natural hazards.

Furthermore, the cost for financing, the so-called annuity cost, can change over time due to macroeconomic changes which might be apt to influence the interest rate.

Electricity cost for the extraction of geothermal fluid may vary over time, due to changes in the price for electricity per kWh, which itself is determined by a complex set of variables. The commonly used concept of levelized cost of electricity (LCOE) calculates the price according to the levels of investment costs (C_I), operation and maintenance costs (C_M), fuel costs (C_F), and electricity generation (E) per year. LCOE uses the same discounting profile as NPV, and discounts the separate variables with a discount factor r over the span of I periods. LCOE can be calculated as [112]:

$$LCOE = \frac{\sum_{i=1}^{I} \frac{C_I + C_M + C_F}{(1+r)^i}}{\sum_{i=1}^{I} \frac{E_i}{(1+r)^i}} \tag{34}$$

Each individual variable of the electricity price itself is again prone to uncertainty and indistinct development over time due to effects partly discussed in this chapter. Additionally the electricity cost are subject to change as the production rate and the drawdown of a reservoir can change substantially.

4.1.3 Benefit and Uncertainty

Not only the cost side of the optimization underlies uncertainty. As equation 18 shows, the calculation of benefits for low temperature geothermal projects include two variables that are subject to change: price and demand. Both variables are interdependent. Constraint

2 of the optimization problem states that the production for period i cannot exceed the demand for the period i. Assuming a decline in demand, the production cannot hold its level and must be adapted. The probability of demand changes is difficult to predict as many influencing factors need to be taken into account.

One of the most influencing factors of demand for hot water is the annual temperature profile. If the seasonal temperature amplitude gets smaller, demand changes will occur. Additionally and more fundamentally, if the annual temperature will rise or fall, impacts on the demand for hot water are implicated. To answer the question of how regional and global temperature profiles change, hundreds of scientists work in interdisciplinary cooperation. One of leading research groups regarding climate change is the Intergovernmental Panel on Climate Change (IPCC). In its latest assessment report, the global and regional temperature development is analyzed and discussed in great depth. Nevertheless, it is difficult to forecast an exact change, as assumptions are manifold. Figure 20 shows the projected global mean surface temperature for different scenarios which where calculated by the IPCC.

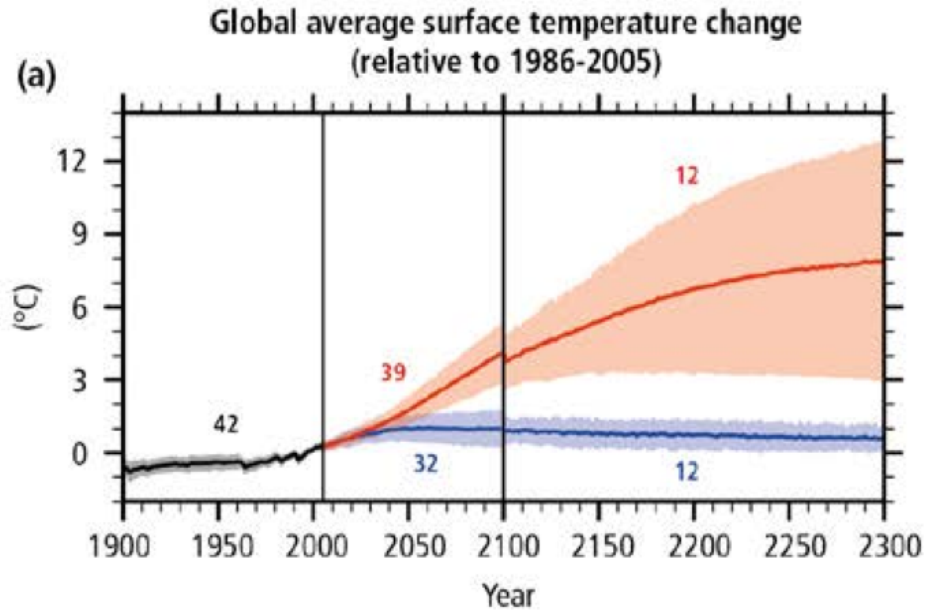

Figure 20: Time series of global annual change in mean surface temperature for the 1900 to 2300 period from the fifth assessment report of the IPCC [12]

The breadth of forecast results pose a difficult for exact future predictions, especially when long-term forecasting is intended.

Furthermore, demand can be changed by customer migration. If the geothermal low temperature project serves a certain area, its demand is dependent on the population of the

area. Population changes, e.g rural depopulation, are very common and need to be taken into account. Although forecasting of population migration can be fairly exact on a macroscopic scale [113], human behavior is challenging to forecast in general [114].

Another factor, one which interlocks price and demand, has to be included: the potential of competition. If a competitor produces the same product at a lower price, demand will drop for the project. This is based on Mankiw's assumption that rational people think at the margin [115]. The probability of new competitors is highly dependant on the barriers to entry [116] [117]. In his 1979 article, Michael E. Porter explains six distinct influential variables that determine the level of the barrier: Economies of scale, product differentiation, capital requirements, cost disadvantages independent of size, access to distribution channels and government policy. Although analyzing which of these variables apply to the exploitation of low temperature geothermal resources goes beyond the scope of this thesis, it is of interest for future research. Nevertheless, the uncertainty involved in the forecasting of competition can be regarded as high.

In line with Porter's five forces analysis, another source of uncertainty has to be analyzed: the threat of substitution. If, for example, different, cheaper sources for residential heating are provided to the community that is the main customer of the geothermal project, demand will be reduced accordingly.

Another factor which shows the interdependence of price and demand is the price elasticity of demand. As heat is a basic human need, the price elasticity is usually categorized as rather inelastic [118]. Nevertheless, research has shown that regional differences exist [119]. Furthermore, the amount of heating source options seems to have an influence on the elasticity [120].

In addition to the price elasticity of demand, the income elasticity of demand is of interest. Typically regarded as relatively inelastic [118], the income elasticity does not seem to have a large influence on the demand for heating. However, increasing income can cause demand increase for space heating if the income increase leads to the purchase of more energy intensive housing (e.g. bigger floor area).

4.2 Lumped Parameter Modeling and Uncertainty

In addition to identifying potential sources of uncertainty for the economic optimization, the influence of decreasing uncertainty on LPM is analyzed.

Figures 21 to 24 show the measured production and drawdown data for all four fields separately from 2007 to 2009. The graphs showing the complete set of measured data can be found in Appendix A and are excluded from the main part of the thesis in order to improve readability. The sets of measured data were used for the validation of the model results. A seasonal variation of production and drawdown with a significantly higher production mass flow during the winter months is shown. Furthermore drawdown minima and maxima follow production minima and maxima in with a slight deviation.

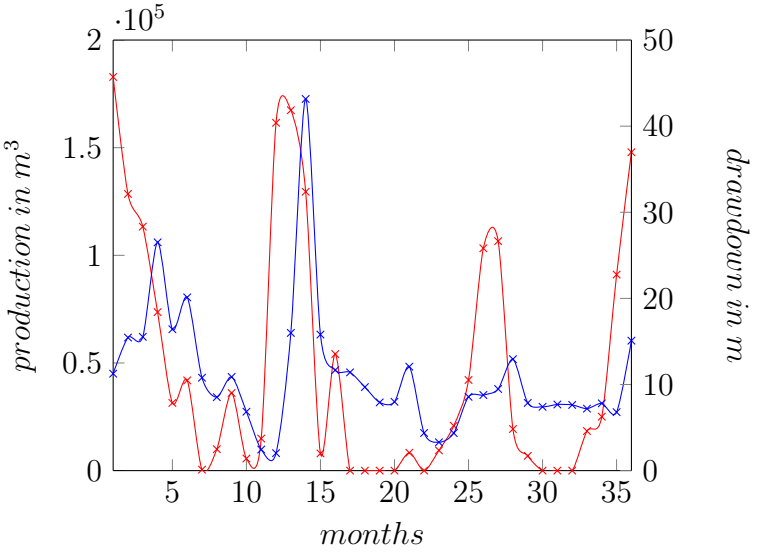

Figure 21: Production and drawdown data from Ellidaar 2007 - 2009; production is displayed by the red line; drawdown data from reference well RV-27 is displayed by the blue line

After processing the operational data according to the routine described in chapter 3.5, PyLumpfit was used to fit an LPM to the five data sets of Ellidaar, Laugarnes, Reykir, Reykjahlid, and Reykir and Reykjahlid combined.

For Ellidaar, the production data was taken from wells RV-23, RV-26, RV-29, RV-30, RV-31, RV-36, RV-37 and RV-39. As only one reference well - RV-27 - is located in this field, the measured data from this borehole was used accordingly.

For Laugarnes, the production data was taken from wells RV-5, RV-9, RV-10, RV-11, RV-15, RV-17, RV-19, RV-20, RV-35 and RV-38. Laugarnes features two reference wells - RV-7 and RV-34. For fitting the data both reference data sets were used.

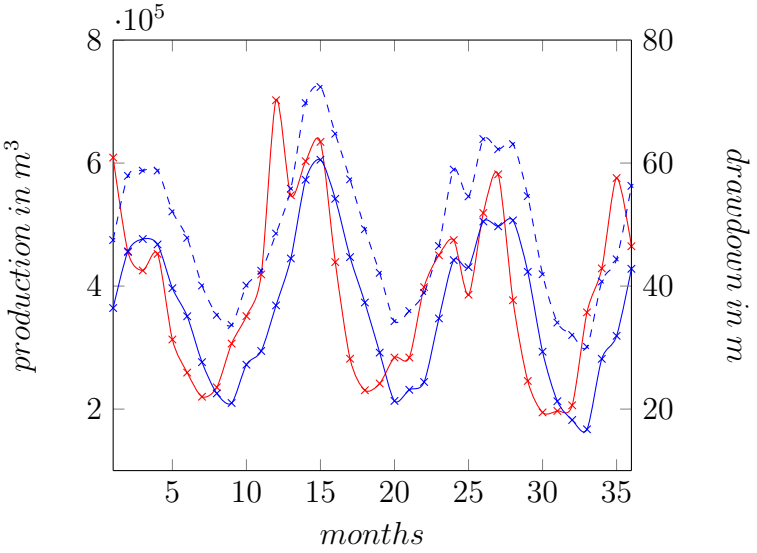

Figure 22: Production and drawdown data from Laugarnes 2007 - 2009; production is displayed by the red line; drawdown data from reference well RV-7 is displayed by the blue line; RV-34 by the dashed blue line

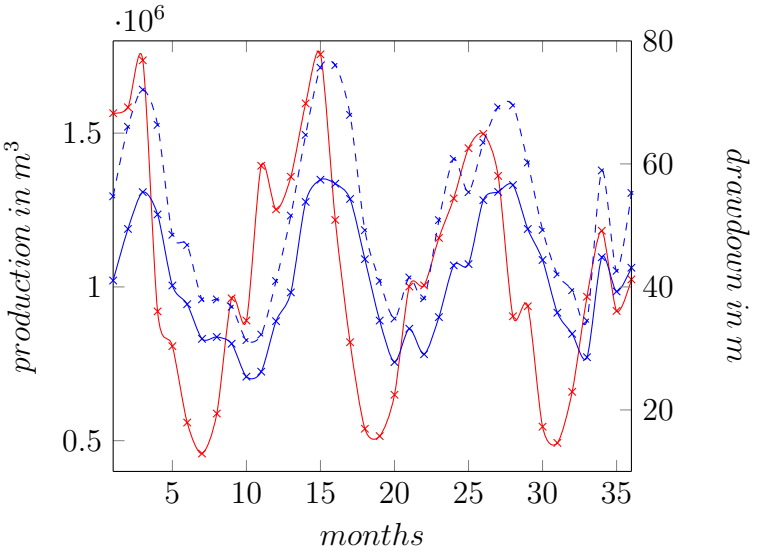

Figure 23: Production and drawdown data from Reykir 2007 - 2009; production is displayed by the red line; drawdown data from reference well MG-1 is displayed by the blue line; SR-32 by the dashed blue line

For Reykir, the production data was taken from wells MG-3, MG-4, MG-6, MG-8, MG-9, MG-11, MG-12, MG-13, MG-14, MG-15, MG-16, MG-17, MG-18, MG-20, MG-22, MG-23, MG-24, MG-25, MG-26, MG-27, MG-30 and MG-31. Two reference wells are located within the fields premises - MG-1 and SR-32.

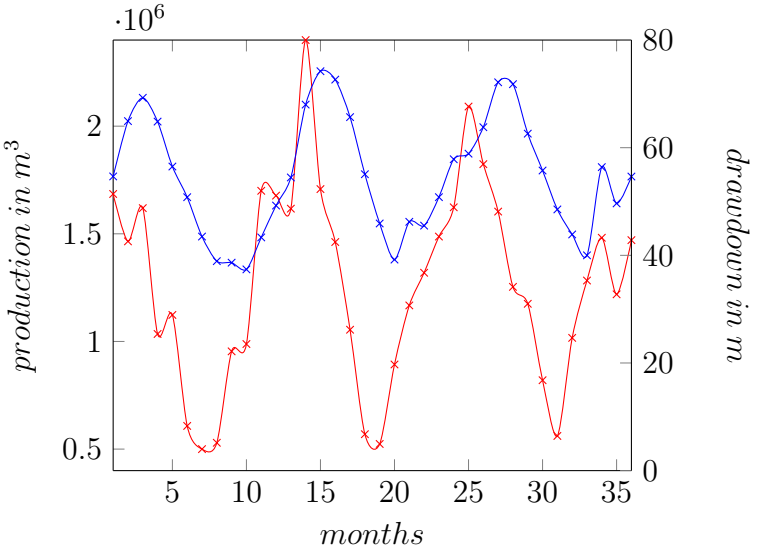

Figure 24: Production and drawdown data from Reykjahlid 2007 - 2009; production is displayed by the red line; drawdown data from reference well MG-28 is displayed by the blue line

For Reykjahlid, the production data was taken from wells MG-5, MG-19, MG-21, MG-29, MG-32, MG-33, MG-34, MG-35, MG-36, MG-37, MG-38 and MG-39. Coming from the only reference well - data from MG-28 was used for fitting the data to the model.

Generally the drawdown data from reference wells should cover a large time span of production. For some of the fields, this could not be followed, since the quality of the model fit was better for the reference well, which provided data for a shorter period of time.

4.2.1 Initial Fit

The field data was gradually used as input. During the first step, production and drawdown data from the whole available period was selected and the model was run. This was done for an open and closed one tank model, an open and closed two tank model and an open and closed three tank model. Drawdown was defined positive in the downward direction. Production was defined as growing positively. The initial water level was set to be 0. The data had to be converted into the SI units that are used by PyLumpfit. The production data was provided by OR in cubic meters per month. The conversion into kg/s was made with a multiplication factor which resembles the density of the fluid at the measured temperature. Table 2 shows the different average densities assumed for the three fields:

Generally, the coefficient of determination was higher for model fits of higher complexity. The best results are explained in the following chapters.

Table 2: Density conversion factors

Field	Assumed Temp. (C)	Density (kg/m3)	Conversion Factor
Ellidaar	90	965	0.965
Laugarnes	130	935	0.935
Reykir and Reykjahlid	85	968	0.968

4.2.1.1 Ellidaar

For the Ellidaar geothermal field, a good fit was obtained with a one tank open model. The coefficients of determination remained on a medium high level of 0.67 for all models with increased complexity. The intial fit is displayed in Appendix B Figure 38 a-f.

4.2.1.2 Laugarnes

PyLumpfit produced valuable results for the geothermal area of Laugarnes when fitting the data to reference well RV-34. A good fit was obtained with a one tank, two tank and three tank open approach. The coefficient of determination measured 0.71 for the one tank open approach and did not increase with increasing complexity and hence, the one tank open model was chosen as the best fit for RV-34. Fitting the data to RV-7 did produce valuable results as well, although the coefficient of determination stayed at a comparably low level of 0.67 for models of higher complexity. The reason for that is subject to further research as it is not clear from the data why the fitting has a poorer quality than the fitting of RV-34, especially when comparing the data of RV-7 to the fairly similar data of RV-34. The initial fits for the Laugarnes geothermal field, using RV-7 and RV-34 as the reference wells, is displayed in Appendix B Figure 40 a-f.

4.2.1.3 Reykir and Reykjahlid

Despite the geographical and geological closeness of the two fields, the author found it to be of interest to fit a model to the individual data sets, as the reference wells are relatively far apart from each other.

Fitting the operational data of the geothermal field Reykir while using well SR-32 for the drawdown measurements, produced valuable results. The coefficient of determination reached a level of 0.67 with a one tank open model. For a two tank closed model, the level increased to 0.68 and for a two tank open model the coefficient leveled off at 0.72. Further increases in complexity did not lead to higher levels. Therefore the two tank open

approach was used as the best fit. Using data from reference well MG-1 did lead to a slightly lower quality fit, as the maximum level for the coefficient of determination was 0.69 .

The results of Reykir's initial fit, using data from reference wells SR-32 and MG-1, are displayed in Appendix B Figure 42 a-f.

Fitting Reykjahlid's data, using reference well MG-28 did not produce valuable results as the level of the coefficient of determination did not exceed 0.15. The initial fits for the Reykjahlid geothermal field, using MG-28 as the reference well is displayed in Appendix B Figure 43 a-f.

When using Reykir and Reykjahlid operational data together the results were contradictory to the stand alone results. Fitting with data from Reykir's reference wells MG-1 and SR-32 did not produce valuable results. However, Reykjahlid's reference well MG-28 now produced a fit with a coefficient of determination of 0.71 while using a one tank open model.

4.2.1.4 Complete Overview

Table 3 gives an overview of all initial fits, displaying the R^2 for different model complexities.

Table 3: Initial R^2 values with increasing model complexity

	1 closed	1 open	2 closed	2 open	3 closed	3 open
Ellidaar RV-27	0.00	0.67	0.67	0.67	0.67	0.67
Laugarnes RV-7	0.00	0.67	0.67	0.67	0.67	0.67
Laugarnes RV-34	0.00	0.71	0.00	0.71	0.66	0.71
Reykjahlid MG-28	0.00	0.15	0.00	0.15	0.15	0.15
Reykir MG-1	0.00	0.62	0.64	0.69	0.69	0.66
Reykir SR-32	0.00	0.67	0.68	0.72	0.72	0.72
R and R MG-1	0.00	0.58	0.00	0.58	0.48	0.48
R and R SR-32	0.00	0.44	0.00	0.44	0.42	0.42
R and R MG-28	0.00	0.71	0.00	0.71	0.70	0.70

Table 4 gives an overview of all inital fits, displayed as the $\bar{R}^2$ for different model complexities.

Table 4: Initial $\bar{R}^2$ values with increasing model complexity

	1 closed	1 open	2 closed	2 open	3 closed	3 open
Ellidaar RV-27	0.00	0.67	0.67	0.67	0.67	0.67
Laugarnes RV-7	0.00	0.48	0.46	0.46	0.46	0.46
Laugarnes RV-34	0.00	0.71	-0.01	0.71	0.65	0.70
Reykjahlid MG-28	0.00	0.14	-0.01	0.14	0.14	0.13
Reykir MG-1	0.00	0.62	0.64	0.69	0.69	0.65
Reykir SR-32	0.00	0.67	0.68	0.72	0.72	0.72
R and R MG-1	0.00	0.58	-0.01	0.57	0.47	0.47
R and R SR-32	0.00	0.44	-0.01	0.43	0.41	0.41
R and R MG-28	0.00	0.71	-0.01	0.71	0.70	0.69

4.2.2 Uncertainty and LPM

As the second step, the data time range was reduced to 60 months and a fit was tried to be achieved. This was done for all supported model complexities. All further iterations were run with the same additional amount of data, e.g. the second run incorporated 120 months of operational data, the third run 240 and so forth. By doing this, the uncertainty about how the water table of the reservoir behaves with ongoing production was constantly decreased as the model gained access to operational data gradually. This was done for each reference well individually. Appendix C shows a table with the results.

It was determined that when reducing the amount of input data, the model complexity of the best fit does not change.

Reykjahlid alone showed no satisfactory results, as was to be expected because of the weak initial fit. Ellidaar showed no satisfactory results either. In this case, the development of the coefficient of determination is especially interesting, as its initial fit only reached a high level for the coefficient of determination when using a lot of data points. PyLumpfit was not able to create a reasonable fit for Ellidaar when the model used up to the first 300 months as input. Figure 25 shows the development of the coefficient of determination and the yearly production volume. Good fits are obtained when the annual production values plummet towards 0. The quality of the fit gets better the longer the production stays on minimal levels.

In order to increase the amount of information that the development of the coefficients of determination provides, a control profile with made up operational data was created. The production data was created in a way that follows seasonal patterns with an annually repetitive sine curve. This behavior was chosen as it can be found in the measured operational data as well (compare Figures 21 - 24).

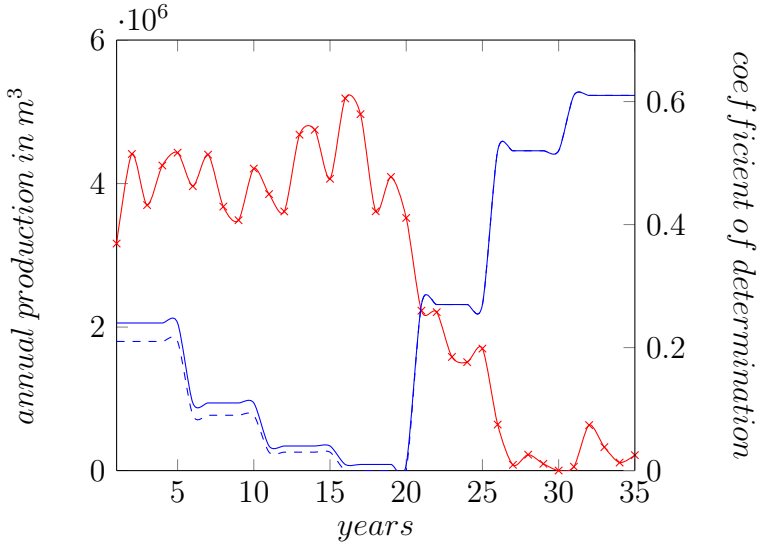

Figure 25: Development of annual production data (red) and R^2 (blue, solid), $\bar{R}^2$ (blue, dashed) for the geothermal field of Ellidaar 1970 - 2004

The production of time period i is calculated as:

$$\dot{m}_i = [sin(i \cdot \frac{1}{6}\pi + \frac{1}{6}\pi) + 2] \cdot 100,000 \tag{35}$$

The drawdown data depends on the production data and is slightly shifted in time, in order to produce a data set that simulates the real physical behavior of geothermal reservoirs. The calculation of the drawdown response is related to equations 5-7 and represents a one tank open system. More details can be found in Appendix E. The drawdown of time period i is calculated as:

$$h_i = h_{i-1} + \frac{\dot{m}_{i-2} - \dot{m}_{i-3}}{7500} \tag{36}$$

where $h_1 = 56\frac{2}{3}$. The initial level of the drawdown data was chosen randomly.

Theoretically this model should obtain a good fit with a one tank open model. As expected, the best fit was obtained with an one tank open model. Figure 26 shows the initial behavior of the coefficient of determination with increasing data input of up to 300 data points. Increasing quality was measured with even more data points, but the limited time frame from which real operational data is available, limited the practicality of using information from such a development.

For comparison of results, the coefficients of determination are normalized on a scale of 0 to 1 by using the following equations:

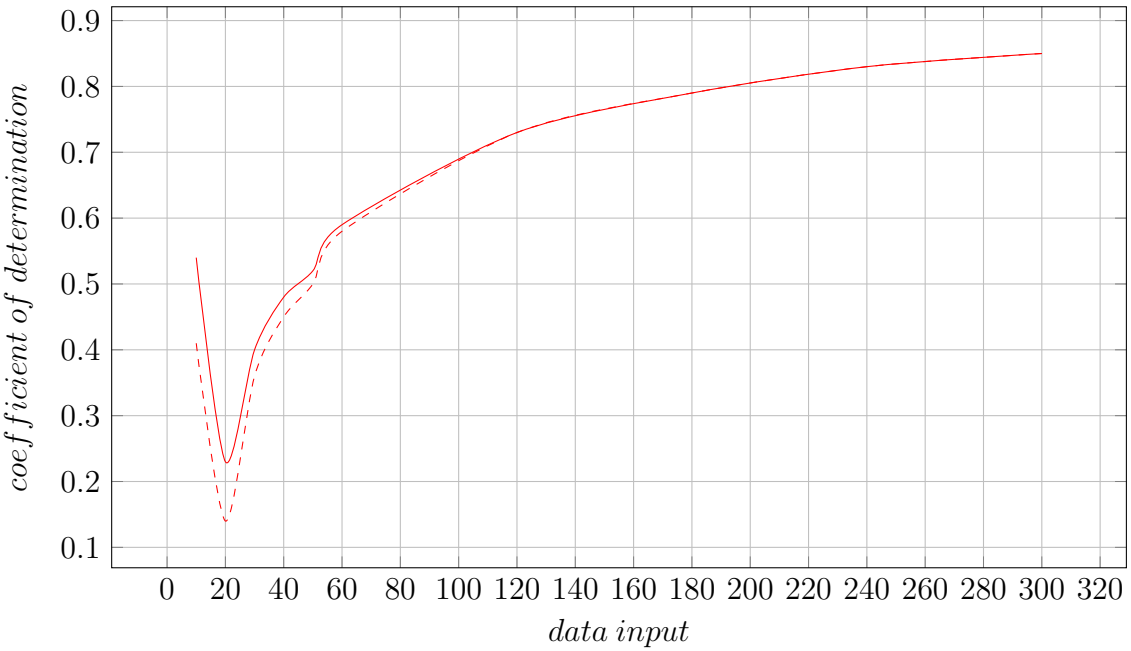

Figure 26: Development of the control model's R^2 (red, solid) and $\bar{R}^2$ (red, dashed) value with increasing data input

$$R^2_{Ni} = \frac{R^2_i}{R^2_{max}} \tag{37}$$

$$\bar{R}^2_{Ni} = \frac{\bar{R}^2_i}{\bar{R}^2_{max}} \tag{38}$$

where R^2 is the coefficient of determination, i the time period and R^2_{max} the maximum coefficient of determination which was reached within the first 300 months. By doing this, a comparison of normalized coefficients of determination is possible. A steep increase of the coefficient of determination occurs when few data points are available. Therefore the resolution of the data input increase was chosen to be higher in the beginning. A base increase of 10 data points was used until the level of 60 was reached. This was chosen as a compromise between computational time and accuracy. Figure 27 shows the results for Laugarnes RV-7, Laugarnes RV-34, Reykir MG-1, Reykir SR-32 and Reykir/Reykjahlid MG-28. The according data is displayed in Table 5 and Table 6. Ellidaar and Reykjahlid stand-alone were not considered for this step as their initial fits were not on a satisfactory level. The model complexity was chosen to be in line with the initial best fit.

The development of R^2 and $\bar{R}^2$ behaves only partially similarly for the separate cases. With an increased amount of data, the coefficients of determination generally acquire a higher value. Nevertheless, for some cases, this development is interjected with a contrary

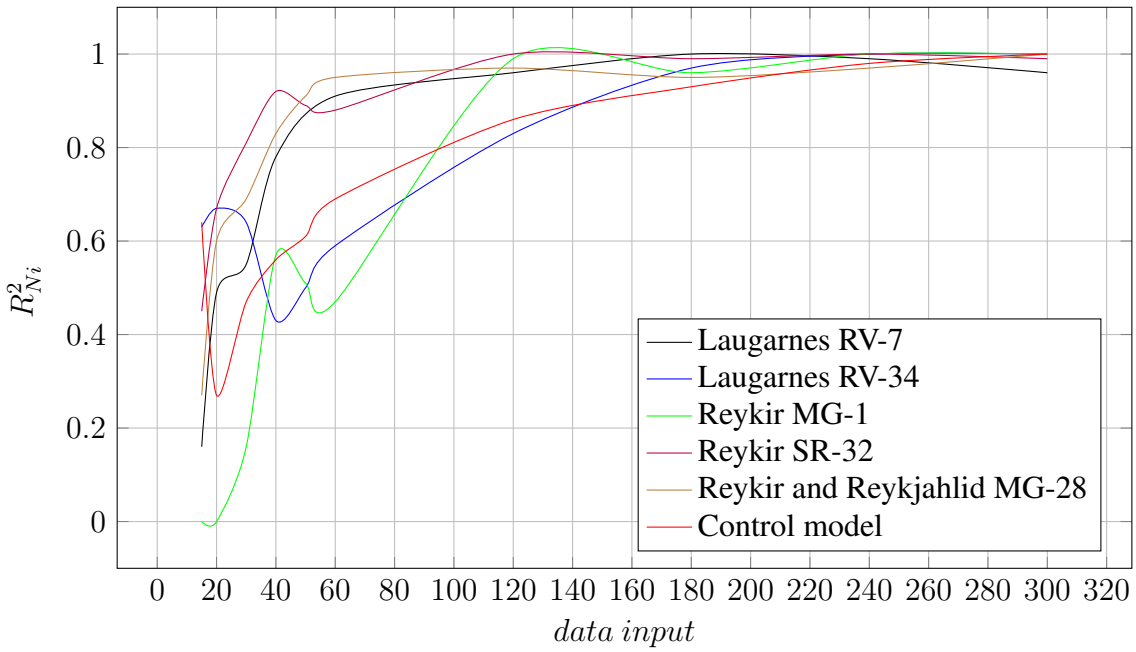

Figure 27: R^2_{Ni} values with decreasing uncertainty

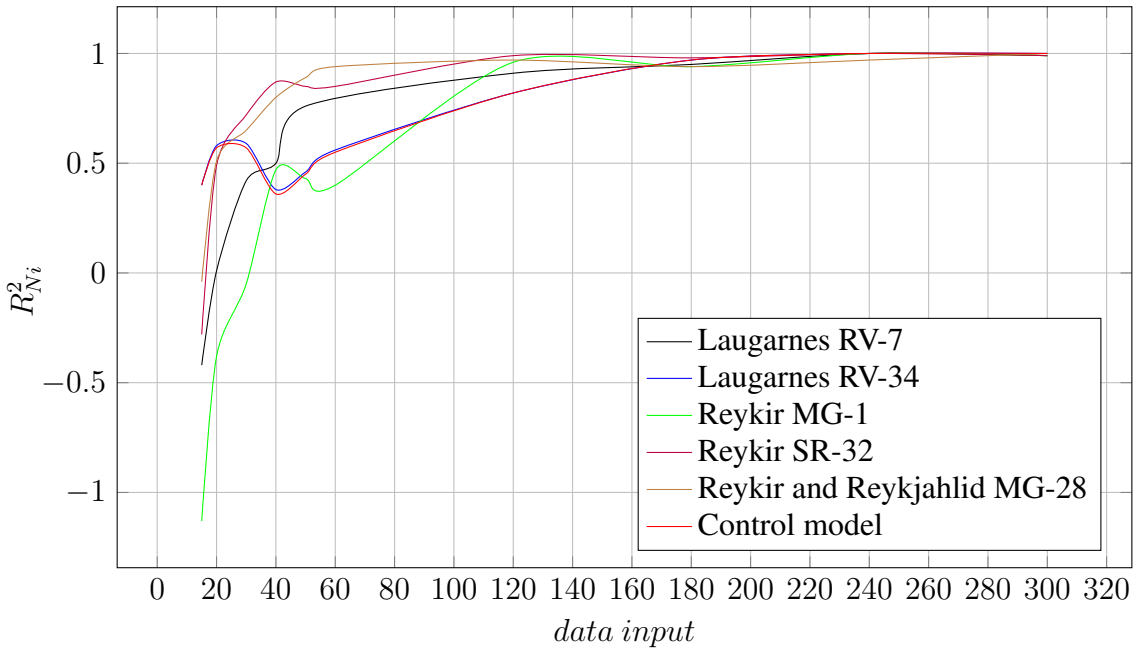

Figure 28: $\bar{R}^2_{Ni}$ values with decreasing uncertainty

Table 5: Development of the normalized R^2 values with decreasing uncertainty

	Normalized Coefficient of Determination R^2					
data input	L RV-7	L RV-34	R MG-1	R SR-32	RR MG-28	Control Model
15	0.16	0.63	0.00	0.45	0.27	0.64
20	0.49	0.67	0.00	0.67	0.60	0.27
30	0.55	0.64	0.16	0.81	0.69	0.47
40	0.78	0.43	0.57	0.92	0.83	0.56
50	/	0.50	0.51	0.89	0.91	0.61
60	0.91	0.59	0.47	0.88	0.95	0.69
120	0.96	0.83	0.99	1.00	0.97	0.86
180	1.00	0.97	0.96	0.99	0.95	0.93
240	0.99	1.00	1.00	1.00	0.97	0.98
300	0.96	1.00	1.00	0.99	1.00	1.00

Table 6: Development of the normalized $\bar{R}^2$ values with decreasing uncertainty

	Normalized Coefficient of Determination $\bar{R}^2$					
data input	L RV-7	L RV-34	R MG-1	R SR-32	RR MG-28	Control Model
10	-0.42	0.40	-1.13	-0.28	-0.04	0.40
20	0.01	0.58	-0.38	0.49	0.51	0.57
30	0.42	0.59	-0.05	0.72	0.65	0.57
40	0.50	0.38	0.47	0.87	0.80	0.36
50	/	0.46	0.43	0.85	0.89	0.45
60	-0.05	0.56	0.40	0.85	0.94	0.55
120	0.91	0.82	0.96	0.99	0.97	0.82
180	0.95	0.97	0.94	0.98	0.94	0.97
240	1.00	1.00	1.00	1.00	0.97	1.00
300	0.99	1.00	0.99	0.99	1.00	1.00

movement. For example, L RV-34 shows a decrease between 30 and 40 data points. When comparing the drawdown data of L RV-34 to other reference wells, the values behave in a non conform way. The reason for this behavior cannot be explained with varying production, as L RV-7, which responds to the same production values, shows continuously growing coefficients of determination. Further research might be able to find the reason for L RV-34's behavior. The same behavior can be found when analyzing R MG-1, where the coefficient of determination declines between 40 and 60 data points, whereas R SR-32 does not show this inconsistency. Further analysis with higher resolution showed that the decline takes place between 40 and 70, without being connected to abnormal drawdown or production behavior. The control model shows a monotonic increase from 30 data points on, but behaves oppositely when very few data points are used as input for PyLumpfit. This might be due to the strong seasonality of the control model. Further research might prove that in order to achieve a stronger fit, a whole seasonal cycle must be present. At the moment, the data suggest that this is the case, but the statement has to be regarded as speculative.

The level of all R^2_{Ni} and $\bar{R}^2_{Ni}$ values reaches satisfactory levels of 80% and more when ten years of monthly data were used as input. For L RV-7, R SR-32 and RR MG-28 this level was reached with data input from 30 to 60 months. Nevertheless, ten seasonal cycles were considered to be the appropriate amount of data to bring the coefficients of determination to the system specific maximum values.

For comparison of the results with different control models, three additional models were created. Control model two is a one tank open model which features a yearly increase in production and drawdown of one percent. Control model three is a one tank open model which faces an one percent decline of production and drawdown per annum. Control model four is a two tank open model with an annual production decrease of five percent while the drawdown reacts slower with only two percent decrease. Figure 29 shows the development of the normalized coefficients for control model one to four. All control models behave in a very similar way.

4.2.3 Drawdown Forecasting

In addition to the analysis of the development of the coefficients of determination with increasing operational data, a drawdown forecast for selected wells was made. For this analysis Reykir SR-32 and Laugarnes RV-34 were chosen, as both showed good initial fits and satisfactory development of the model fit with increased data input.

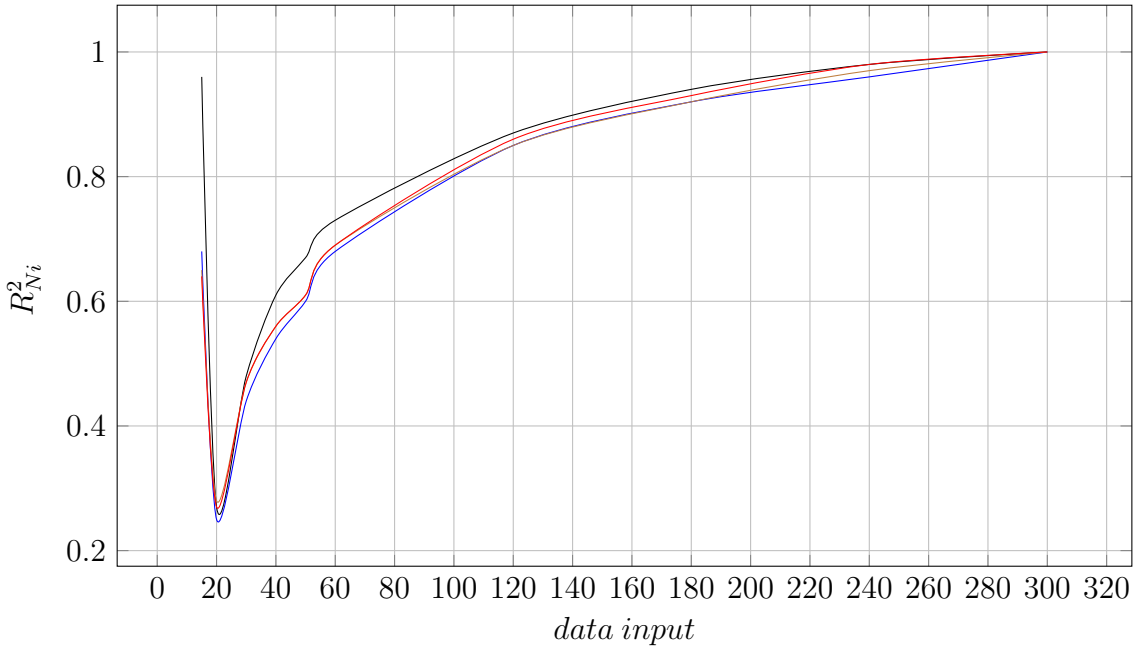

Figure 29: R^2_{Ni} values with decreasing uncertainty - control model one in red, two in brown, three in blue and four in black

For Reykir SR-32 a two tank open model was used as a base and the production was forecasted on the premise that it alternates within the range of the main 80% of the according data input. To calculate the main 80%, the top and bottom 10% are cut off. The maximum value was set to occur during the months of December to February, as then the demand for heating in Iceland is the biggest. The minimum value was set to be used from June to August, the period with the least demand for hot water. Starting point of the operational data was chosen to be March 1980, as this date marks the start of data collection from reference well SR-32. The yearly production was assumed to be stable.

For Laugarnes RV-34 a one tank open model was used. The same process was applied as in the case of Reykir. The starting point was chosen to be the first of February 1985.

Table 7 shows the data range used for the forecasting.

For Reykir the water level showed a decreasing trend for the forecasts with data input of 60, 120 and 180 months. 240 and 300 months data input stabilized the water level trend to a level development. When using the main 80% of the production data of the first 60 months throughout the forecasting process, the decreasing trend continued to be visible until 240 months data input. The according graphs can be found in Appendix D. For Laugarnes a level development of the drawdown was visible throughout all iterations. The forecasted water level showed the same trend over all iterations: it followed production closely and gave a fairly good indication if production was actually held at a stable level.

Table 7: Production range used for forecasting - main 80% of the monthly production values for Laugarnes and Reykir - values in m^3

	Laugarnes		Reykir	
months	min	max	min	max
60	292620	725460	1044050	1663220
120	234909	674673	1043545	1874540
180	204709	659525	766373	1796883
240	207120	652385	586048	1729802
300	220151	644037	586454	1719307

Overall, the water level seemed to have had a slightly negative trend, despite the model being open.

Figure 30 shows the drawdown forecast for Laugarnes and Figure 31 shows the forecast for Reykir.

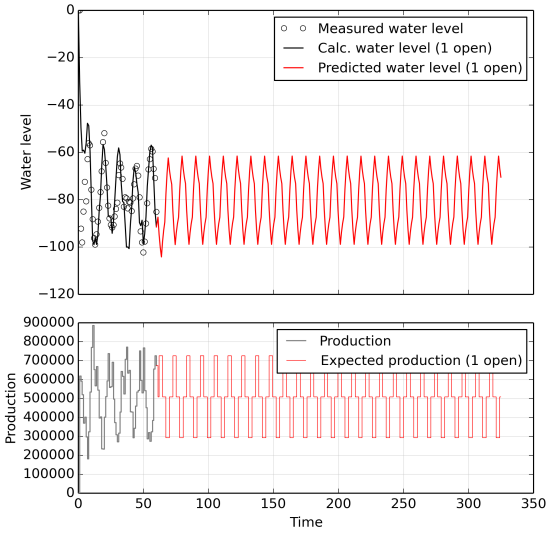

(a) Forecast with 60 months data input

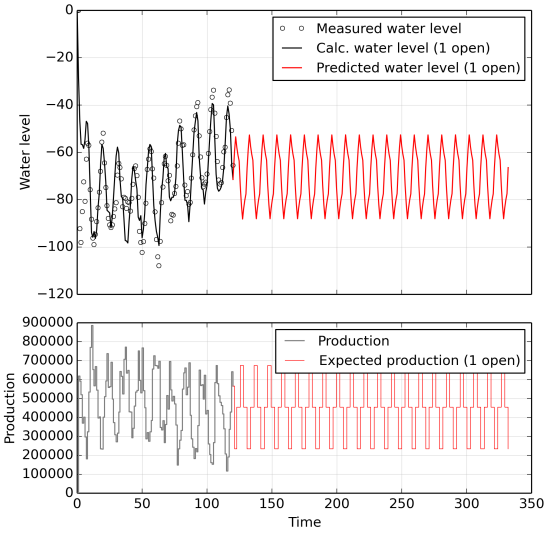

(b) Forecast with 120 months data input

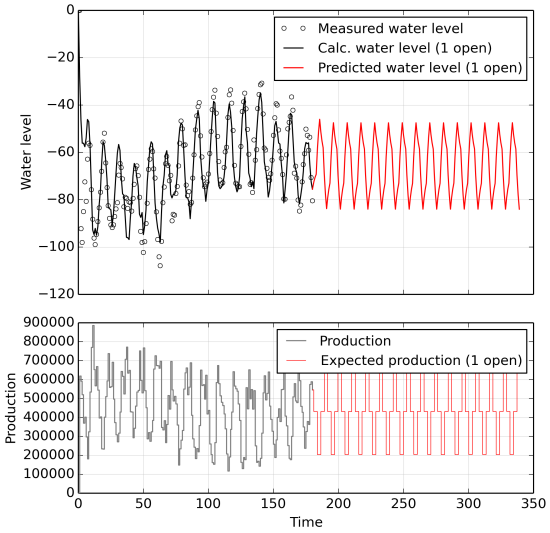

(c) Forecast with 180 months data input

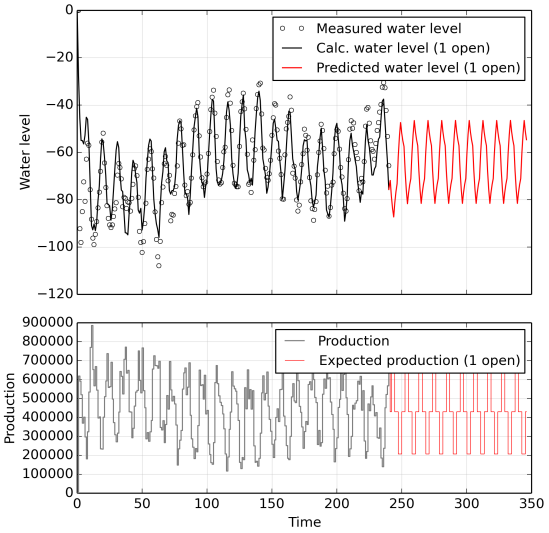

(d) Forecast with 240 months data input

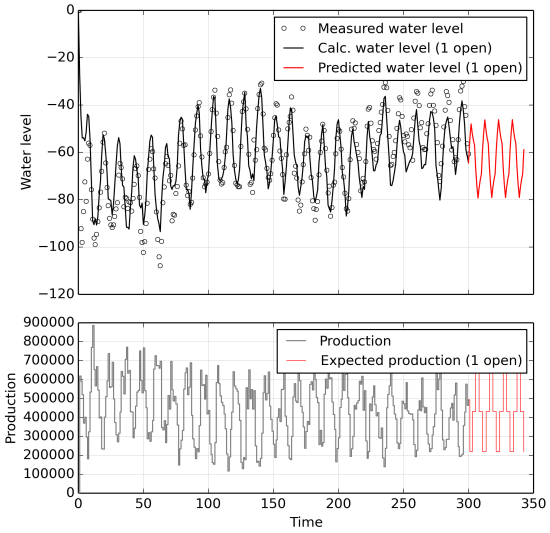

(e) Forecast with 300 months data input

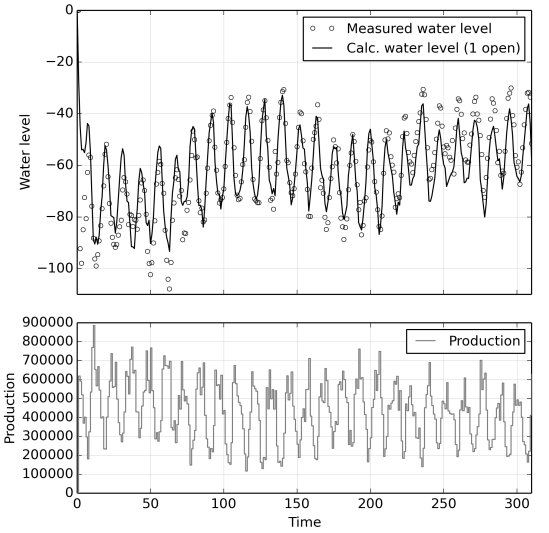

(f) Initial fit

Figure 30: Drawdown forecast for Laugarnes

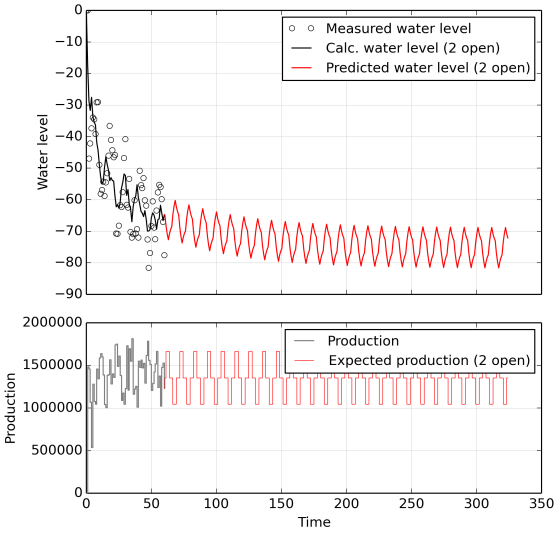

(a) Forecast with 60 months data input

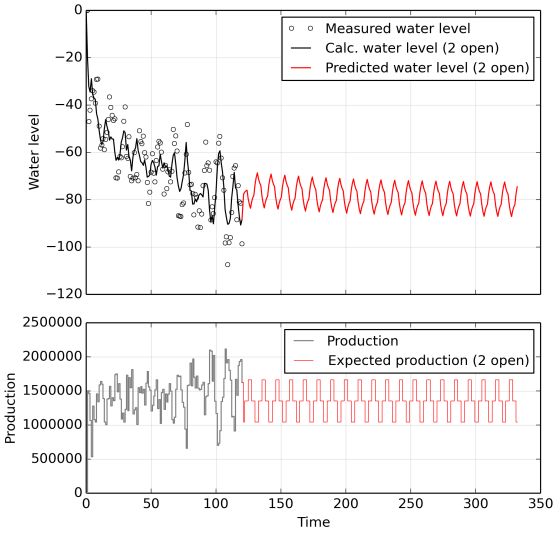

(b) Forecast with 120 months data input

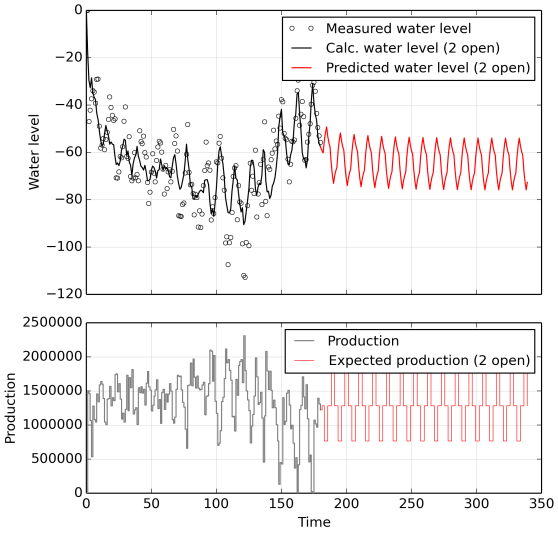

(c) Forecast with 180 months data input

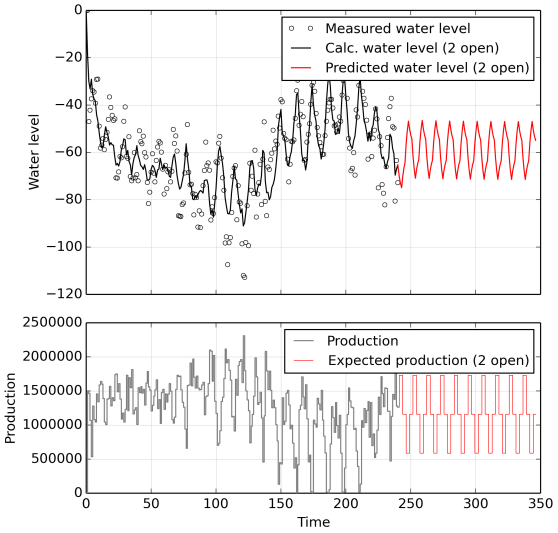

(d) Forecast with 240 months data input

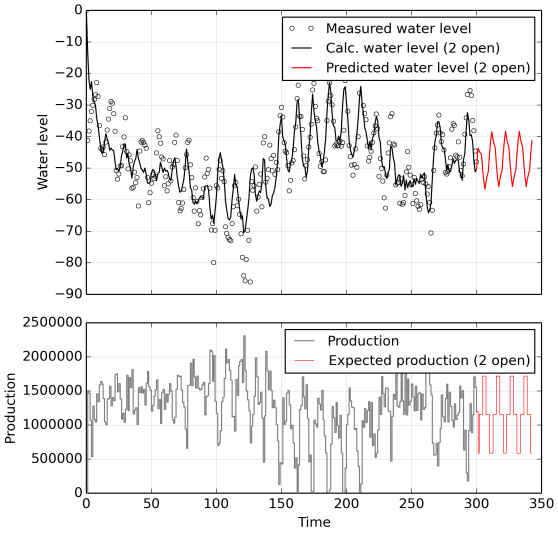

(e) Forecast with 300 months data input

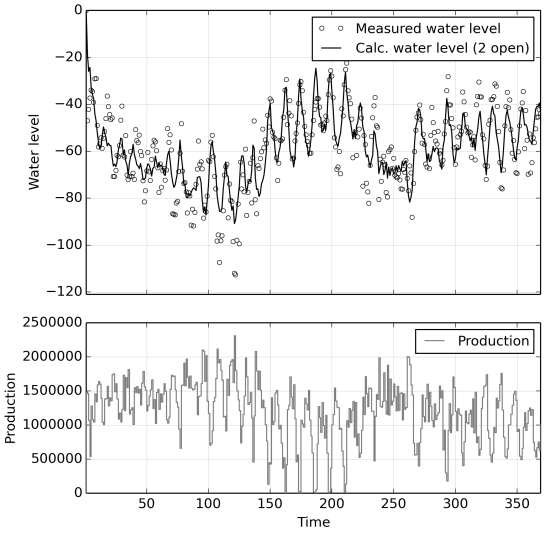

(f) Initial fit

Figure 31: Drawdown forecast for Reykir

Chapter 5

Conclusion

This chapter discusses the results and summarizes the research and points out possible future research opportunities.

5.1 Summary

After introducing the scientific background of the origin and usage possibilities of geothermal energy, the concept of reservoir modeling has been explained and different types of reservoir modeling techniques were analyzed. The cost and time saving lumped parameter modeling approach was chosen to be the main focus of the thesis.

Operational data was obtained from Orkuveita Reykjavikur and covered 300+ months of drawdown and production history of the fields Ellidaar, Laugarnes, Reykir and Reykjahlid.

After processing and cleaning the raw data, an initial model fit was attempted by minimizing the sum of squared differences between the model function and the observed values. An appropriate model fit was determined with the R^2 and $\bar{R}^2$ values. The operational data was divided into data input packs of 60 data points and a fit was tried to be achieved. Additionally, control models with imaginary data were created, in order to compare the results to stable, seasonal data. The results showed that a higher resolution of data input points was needed in the beginning, as the model iterations with 60 data points already showed a significantly high coefficient of determination. Hence models were fitted with 15, 20, 30, 40, 50, 60, 120, 180, 240 and 300 data points. This showed some interesting behavior of the coefficient of determination, as its development was analyzed for the Ellidaar geothermal area. The goodness of fit did develop its maxima when production

dropped to its minimum levels. Overall, best fits did not show differences in model complexity with decreasing uncertainty. Both models from real data and models from control data showed the same development with decreasing uncertainty. After 10 seasonal cycles the R^2 and $\bar{R}^2$ values reached at least 80% of the reservoir/reference well maxima.

For the economical optimization part of the thesis, net present value maximization was chosen to be the objective function, as this represents the industry standard. The concept of net present value calculations was explained and the influence of the discount rate was pointed out. In order to calculate a stable discount rate, the weighted average cost of capital model was used, which allows a rather stable discounting as long as the underlying capital structure of the project does not change. Furthermore, the cash flow of a low temperature geothermal project was discussed and a modular approach with different influential variables within the cost and benefit model was proposed. These variables might show indistinct behavior over time and were therefore identified as potential sources of uncertainty.

5.2 Discussion

The results of analyzing the different variables, which are subject to change during an economical optimization with the goal to maximize the NPV of a low temperature geothermal project, are discussed in chapter 4. Almost all variables that influence the outcome of the optimization are subject to an extensive amount of uncertainty. While analyzing the possible changes a variable can undergo, it became obvious that each variable has a subset of influencing variables itself. In many cases, these sub-variables themselves are prone to indistinct behavior as they are influenced again by other variables. One example to show this behavior is equipment cost in the investment period. Figure 32 gives an overview of the influencing factors of some of the variables and sub-variables.

This example was chosen to show the multiple points of attack for uncertainty. In Figure 32 only the influencing sub-variables for one variable per level are shown. In reality, not only the feedstock price for the equipment cost has further sub-variables that are prone to uncertainty. Labor cost has different influencing factors as well. Some parts of the cost model, which is used for optimization, are much more exposed to uncertainty than one would think at first. In many optimization analyses for geothermal low temperature projects, equipment cost are given as a constant or are sometimes even just limited to cost for pumps. This behavior excludes all other physical equipment that is needed to run a

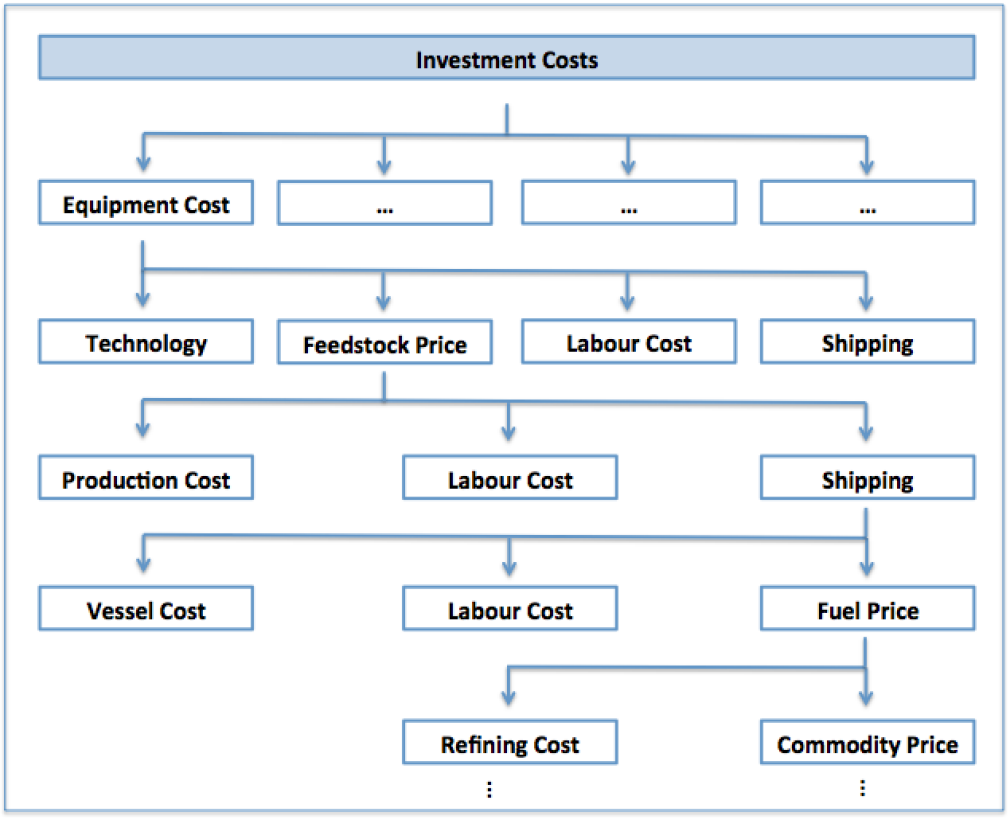

Figure 32: Sources of uncertainty for equipment cost during the investment period

geothermal exploitation project and rejects the reality of variables with indistinct behavior over time.

In chapter 2.2.1.1 one of the basic ideas of modeling is stated as the shortening of reality. A model therefore, by definition, reduces the amount of information that reality provides. It is unrealistic to assume all sources of uncertainty can be included in an optimization problem. The question is rather, which variables should be allowed to fluctuate and how the outcome of optimization can be made more realistic. The answer to this question is dependent on the background of the model user: an economist might choose different variables than an engineer. These choices might alter the model outcome but are necessary in order to create an optimization model that is manageable and does not complicate the usability or reduce the usefulness. For research purposes, the complete set of sources of uncertainty is regarded as interesting and significant. In an industrial setting, the model might face a decreased amount of sources of uncertainty in order to improve practicality.

Chapter 4 analyzed one of the options through which optimization results can be made more realistic: lumped parameter modeling.

The forecast of how physical properties of the reservoir react to production is one the questions that needs to be answered in order to maximize the quality of an optimization outcome. Chapter 3 stated that one option that is commonly used for modeling these physical reactions is lumped parameter modeling. The main outcomes of the question how uncertainty influences the outcome of lumped parameter modeling are the following.

1. Increasing availability of operational data/decreasing uncertainty has no influence on the complexity of the best fitting model. All iterations showed this result. This can save computational time and resources, as not all different levels of complexity need to be simulated once the best fit is determined.

2. The development of the coefficient of determination with decreasing uncertainty can be regarded as important. The example of Ellidaar showed clearly that a good initial fit can be misleading. Further analysis of the coefficient's development showed distinct deficiencies when reducing the amount of available data for input.

3. For all tested reservoirs, using ten seasonal cycles of data allows the model to reach 80% or more of the maximum coefficient of determination. This outcome can be of high practical value, as it implicates very good forecasting possibilities are available after the indicated time span.

4. Drawdown forecasting is apt to produce valuable results if the model fit has an appropriate coefficient of determination. Predictions if the simulated production is within the sustainable production limit are possible.

In general, decreasing uncertainty seems to have positive effects for the outcome of lumped parameter modeling. Nevertheless, the results are only improved up to a certain point which can be reached at different levels of uncertainty. It would be of interest for future research to analyze where the economical optimum for uncertainty decrease is located.

A better model fit generally means more accurate knowledge on how the reservoir would react to production changes. Consequently, qualitatively better drawdown forecasting possibilities are generated. Using these forecasting possibilities is an important step for maximizing the quality of the optimization output, as realistic production limits are needed in order to improve the accuracy of the optimization model.

As already stated, the research shows that a well-specific maximum of the model fit is reached after ten seasonal cycles. At this point the degree of uncertainty is comparably low and the model can be used as a tool to produce valuable output for the economical op-

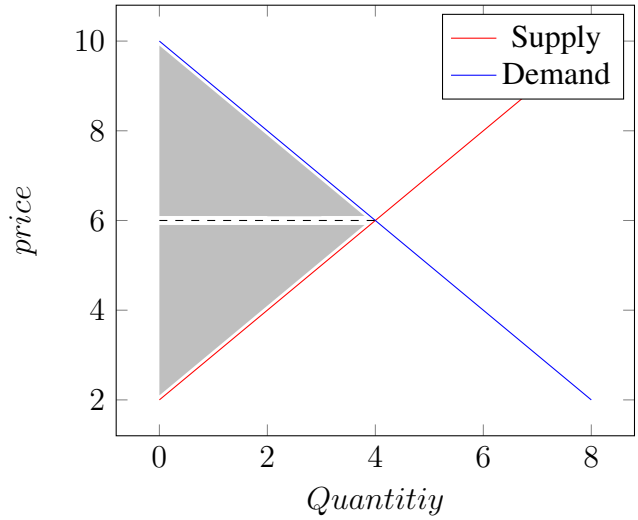

Figure 33: Maximized surplus at equilibrium; shaded area represents surplus

timization. Furthermore, the model is apt to show the reservoir's current sustainable production limit and if the reservoir's production is within the sustainable production range or not. This information is of utmost importance when the nature of NPV calculations is considered.

Maximizing the NPV of a project is considered the standard objective function for a lot of economic optimization problems. This stems from the fact that a maximized NPV is regarded as desirable by most companies, since it maximizes the value a company can get from a project if the time value of money is considered. A high discount rate might devalue future earnings severely and consequently short-term production over the sustainable production limit might be considered optimal as the estimated value for production decreases rapidly over time. A simple example of the influence of the discount rate is displayed in Figure 10. Without knowing how the reservoir would react to excessive production, it is not possible to find realistic economical production values.

One alternative to NPV maximization is minimizing the deviation between supply and demand. Considering economic theory, a minimized supply demand deviation should stabilize untaxed prices for consumers and create the maximized social welfare, since consumer and producer surplus are maximized as a whole, while deadweight losses are minimized and theoretically non-existent if supply equals demand. This is displayed conceptually in Figure 33, where the gray shaded area represents the maximized surplus at an economic equilibrium.

In reality, temporary surplus production or deficit cannot be outruled. When not maximizing the NPV but minimizing the supply demand deviation, the level of uncertainty is shifted to the price independent variables that determine demand. Taking the results

of chapter 4.2.3 into account, demand would still react to climate change and population migration. Other variables that are subject to uncertainty and are influencing the optimization of NPV results, for example different cost structures etc., would become obsolete. It is of academic interest to investigate this further, but it is speculative if minimizing supply demand deviation has the potential of broad scale application in private run industries.

5.3 Future Research Opportunities

The purpose of this thesis was to focus on the development of the LPM fit under decreasing uncertainty. Consequently, some of the parameters that are incorporated in the LPM result have been outside of the focal area and were not part of the analysis. Two of those parameters, are the storage coefficients (K) and the resistance levels (σ). It might be of interest for future research to analyze the development of these parameters and compare the outcome to the development of the model fit with decreasing uncertainty.

The analysis has been undertaken with operational data from four different fields in Iceland. In order to prove the reliability of the results, a larger, international sample group would be interesting to analyze. More samples would most likely lead to more best fits of higher model complexity. If this is the case, the application of the Akaike Information Criterion as one of the parameters that provides information about the model fit could be of interest, as it penalizes higher model complexity [121]. Furthermore, the development of the model fit after 300 months of data input is of scientific interest. As the operational data available only spans a certain time frame, it was not possible to analyze the development of the goodness of fit for very long term data series. It would be interesting to use operational data from reservoirs where data has been collected for 50 or more years.

The thesis proposed several different sources of uncertainty for economical optimization when using NPV maximization as the goal. The quantification of the effects arising due to these sources of uncertainty is apt to be the major part of future theses' topics. Additionally, the NPV model could be extended by a terminal value calculation which takes the long-term development into account. Due to the high uncertainty that arises when long-term effects are analyzed, a quantification of the terminal value and its uncertainty might be interesting.

To conclude, the research for this thesis discusses the main sources of uncertainty for economic optimization of low temperature geothermal resources. Furthermore, it analyzed and explained the role of decreasing uncertainty for model fits by lumped parameter mod-

eling and proposed 10 seasonal cycles as a threshold for stabilizing the model fit. This time horizon can act as a stabilizing factor in the economic optimization and improve the accuracy of economic forecasting. Nevertheless, it would be of interest to extend the research focus and answer some of the questions that were beyond the scope of this thesis. Additionally, further practical analyses would be beneficial for proving the consistency in the coherence of the research results.

References

[1] State Government Victoria - Department of state development, business and innovation, "Renewable resourceful victoria," February 2010.

[2] U. S. Energy Information Admnisitration, "International energy statistics."

[3] J. McDowell and P. White, "Updated resource assessment and 3-d geological model of the mita geothermal system, guatemala," in *Geothermal Resources Council 2011 Annual Meeting, October 23-26, 2011, San Diego, California*, vol. 35. Geothermal Resources Council, 2011, pp. 99–107.

[4] O. E. Vallejos, *A conceptual reservoir model and numerical simulation studies for the Miravalles geothermal field, Costa Rica*. United Nations University, 1996.

[5] G. Gunnarsson, A. Arnaldsson, and A. L. Oddsdóttir, "Model simulation of the geothermal fields in the hengill area, south-western iceland," in *Proceedings World Geothermal Congress*, 2010.

[6] S. S. Gylfadóttir, "Reservoir assessment and modelling of geothermal systems," lecture Slides, Subsurface Exploration 2014 - ISE course.

[7] S. R. Sigurdardóttir, "Optimization for sustainable utilization of low temperature geothermal systems," Ph.D. dissertation, Reykjavik University, 2013.

[8] P. I. Daniel, "Natural resource taxation," in *Management of Natural Resources in Sub-Saharan Africa - Kinshasa Conference*, 2012.

[9] U. S. Energy Information Admnisitration, "US crude oil and natural gas proved reserves 2012."

[10] E. Gunnlaugsson, G. Gislason, G. Ivarsson, and S. P. Kjaran, "Low-temperature geothermal fields utilized for district heating in reykjavík, iceland," in *Proceedings World Geothermal Congress*, 2000.

[11] G. Ivarsson, "Heating utility in reykjavik - water production 2010," Orkuveita Reykjavikur, Tech. Rep., 2010.

[12] Intergovernmental Panel on Climate Change, "Fifth assessment report," 2014.

[13] U. S. Energy Information Administration, "Internation energy outlook 2013."

[14] ——, "International energy outlook 2014."

[15] United Nations, "United nations climate change conferences 1 - 20."

[16] A. Giddens, "The politics of climate change," *Policy Network*, 2009.

[17] N. H. Stern, *Stern Review: The economics of climate change*. HM Treasury London, 2006.

[18] BP, "Bp energy outlook 2035."

[19] A. Evans, V. Strezov, and T. J. Evans, "Assessment of sustainability indicators for renewable energy technologies," *Renewable and sustainable energy reviews*, vol. 13, no. 5, pp. 1082–1088, 2009.

[20] L. Rybach, "Geothermal energy: sustainability and the environment," *Geothermics*, vol. 32, no. 4, pp. 463–470, 2003.

[21] ——, "Geothermal sustainability," in *Proceedings European Geothermal Congress, Unterhaching, Germany*, 2007.

[22] R. DiPippo, *Geothermal Power Plants: Principles, Applications and Case Studies*. Elsevier Science, Jul. 2005.

[23] M. A. Grant and P. F. Bixley, *Geothermal Reservoir Engineering, Second Edition*, 2nd ed. Burlington, MA: Academic Press, Mar. 2011.

[24] E. Huenges and P. Ledru, *Geothermal Energy Systems: Exploration, Development, and Utilization*. John Wiley & Sons, Apr. 2010.

[25] B. J. Skinner and B. W. Murck, *Blue Planet An Introduction to Earth System Science, 3rd Edition*, 3rd ed. Hoboken, NJ: Wiley, Jan. 2011.

[26] K. Bjorlykke, *Petroleum Geoscience: From Sedimentary Environments to Rock Physics*. Springer Science & Business Media, Sep. 2010.

[27] J. W. Tester, E. M. Drake, and M. J. Driscoll, *Sustainable Energy: Choosing Among Options*. Cambridge, MA: Mit Pr, 2012.

[28] K. Burke and W. S. F. Kidd, "Were archean continental geothermal gradients much steeper than those of today?" *Nature*, vol. 272, no. 5650, pp. 240–241, 1978.

[29] I. Stober, *Geothermal Energy: From Theoretical Models to Exploration and Development*. New York: Springer, 2013.

[30] R. Cataldi, S. F. Hodgson, J. W. Lund, G. R. Council, and I. G. Association, *Stories from a Heated Earth: Our Geothermal Heritage*. Sacrament Calif: Geothermal Resources Council, Jul. 1999.

[31] R. Cataldi and P. Chiellini, "Geothermal energy in the mediterranean area before the middle ages," in *Proceedings World Geothermal Congress*, 1995, pp. 373–380.

[32] J. W. Lund, "Balneological use of thermal waters," *International Geothermal Days, Bad Urach, Germany*, 2001.

[33] H. Quick, J. Michael, H. Huber, and U. Arslan, "History of international geothermal power plants and geothermal projects in germany," in *Proceedings World Geothermal Congress*, 2010.

[34] D. A. Glowka, "The role of r and d in geothermal drilling cost reduction," Sandia National Labs., Albuquerque, NM (United States), Tech. Rep. SAND–97-1469C; CONF-971048–4, Jul. 1997.

[35] J. W. Tester and H. J. Herzog, *Economic predictions for heat mining: a review and analysis of hot dry rock (HDR) geothermal energy technology*. Energy Laboratory, Massachusetts Institute of Technology, 1990.

[36] S. L. Milora and J. W. Tester, "Geothermal energy as a source of electric power: Thermodynamic and economic design criteria," *NASA STI/Recon Technical Report A*, vol. 77, p. 16623, 1976.

[37] D. L. Norton, "Theory of hydrothermal systems," *Annual Review of Earth and Planetary Sciences*, vol. 12, no. 1, pp. 155–177, 1984.

[38] V. Hardardottir, "Metal-rich scales in the reykjanes geothermal system, SW iceland: sulfide minerals in a seawater-dominated hydrothermal environment," Ph.D. dissertation, University of Ottawa, 2011.

[39] S. Arnorsson, "Major element chemistry of the geothermal sea-water at reykjanes and svartsengi, iceland," *Mineralogical Magazine*, vol. 42, no. 322, p. 209, 1978.

[40] H. Gupta, *Geothermal Energy: An Alternative Resource for the 21st Century*. Elsevier Science, 2006.

[41] R. Allis, "Insights on the formation of vapor-dominated geothermal systems," in *Proceedings World Geothermal Congress*, 2000, pp. 2489–2496.

[42] S. E. Ingebritsen and M. L. Sorey, "Vapor-dominated zones within hydrothermal systems: Evolution and natural state," *Journal of Geophysical Research: Solid Earth (1978–2012)*, vol. 93, no. B11, pp. 13 635–13 655, 1988.

[43] D. E. White, L. J. P. Muffler, and A. H. Truesdell, "Vapor-dominated hydrothermal systems compared with hot-water systems," *Economic Geology*, vol. 66, no. 1, pp. 75–97, 1971.

[44] D. E. White, "Diverse origins of hydrothermal ore fluids," *Economic Geology*, vol. 69, no. 6, pp. 954–973, 1974.

[45] P. H. Jones, "Geothermal resources of the northern gulf of mexico basin," *Geothermics*, vol. 2, Part 1, pp. 14–26, 1970.

[46] J. H. S. Duffield, Wendell A., *Geothermal Energy: Clean Power from the Earth's Heat*. Diane Publishing, 2003.

[47] S. K. Sanyal, A. Robertson-Tait, M. Kraemer, and N. Buening, "A survey of potential geopressured resource areas in california," in *Eigtheenth Workshop of Geothermal Reservoir Engineering*, 1993.

[48] R. Blackett, J. Satrape, and G. Beeland, "A decade of geothermal development in the united states 1974-1984: a federal perspective," *Geothermal Resources Council Bulletin*, vol. 15, no. 7, pp. 5–14, 1986.

[49] J. Negus-de Wys and M. Dorfman, "The geopressured-geothermal resource: Transition to commercialization," EG and G Idaho, Inc., Idaho Falls, ID (USA), Tech. Rep., 1990.

[50] H. J. Herzog, J. W. Tester, and M. G. Frank, "Economic analysis of heat mining," *Energy sources*, vol. 19, no. 1, pp. 19–33, 1997.

[51] J. W. Tester and H. J. Herzog, "The economics of heat mining: An analysis of design options and performance requirements of hot dry rock (HDR) geothermal power systems," *Energy Syst. Policy*, vol. 25, pp. 33–63, 1991.

[52] Google Press, "Google.org invests more than 10 million dollars in breakthrough geothermal energy technology."

[53] "The future of geothermal energy," Massachusetts Institute of Technology, Tech. Rep., 2006.

[54] H. C. H. Armstead and J. W. Tester, *Heat mining*. Chapman and Hall, 1986.

[55] D. W. Brown, D. V. Duchane, and V. T. Hriscu, *Mining the Earth's Heat: Hot Dry Rock Geothermal Energy*. Berlin ; London: Springer, Apr. 2012.

[56] W. A. Elders, G. O. Fridleifsson, and B. Pálsson, "Iceland deep drilling project: The first well, IDDP-1, drilled into magma," *Geothermics*, vol. 49, p. 1, Jan. 2014.

[57] G. O. Fridleifsson, W. A. Elders, and A. Albertsson, "The concept of the iceland deep drilling project," *Geothermics*, vol. 49, pp. 2–8, Jan. 2014.

[58] W. A. Elders, G. O. Fridleifsson, and A. Albertsson, "Drilling into magma and the implications of the iceland deep drilling project (IDDP) for high-temperature geothermal systems worldwide," *Geothermics*, vol. 49, pp. 111–118, Jan 2014.

[59] G. O. Fridleifsson, O. Sigurdsson, D. Thorbjornsson, R. Karlsdottir, T. Gislason, A. Albertsson, and W. A. Elders, "Preparation for drilling well IDDP-2 at reykjanes," *Geothermics*, vol. 49, pp. 119–126, Jan. 2014.

[60] B. Lindal, *Industrial and other applications of geothermal energy*. United Nations Educational, Scientific and Cultural Organization, 1973.

[61] T. J. Hammons and A. Gunnarsson, "Geothermal sustainability in europe and worldwide," in *Universities Power Engineering Conference, 2008. UPEC 2008. 43rd International*. IEEE, 2008, pp. 1–10.

[62] P. M. Wright, "The sustainability of production from geothermal resources," *Bull. Geo-Heat Center*, vol. 19, no. 2, pp. 9–12, 1998.

[63] R. G. Bloomquist, "Geothermal space heating," *Geothermics*, vol. 32, no. 4–6, pp. 513–526, Aug 2003.

[64] E. Gunnlaugsson, H. Frimannson, and G. Sverrisson, "District heating in reykjavik-70 years experience," in *Proceedings World Geothermal Congress. Kyushu-Tohoku, Japan*, 2000.

[65] A. Ragnarsson, "Utilization of geothermal energy in iceland," in *Proceedings of the International Geothermal Conference IGC-2003*, vol. 10, 2003, pp. 39–45.

[66] J. W. Lund, "Direct utilization of geothermal energy," *Energies*, vol. 3, no. 8, pp. 1443–1471, Aug. 2010.

[67] S. Arason, "The drying of fish and utilization of geothermal energy; the icelandic experience," in *International Geothermal Conference, Reykjavík*, 2003.

[68] H. Stachowiak, *Allgemeine Modelltheorie*. Wien: Springer, 2013.

[69] G. S. Bodvarsson, K. Pruess, and M. J. Lippmann, "Modeling of geothermal systems," *Journal of petroleum technology*, vol. 38, no. 10, pp. 1007–1021, 1986.

[70] W. Cumming, "Geothermal resource conceptual models using surface exploration data," in *Proceedings*, 2009.

[71] M. J. O'Sullivan, K. Pruess, and M. J. Lippmann, "State of the art of geothermal reservoir simulation," *Geothermics*, vol. 30, no. 4, pp. 395–429, 2001.

[72] K. Pruess, *Mathematical modeling of fluid flow and heat transfer in geothermal systems : an introduction in five lectures*. Orkustofnun, 2002.

[73] G. Axelsson, G. Björnsson, and J. E. Quijano, "Reliability of lumped parameter modeling of pressure changes in geothermal reservoirs," in *World Geothermal Congress 2005, Turkey*, 2005.

[74] H. Sarak, M. Onur, and A. Satman, "Applications of lumped-parameter models for simulation of low-temperature geothermal reservoirs," in *Proceedings of the 28th Workshop on Geothermal Reservoir Engineering, Stanford, USA*, 2003, pp. 307–315.

[75] G. Axelsson, "Simulation of pressure response data from geothermal reservoirs by lumped parameter models," in *14th Workshop on Geothermal Reservoir Engineering, Stanford, USA*, 1989, pp. 257–263.

[76] S. S. Gylfadottir, G. Axelsson, and T. Arason, *PyLumpfit User Manual*, July 2014.

[77] H. Sarak, M. Onur, and A. Satman, "Lumped-parameter models for low-temperature geothermal fields and their application," *Geothermics*, vol. 34, no. 6, pp. 728–755, 2005.

[78] F. J. Fabozzi, *Financial modeling of the equity market: from CAPM to cointegration*. John Wiley and Sons, 2006.

[79] S. Kaplan, "The valuation of cash flow forecasts: an empirical analysis," *The Journal of Finance*, vol. 50, no. 4, pp. 1159 – 1094, 2003.

[80] K. Spremann, *Valuation*. Oldenbourg Wissenschaftsverlag, 2004.

[81] N. Moyen, "Valuing risk and flexibility," *Resources Policy*, vol. 22, no. 1/2, pp. 63 – 74, 1996.

[82] E. Brigham and M. Erhardt, *Financial mananagement - theory and practice*. Cengage Learning, 2011.

[83] S. P. Pratt, *Cost of capital: applications and examples*. Wiley, 2010.

[84] S. Armitage, *The Cost of Capital: Intermediate Theory*. Cambridge University Press, Mar. 2005.

[85] K. Spremann, *Portfoliomanagement*. Oldenbourg Wissenschaftsverlag, 2006.

[86] U. S. Energy Information Administration, "Annual energy outlook."

[87] J. D. Hamilton, "Understanding crude oil prices," National Bureau of Economic Research, Tech. Rep., 2008.

[88] ——, "What is an oil shock?" *Journal of Econometrics*, vol. 113, pp. 363–398, April 2003.

[89] ——, "Nonlinearities and the macroeconomic effects of oil prices," *Macroeconomic Dynamics*, vol. 15, pp. 364–378, 2011.

[90] Y.-W. Cheung, M. D. Chinn, and A. G. Pascual, "Empirical exchange rate models of the nineties: Are any fit to survive?" *Journal of International Money and Finance*, vol. 24, no. 7, pp. 1150–1175, 2005.

[91] M. D. Chinn and R. A. Meese, "Banking on currency forecasts: How predictable is change in money?" *Journal of International Economics*, vol. 38, no. 1, pp. 161–178, 1995.

[92] C. Engel, "Can the markov switching model forecast exchange rates?" *Journal of International Economics*, vol. 36, no. 1, pp. 151–165, 1994.

[93] R. Meese and K. Rogoff, "The out-of-sample failure of empirical exchange rate models: sampling error or misspecification?" in *Exchange rates and international macroeconomics*. University of Chicago Press, 1983, pp. 67–112.

[94] L. Kilian and M. P. Taylor, "Why is it so difficult to beat the random walk forecast of exchange rates?" *Journal of International Economics*, vol. 60, no. 1, pp. 85–107, 2003.

[95] A. Abhyankar, L. Sarno, and G. Valente, "Exchange rates and fundamentals: evidence on the economic value of predictability," *Journal of International Economics*, vol. 66, no. 2, pp. 325–348, Jul. 2005.

[96] S. Thorhallsson and B. M. Sveinbjornsson, "Geothermal drilling cost and drilling effectiveness," *Short Course on Geothermal Development and Geothermal Wells, UNU-GTP, Santa Tecla, El Salvador*, 2012.

[97] V. Stefansson, "Investment cost for geothermal power plants," *Geothermics*, vol. 31, no. 2, pp. 263–272, 2002.

[98] International Finance Corporation, "Success of geothermal wells: A global study," World Bank Group, Tech. Rep., 2013.

[99] S. K. Sanyal and J. W. Morrow, "An investigation of drilling success in geothermal exploration, development and operation," *Geothermal Resources Council: Transactions*, vol. 35, pp. 233–237, 2011.

[100] M. Wendel, M. Hiegl, F. Jaudin, A. Poux, and others, "GEOFAR–financing geothermal energy in european regions," in *Proceedings World Geothermal Congress 2010*, 2010.

[101] H. Asaue, T. Kubo, T. Yoshinaga, and K. Koike, "Characterization of temporal change of deep resistivity around geothermal reservoir using magnetotelluric survey," in *Proceedings, World Geothermal Congress, April 25-29, Bali, Indonesia*, 2010.

[102] R. L. Detwiler, J. J. Roberts, W. Ralph, and B. P. Bonner, "Modeling fluid flow and electrical resistivity in fractured geothermal reservoir rocks," in *Proceedings, Twenty Eighth Annual Geothermal Reservoir Engineering Workshop, January 27-29, Stanford, USA*, 2003, pp. 301–306.

[103] L. S. Georgsson and R. Karlsdóttir, "Resistivity methods-DC and TEM with examples and comparison from the reykjanes peninsula and Öxarfjördur, iceland," *Short Course V on Exploration for Geothermal Resources, organized by UNU-GTP, GDC and Kengen, Kenya*, 2010.

[104] J. Taron and D. Elsworth, "Thermal–hydrologic–mechanical–chemical processes in the evolution of engineered geothermal reservoirs," *International Journal of Rock Mechanics and Mining Sciences*, vol. 46, no. 5, pp. 855–864, Jul. 2009.

[105] H. Franzson, E. Gunnlaugsson, K. Árnason, K. Saemundsson, B. Steingrimsson, and B. S. Hardarson, "The hengill geothermal system, conceptual model and thermal evolution," in *Proceedings World Geothermal Congress*, 2010.

[106] E. Gunnlaugsson, "District heating in reykjavík; past–present–future," in *UNU Geothermal Training Programme. 30th Anniversary Workshop, Reykjavík, Iceland*, 2008.

[107] M. Martinovic, *Lumped and distributed parameter models of the Mosfellssveit geothermal field, SW-Iceland*. United Nations University, 1990, no. 9.

[108] D. R. Anderson, D. J. Sweeney, and T. A. Williams, *Statistics for business and economics*. West Pub. Co., 1984.

[109] T. T. Allen, *Introduction to Engineering Statistics and Lean Sigma: Statistical Quality Control and Design of Experiments and Systems*. Springer Science & Business Media, 2010.

[110] A. Jeffrey, *Advanced Engineering Mathematics*. Academic Press, Jun. 2001.

[111] J. D. Hoffman and S. Frankel, *Numerical Methods for Engineers and Scientists, Second Edition,*. CRC Press, 2001.

[112] W. E. Glassley, *Geothermal Energy: Renewable Energy and the Environment, Second Edition*. CRC Press, Oct. 2014.

[113] H. T. Heide, "Migration models and their significance for population forecasts," *The Milbank Memorial Fund Quarterly*, vol. 41, no. 1, pp. 56–76, Jan. 1963.

[114] G. S. Becker, *The Economic Approach to Human Behavior*. Chicago: University of Chicago Press, Sep. 1978.

[115] N. G. Mankiw, *Principles of Economics*, 6th ed. Mason, OH: Cengage Learning, Feb. 2011.

[116] M. E. Porter, *How competitive forces shape strategy*. Harvard Business Review Boston, 1979, vol. March/April.

[117] ——, *The Five Competitive Forces That Shape Strategy*. Harvard Business Review Boston, 2008.

[118] P. C. Reiss and M. W. White, "Household electricity demand, revisited," National Bureau of Economic Research, Working Paper 8687, Dec. 2001.

[119] M. A. Bernstein, J. M. Griffin, and S. Infrastructure, *Regional differences in the price-elasticity of demand for energy*. National Renewable Energy Laboratory, 2006.

[120] R. Nesbakken, "Energy consumption for space heating: A discrete–continuous approach," *Scandinavian Journal of Economics*, vol. 103, no. 1, pp. 165–184, 2001.

[121] H. Akaike, "A new look at the statistical model identification," *Automatic Control, IEEE Transactions on*, vol. 19, no. 6, pp. 716–723, 1974.

Appendix A

Production and Drawdown Data

The following two pages show the measured production data of the low temperature geothermal fields Ellidaar, Laugarnes, Reykir and Reykjahlid.

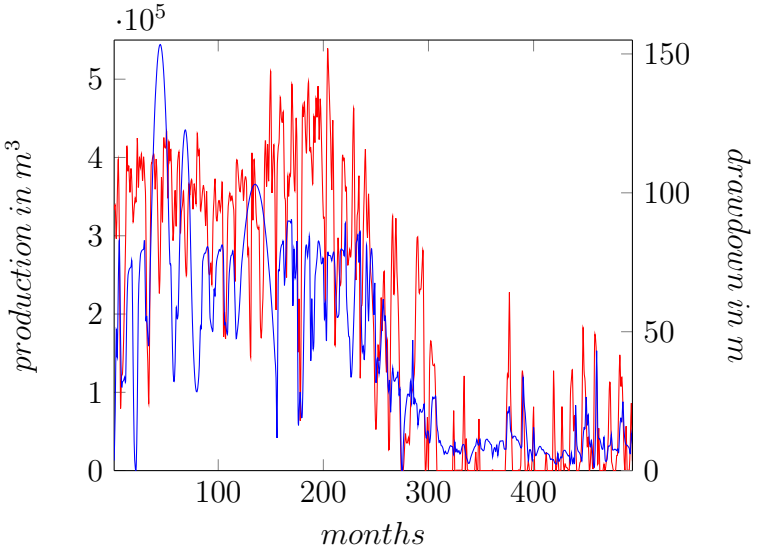

Figure 34: Production and drawdown data from Ellidaar; production is displayed by the red line; drawdown data from reference well RV-27 is displayed by the blue line

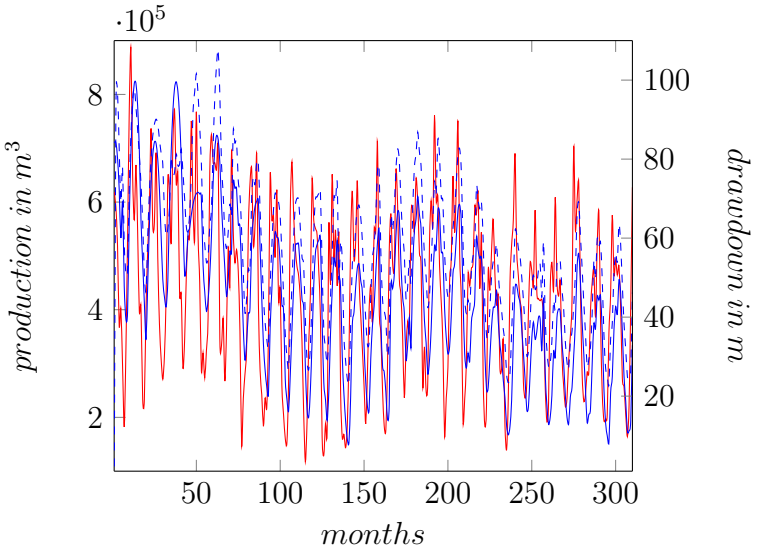

Figure 35: Production and drawdown data from Laugarnes; production is displayed by the red line; drawdown data from reference well RV-7 is displayed by the blue line; RV-34 by the dashed blue line

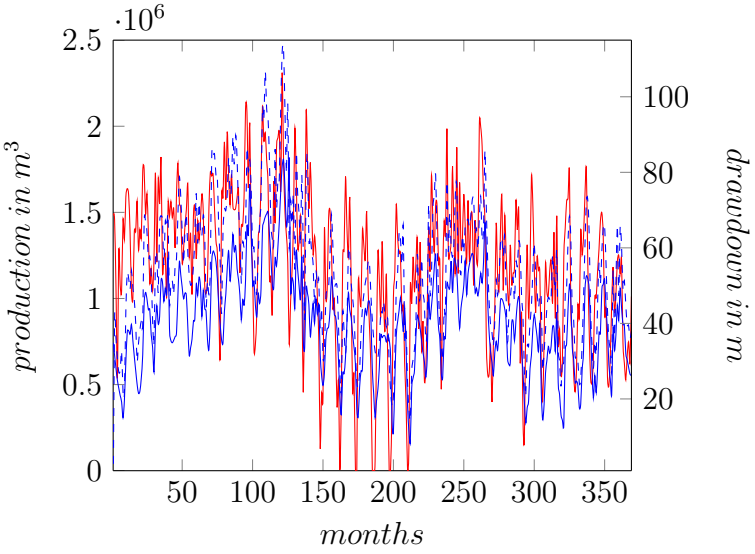

Figure 36: Production and drawdown data from Reykir; production is displayed by the red line; drawdown data from reference well MG-1 is displayed by the blue line; SR-32 by the dashed blue line

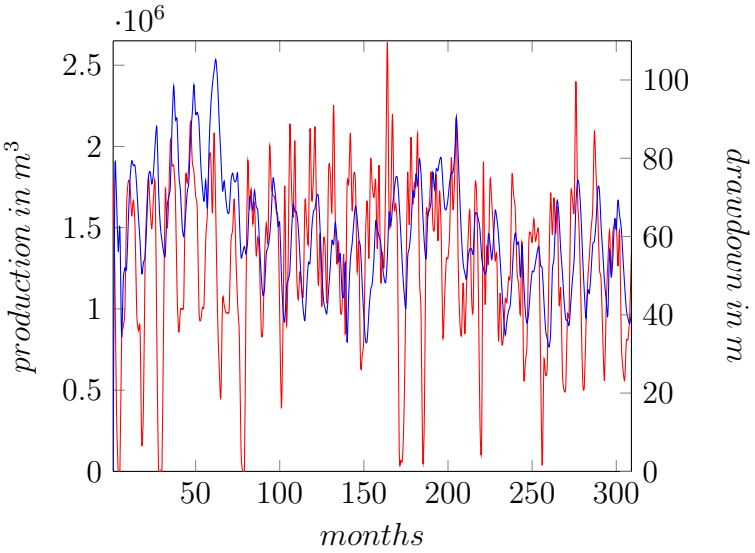

Figure 37: Production and drawdown data from Reykjahlid; production is displayed by the red line; drawdown data from reference well MG-28 is displayed by the blue line

Appendix B

Initial Model Fits

The following pages show the initial LPM fit for Ellidaar, Laugarnes, Reykir and Reykjahlid. The graphs show the production throughout the data collection period, as well as the measured and the calculated water level. The fit for six different model complexities is shown.

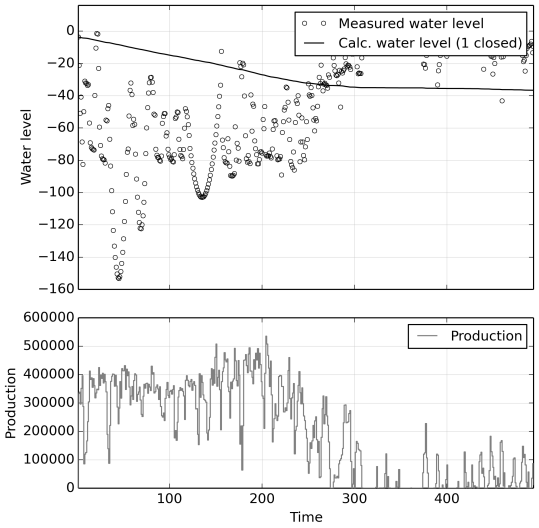

(a) One tank closed system

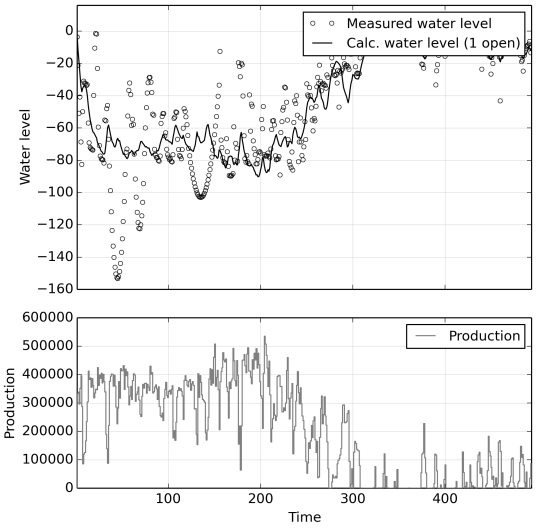

(b) One tank open system

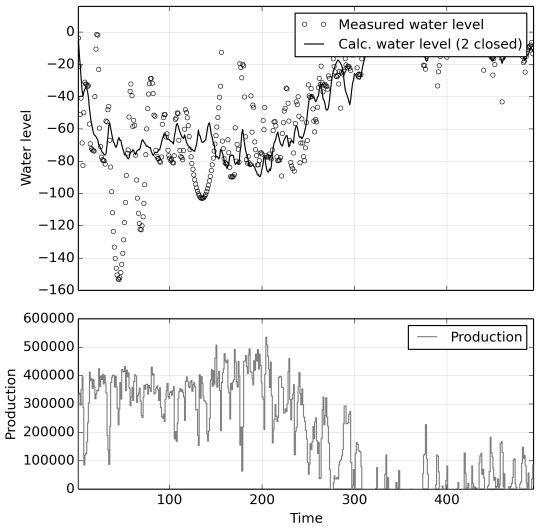

(c) Two tank closed system

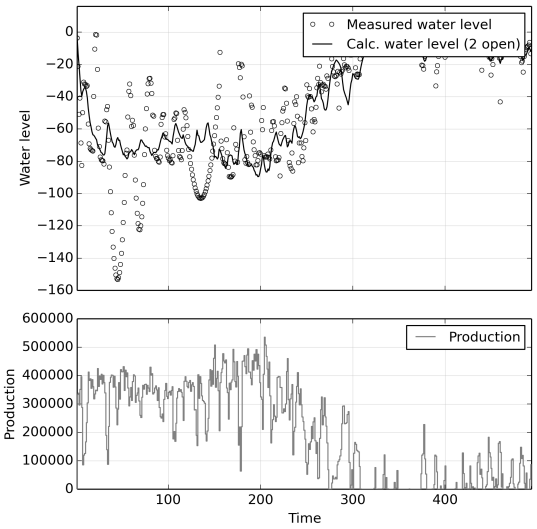

(d) Two tank open system

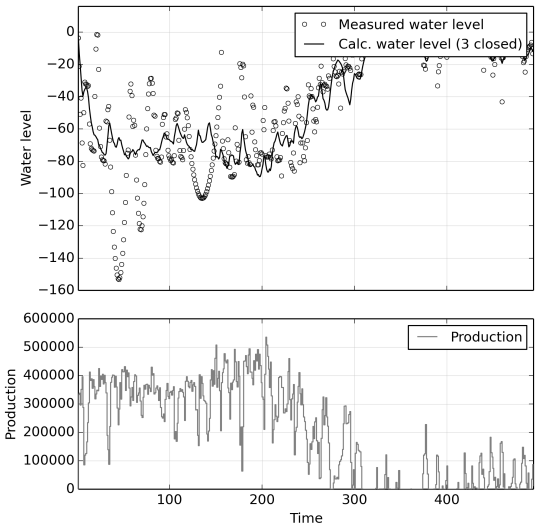

(e) Three tank closed system

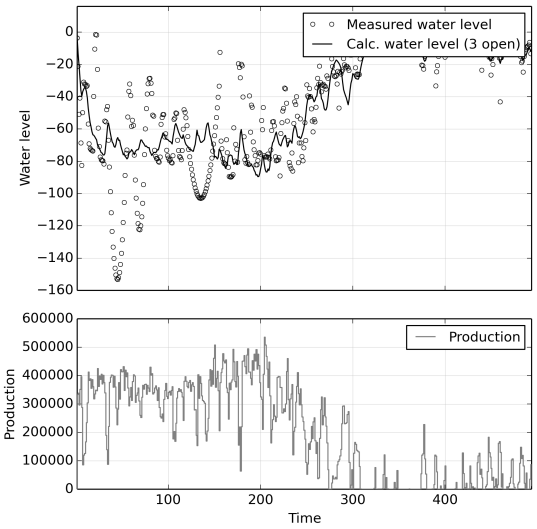

(f) Three tank open system

Figure 38: Ellidaar's initial fit

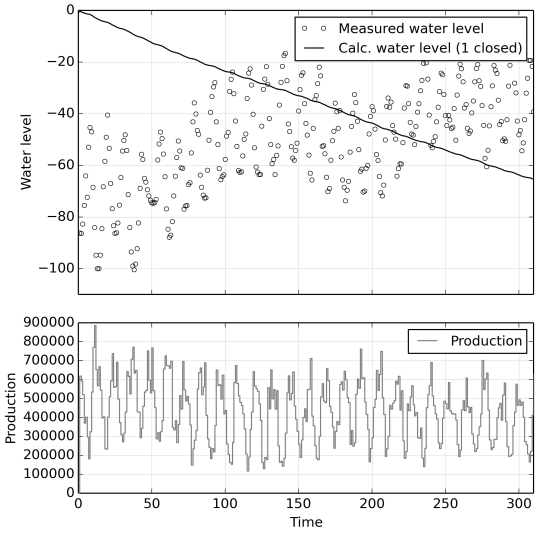

(a) One tank closed system

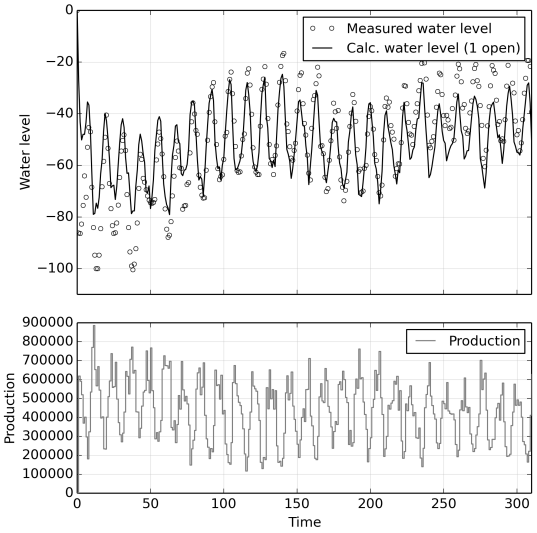

(b) One tank open system

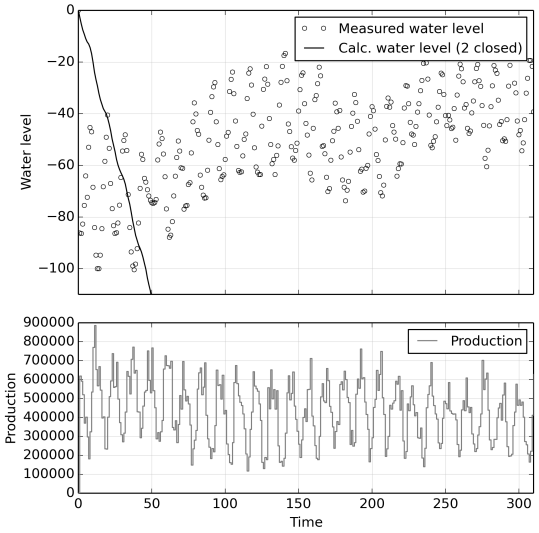

(c) Two tank closed system

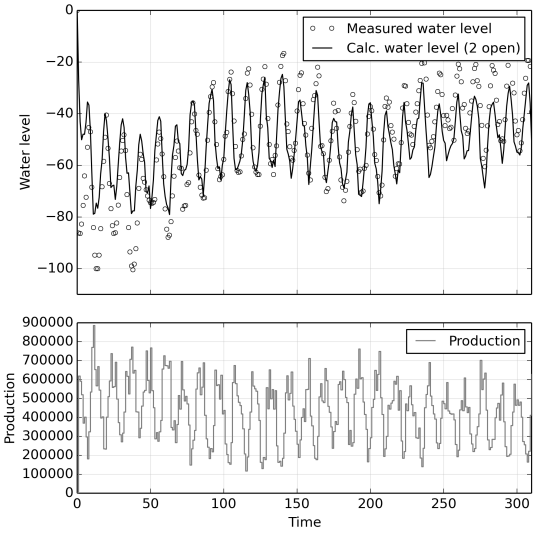

(d) Two tank open system

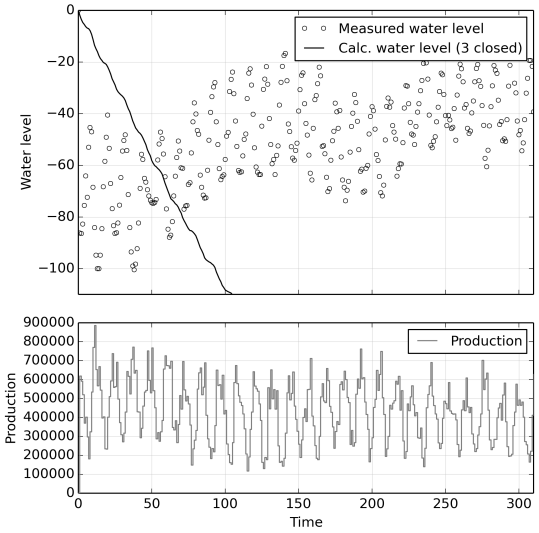

(e) Three tank closed system

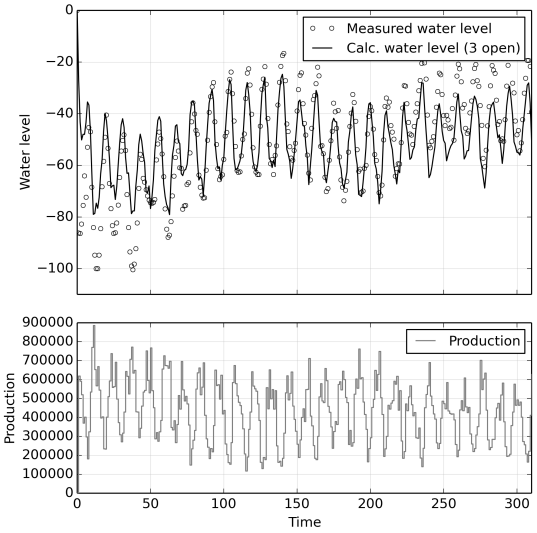

(f) Three tank open system

Figure 39: Laugarnes' initial fit - RV-7

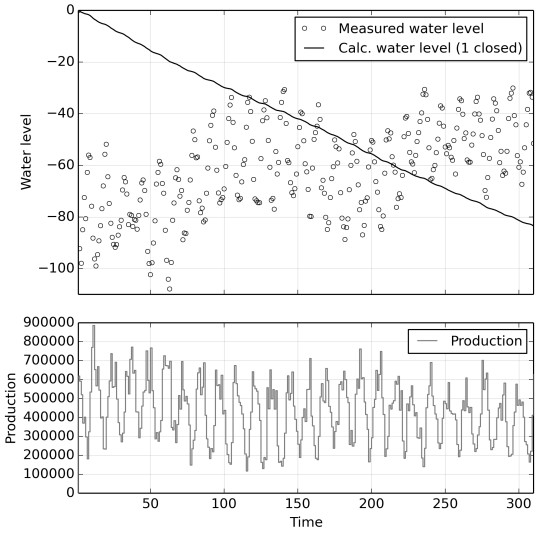

(a) One tank closed system

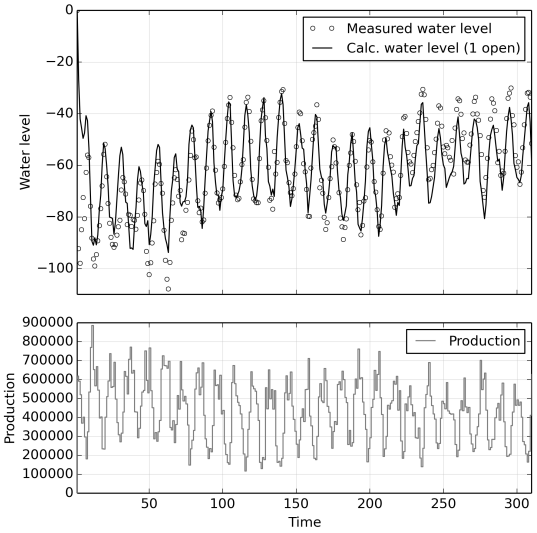

(b) One tank open system

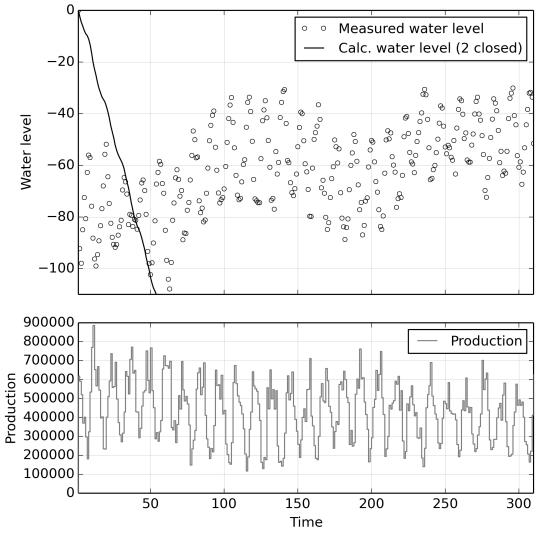

(c) Two tank closed system

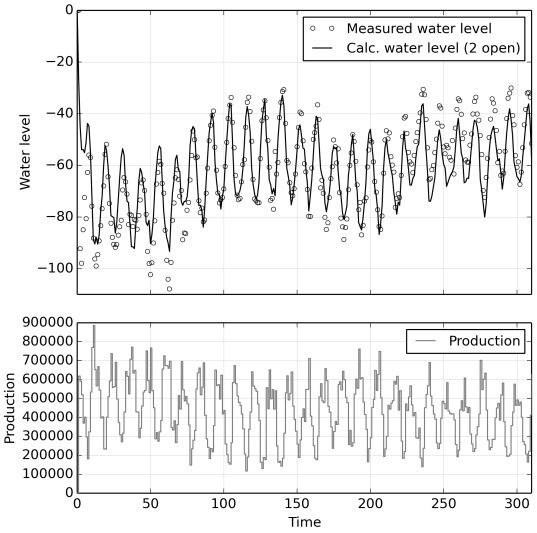

(d) Two tank open system

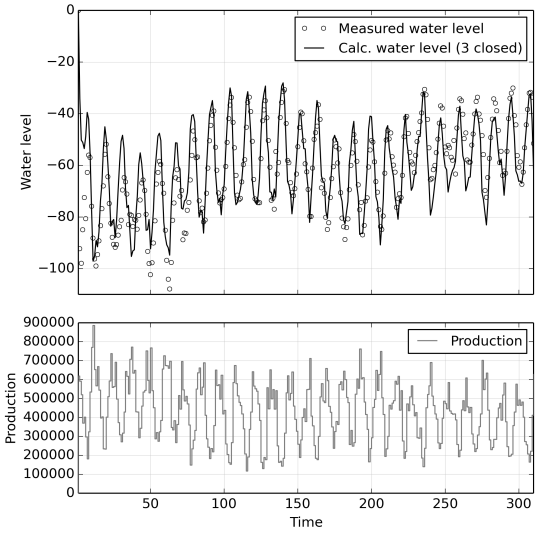

(e) Three tank closed system

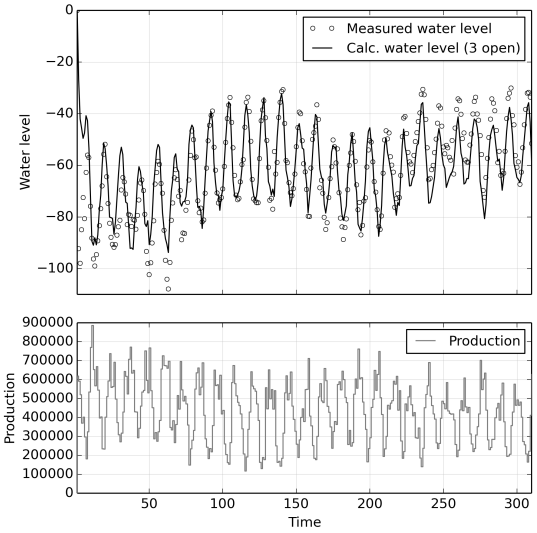

(f) Three tank open system

Figure 40: Laugarnes' initial fit - RV-34

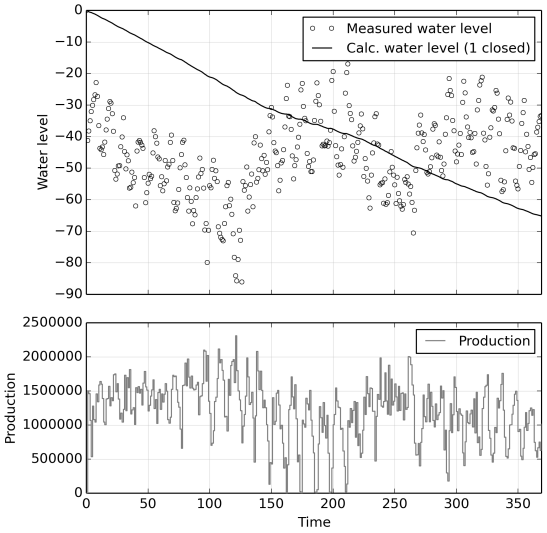

(a) One tank closed system

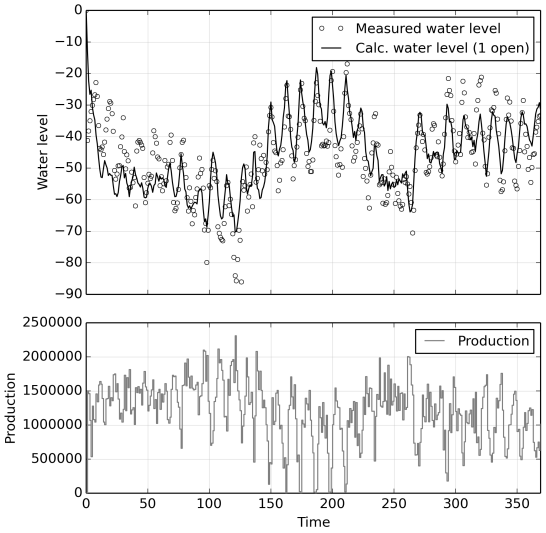

(b) One tank open system

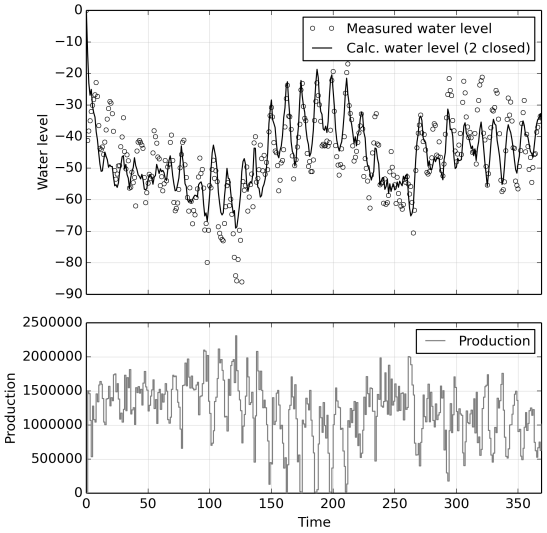

(c) Two tank closed system

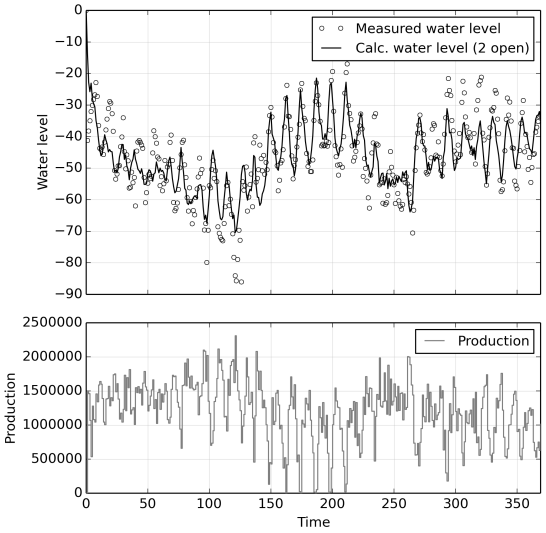

(d) Two tank open system

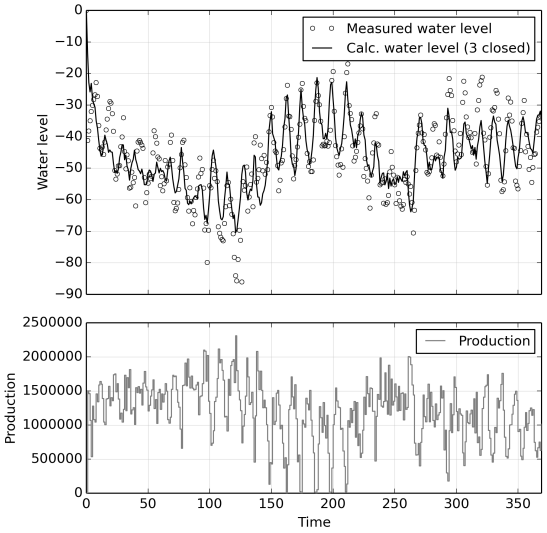

(e) Three tank closed system

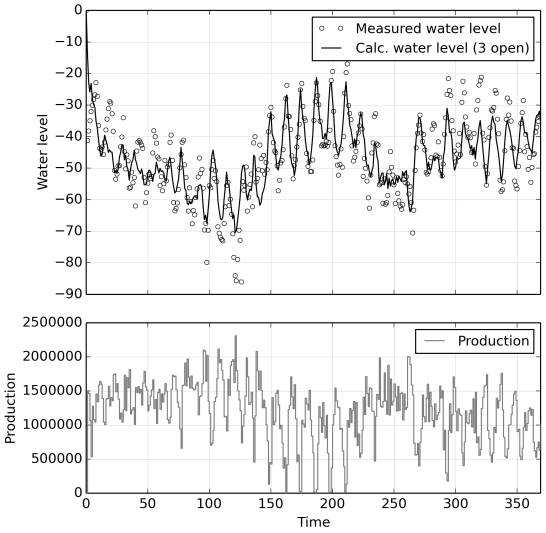

(f) Three tank open system

Figure 41: Reykir's initial fit - MG-1

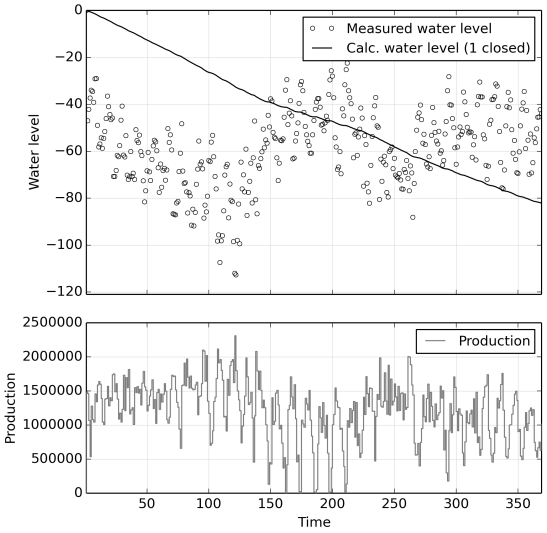

(a) One tank closed system

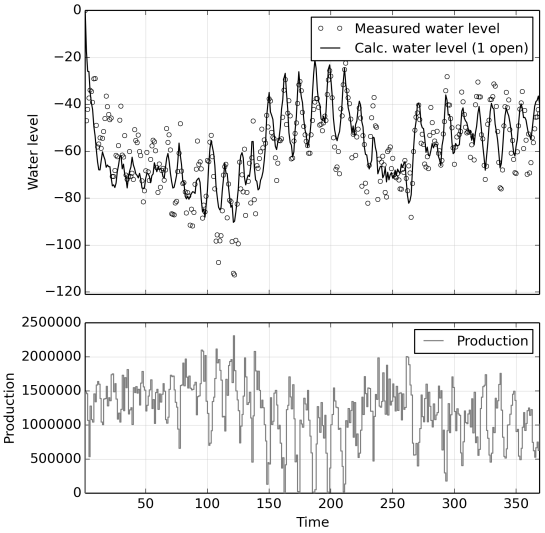

(b) One tank open system

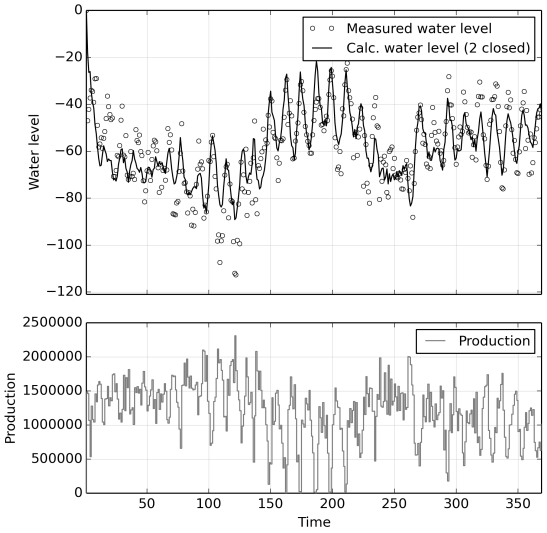

(c) Two tank closed system

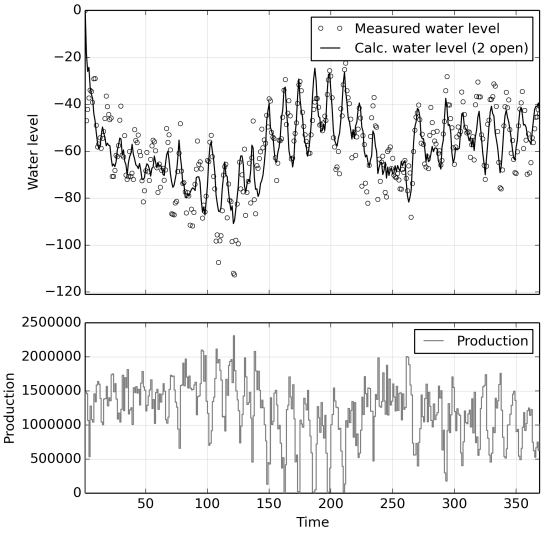

(d) Two tank open system

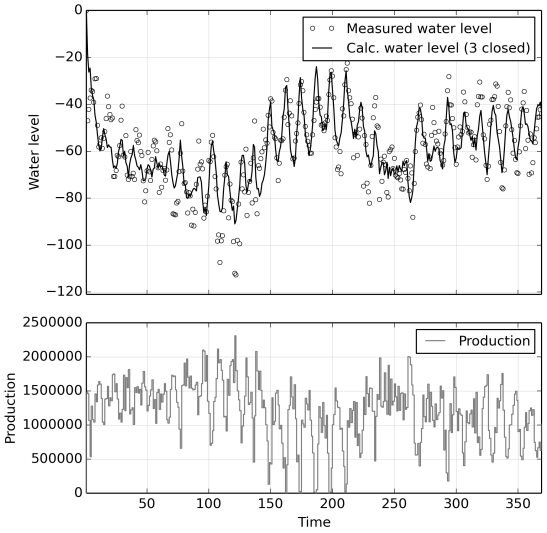

(e) Three tank closed system

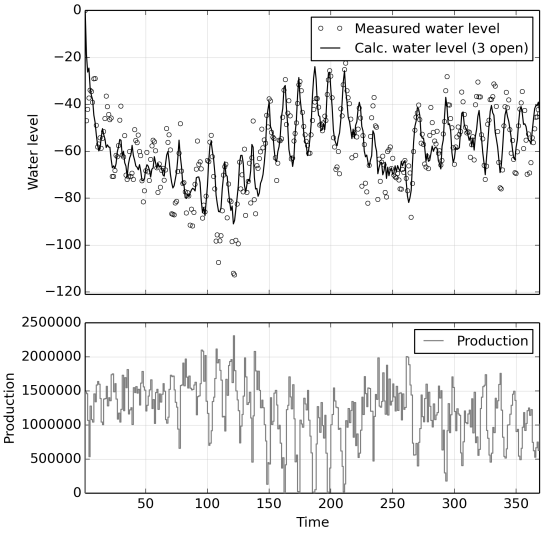

(f) Three tank open system

Figure 42: Reykir's initial fit - SR-32

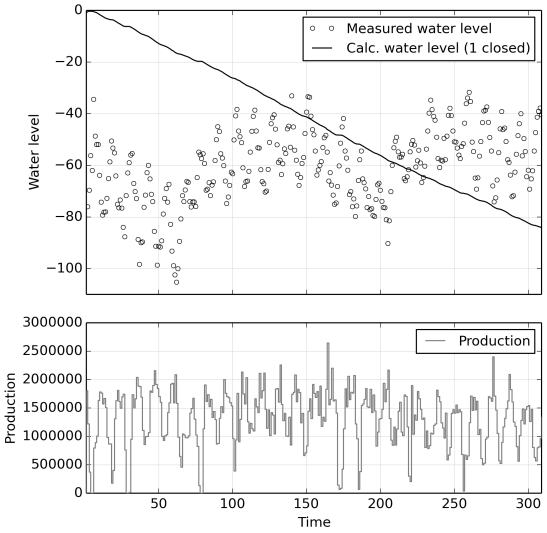

(a) One tank closed system

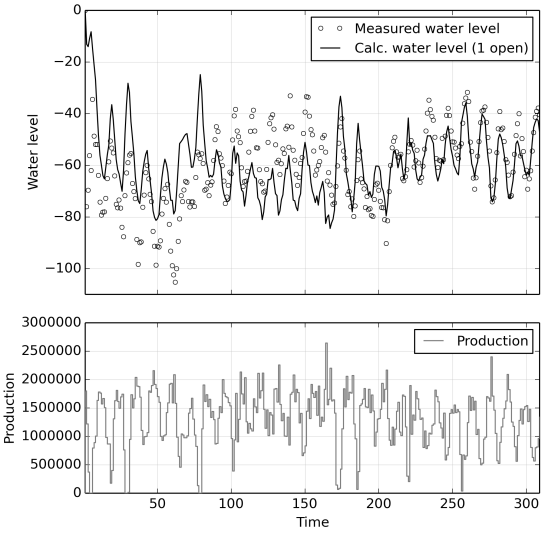

(b) One tank open system

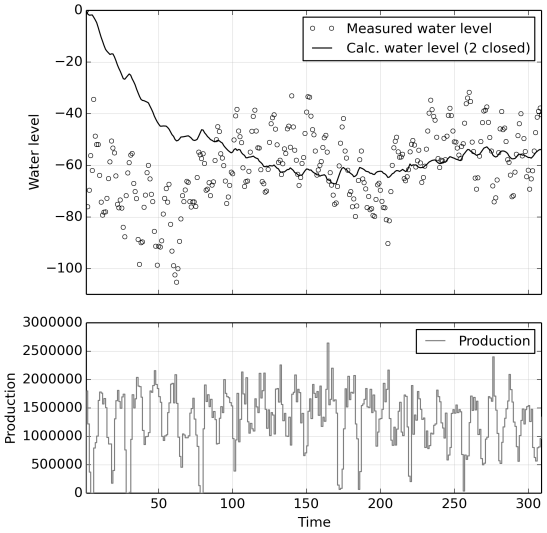

(c) Two tank closed system

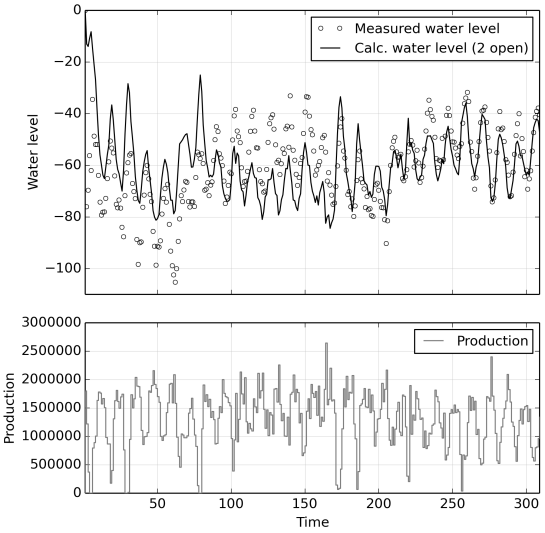

(d) Two tank open system

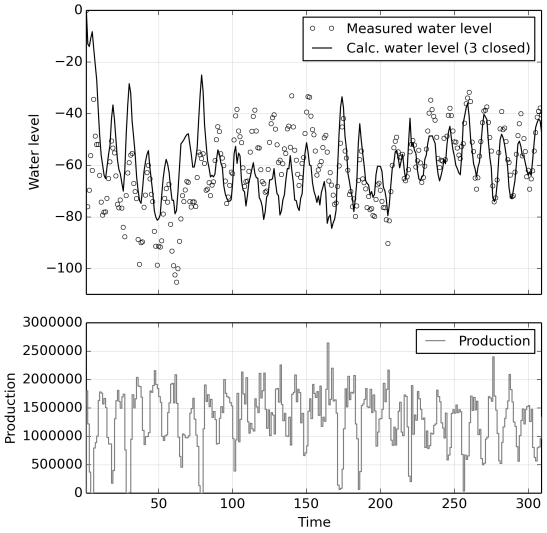

(e) Three tank closed system

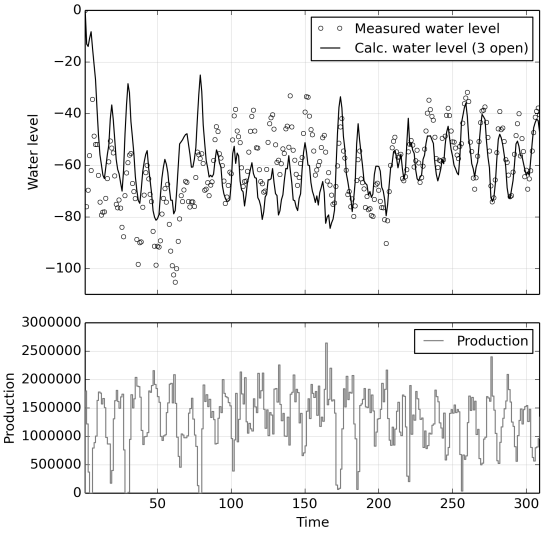

(f) Three tank open system

Figure 43: Reykjahlid's initial fit

Appendix C

Coefficient of Determination Tables

The following two tables show the R^2 and $\bar{R}^2$ values with increasing complexity and decreasing uncertainty.

Table 8: R^2 values for the individual field/reference well with decreasing uncertainty

	data input	**1 closed**	**1 open**	**2 closed**	**2 open**	**3 closed**	**3 open**
Ellidaar RV-27	60	0.00	0.24	0.24	0.24	0.24	0.24
Ellidaar RV-27	120	0.00	0.11	0.10	0.11	0.11	0.11
Ellidaar RV-27	180	0.00	0.04	0.04	0.04	0.04	0.04
Ellidaar RV-27	240	0.00	0.01	0.00	0.00	0.00	0.00
Ellidaar RV-27	300	0.00	0.27	0.27	0.27	0.27	0.27
Laugarnes RV-7	60	0.00	0.63	0.63	0.63	0.63	0.63
Laugarnes RV-7	120	0.00	0.66	0.65	0.66	0.66	0.66
Laugarnes RV-7	180	0.00	0.69	0.00	0.69	0.69	0.69
Laugarnes RV-7	240	0.00	0.68	0.00	0.68	0.67	0.67
Laugarnes RV-7	300	0.00	0.66	0.00	0.66	0.66	0.66
Laugarnes RV-34	60	0.00	0.41	0.41	0.41	0.41	0.41
Laugarnes RV-34	120	0.00	0.58	0.58	0.58	0.58	0.58
Laugarnes RV-34	180	0.00	0.68	0.66	0.68	0.68	0.68
Laugarnes RV-34	240	0.00	0.70	0.00	0.70	0.69	0.69
Laugarnes RV-34	300	0.00	0.70	0.00	0.70	0.68	0.70
Reykjahlid MG-28	60	0.00	0.39	0.39	0.39	0.39	0.39
Reykjahlid MG-28	120	0.00	0.03	0.03	0.03	0.03	0.03
Reykjahlid MG-28	180	0.00	0.00	0.00	0.00	0.00	0.00
Reykjahlid MG-28	240	0.00	0.00	0.00	0.00	0.00	0.00
Reykjahlid MG-28	300	0.00	0.13	0.07	0.13	0.13	0.13
Reykir MG-1	60	0.00	0.21	0.32	0.33	0.33	0.33
Reykir MG-1	120	0.00	0.50	0.69	0.69	0.69	0.69
Reykir MG-1	180	0.00	0.56	0.65	0.67	0.67	0.67
Reykir MG-1	240	0.00	0.57	0.67	0.71	0.71	0.71
Reykir MG-1	300	0.00	0.60	0.65	0.70	0.70	0.70
Reykir SR-32	60	0.00	0.52	0.61	0.64	0.64	0.64
Reykir SR-32	120	0.00	0.59	0.73	0.73	0.73	0.73
Reykir SR-32	180	0.00	0.63	0.68	0.72	0.71	0.71
Reykir SR-32	240	0.00	0.66	0.70	0.73	0.73	0.73
Reykir SR-32	300	0.00	0.66	0.68	0.72	0.72	0.72

Table 9: $\bar{R}^2$ values for the individual field/reference well with decreasing uncertainty

	1 closed	**1 open**	**2 closed**	**2 open**	**3 closed**	**3 open**
Ellidaar RV-27	-0.02	0.21	0.20	0.18	0.17	0.15
Ellidaar RV-27	-0.01	0.09	0.08	0.08	0.07	0.06
Ellidaar RV-27	-0.01	0.03	0.02	0.02	0.01	0.01
Ellidaar RV-27	0.00	0.00	-0.01	-0.02	-0.02	-0.03
Ellidaar RV-27	0.00	0.27	0.26	0.26	0.26	0.26
Laugarnes RV-7	-0.02	0.62	0.61	0.60	0.60	0.59
Laugarnes RV-7	-0.01	0.65	0.64	0.65	0.65	0.64
Laugarnes RV-7	-0.01	0.69	-0.02	0.68	0.68	0.68
Laugarnes RV-7	0.00	0.68	-0.01	0.67	0.66	0.66
Laugarnes RV-7	0.00	0.66	-0.01	0.66	0.65	0.65
Laugarnes RV-34	-0.02	0.39	0.38	0.37	0.36	0.34
Laugarnes RV-34	-0.01	0.57	0.57	0.57	0.56	0.56
Laugarnes RV-34	-0.01	0.68	0.65	0.67	0.67	0.67
Laugarnes RV-34	0.00	0.70	-0.01	0.69	0.68	0.68
Laugarnes RV-34	0.00	0.70	-0.01	0.70	0.67	0.69
Reykjahlid MG-28	-0.02	0.37	0.36	0.35	0.33	0.32
Reykjahlid MG-28	-0.01	0.01	0.00	0.00	-0.01	-0.02
Reykjahlid MG-28	-0.01	-0.01	-0.02	-0.02	-0.03	-0.03
Reykjahlid MG-28	0.00	-0.01	-0.01	-0.02	-0.02	-0.03
Reykjahlid MG-28	0.00	0.12	0.06	0.12	0.12	0.11
Reykir MG-1	-0.02	0.18	0.28	0.28	0.27	0.25
Reykir MG-1	-0.01	0.49	0.68	0.68	0.68	0.67
Reykir MG-1	-0.01	0.56	0.64	0.66	0.66	0.66
Reykir MG-1	0.00	0.57	0.67	0.71	0.70	0.70
Reykir MG-1	0.00	0.60	0.65	0.70	0.69	0.69
Reykir SR-32	-0.02	0.50	0.59	0.61	0.61	0.60
Reykir SR-32	-0.01	0.58	0.72	0.72	0.72	0.72
Reykir SR-32	-0.01	0.63	0.67	0.71	0.70	0.70
Reykir SR-32	0.00	0.66	0.70	0.73	0.72	0.72
Reykir SR-32	0.00	0.66	0.68	0.72	0.72	0.71

Appendix D

Drawdown Forecasting Figures

The next page shows the drawdown forecast for Reykir's SR-32 reference well. Forecasted with the seasonal variation of the main 80% of the production data, taken from the first 60 months.

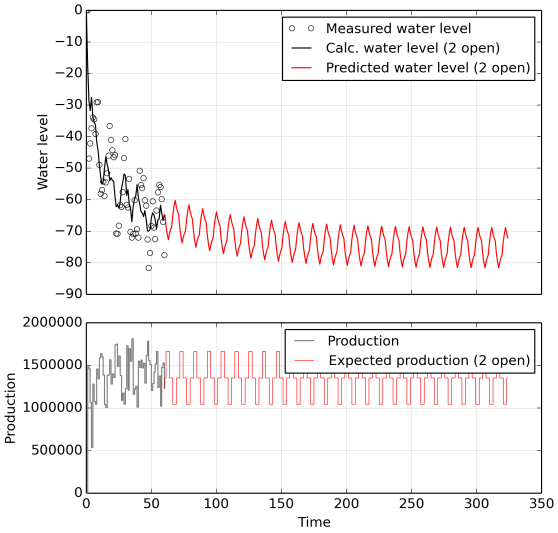

(a) Forecast with 60 months data input

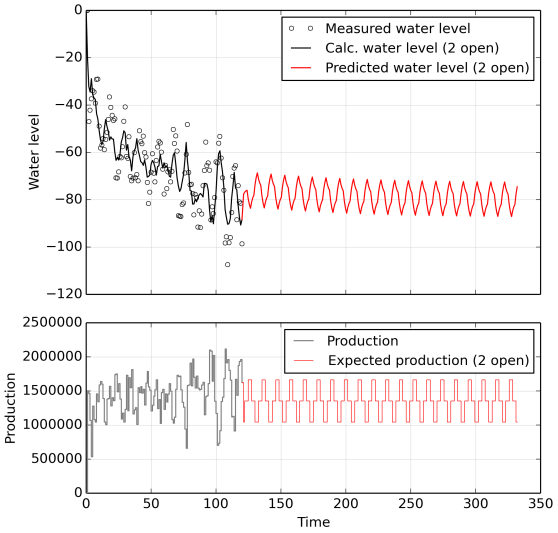

(b) Forecast with 120 months data input

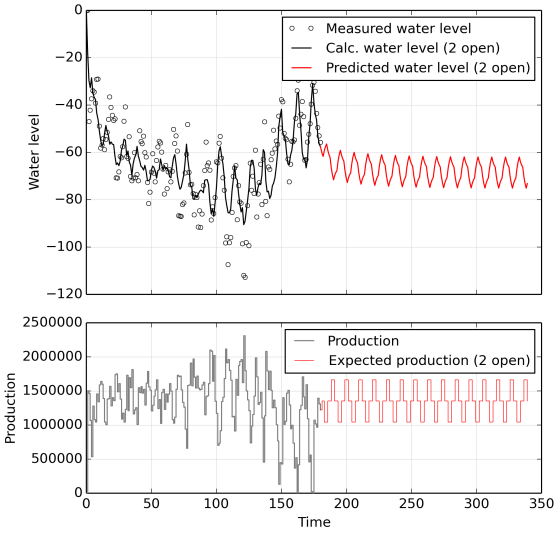

(c) Forecast with 180 months data input

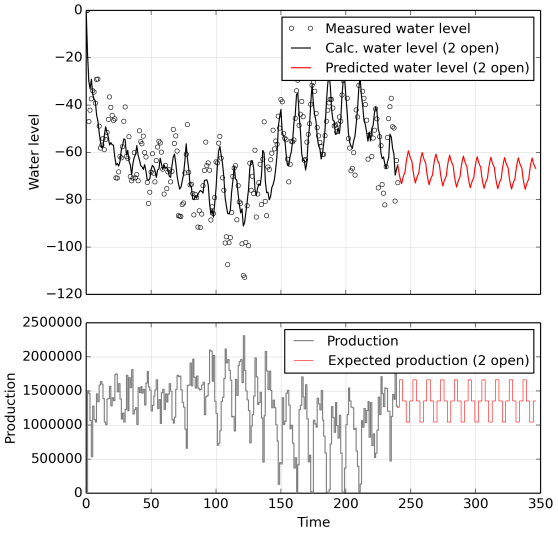

(d) Forecast with 240 months data input

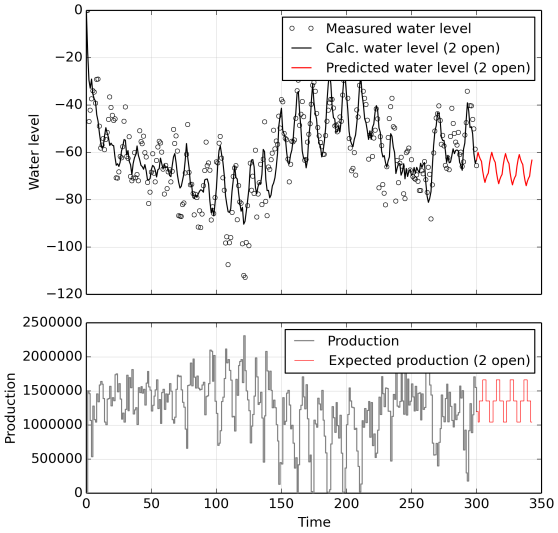

(e) Forecast with 300 months data input

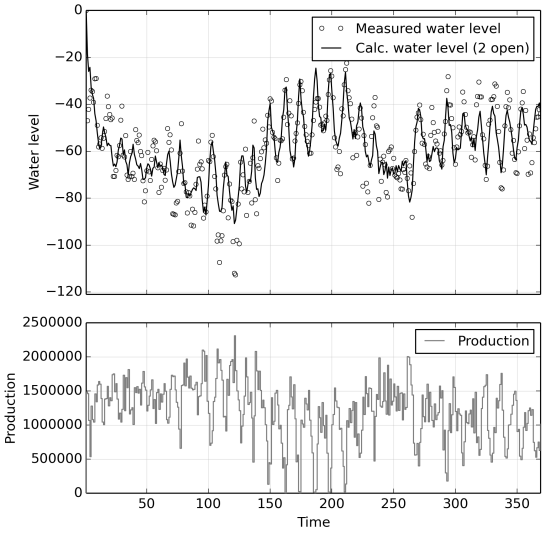

(f) Initial fit

Figure 44: Drawdown forecast for Reykir, input main 80% of the production data from months 1 - 60

Appendix E

Drawdown Response of Control Model

For a one tank open model $h_2 = h_\infty$, therefore:

$$K_1 \frac{h_i - h_{i-1}}{\Delta t} = \sigma_{12}(h_\infty - h_1) + \frac{\dot{m}}{\rho g} \tag{39}$$

By averaging the production one gets:

$$K_1 \frac{h_i - h_{i-1}}{\Delta t} = \sigma_{12}(h_\infty - h_{i-1}) + \frac{\frac{\dot{m}_{i-1}+\dot{m}_i}{2}}{\rho g} \tag{40}$$

This leads to:

$$h_i = \frac{\Delta t \sigma_{12}}{K_1}(h_\infty - h_{i-1}) + h_{i-1} + \frac{\Delta t}{K_1 2\rho g}(\dot{m}_{i-1} + \dot{m}_i) \tag{41}$$

$$h_i = \frac{\Delta t \sigma_{12}}{K_1} h_\infty + \left(\frac{\Delta t \sigma_{12}}{K_1} - 1\right) h_{i-1} + \frac{\Delta t}{K_1 2\rho g}(\dot{m}_{i-1} + \dot{m}_i) \tag{42}$$

School of Science and Engineering
Reykjavík University
Menntavegi 1
101 Reykjavík, Iceland
Tel. +354 599 6200
Fax +354 599 6201
www.reykjavikuniversity.is
ISSN 1670-8539